[redacted]

Copy No. 76

MSC-G-R-66-4
Supplemental Report 6

NATIONAL AERONAUTICS AND SPACE ADMINISTRATION

GEMINI AGENA TARGET VEHICLE 5003

SYSTEMS TEST EVALUATION

(45-Day Report) (U)

Prepared by: Lockheed Missiles and Space Company
Sunnyvale, California

Issued as: Supplement 6

To: Gemini Program Mission Report
Gemini VIII
MSC-G-R-66-4

By: Gemini Mission Evaluation Team
National Aeronautics and Space Administration
Manned Spacecraft Center
Houston, Texas

MANNED SPACECRAFT CENTER
HOUSTON, TEXAS
May 5, 1966

[redacted]

cy#76

D/C 67-83-C

C67-7783

MSC-G-R-66-4
SUPPLEMENTAL REPORT 6
COPY NO.____

~~CONFIDENTIAL~~

LMSC-A817204 5 MAY 1966

SSD-545-66-8 5 MAY 1966

CLASSIFICATION CHANGE

To UNCLASSIFIED
By authority of GDS-GP-4
Changed by L. Shirley Date 9-75
Classified Document Master Control Station, NASA
Scientific and Technical Information Facility

GEMINI AGENA TARGET VEHICLE 5003 SYSTEMS TEST EVALUATION (45-DAY REPORT)(u)

CONTRACT AF 04(695)-545

~~GROUP 4~~
~~Downgraded at 3 year intervals; declassified after 12 years~~

Issued as: Supplement 6
To: Gemini Program Mission Report
Gemini VIII
MSC-G-R-66-4
By: Gemini Mission Evaluation Team
National Aeronautics and Space Administration
Manned Spacecraft Center
Houston, Texas

APPROVED:

M. L. Mercer

M. L. MERCER
MANAGER (ACTING)
NASA AGENA PROGRAMS ENGINEERING

APPROVED:

L. A. Smith

L. A. SMITH
MANAGER
GEMINI PROGRAM

(INFORMATION ON THIS PAGE IS UNCLASSIFIED)

LOCKHEED MISSILES & SPACE COMPANY

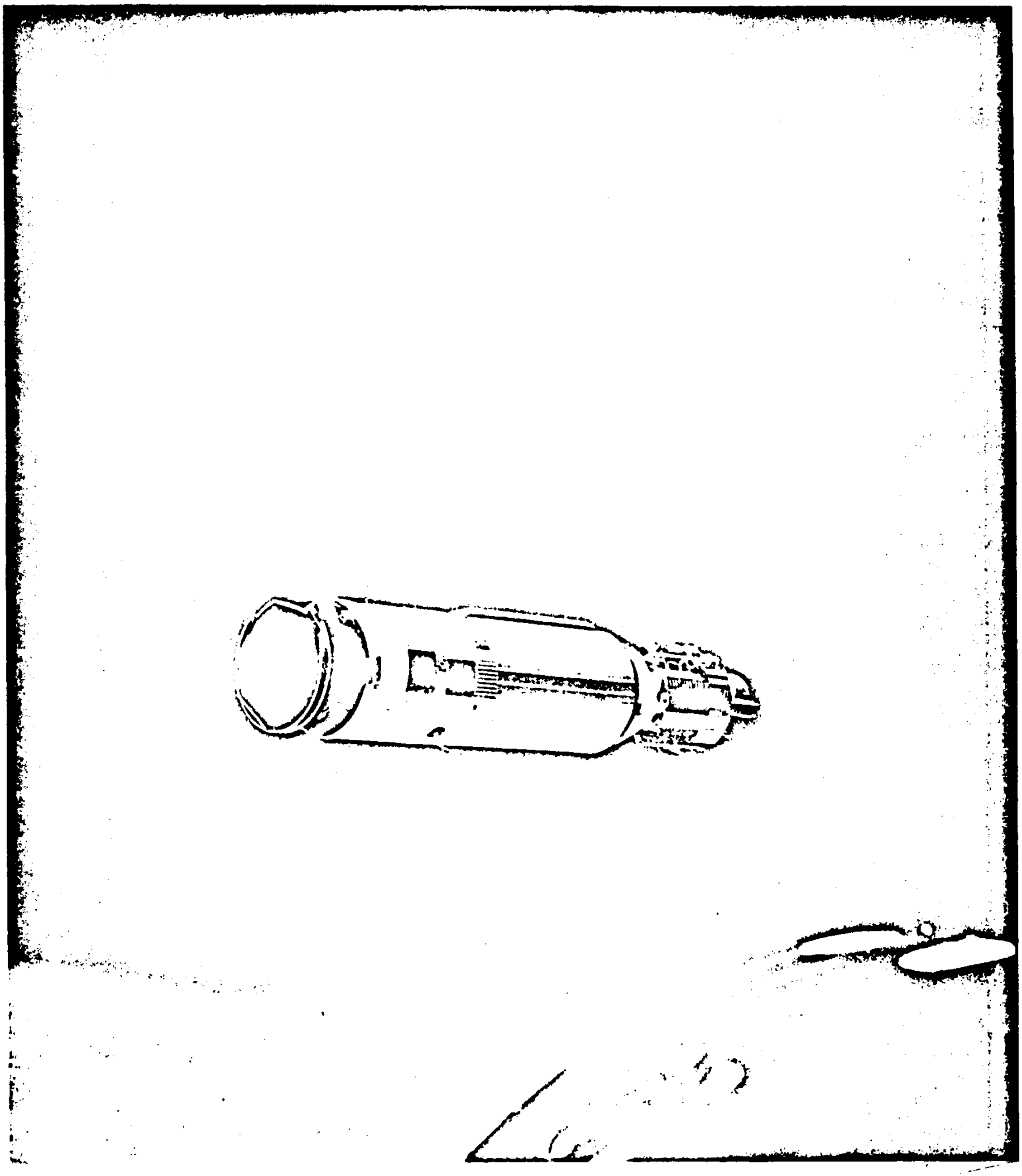

Gemini Agena Target Vehicle as Viewed From the Gemini VIII Spacecraft on Orbit

FOREWORD

This report, prepared by Lockheed Missiles & Space Company in compliance with Contract AF 04(695)-545, documents the flight performance evaluation of Gemini Agena Target Vehicle 5003 launched from the Air Force Eastern Test Range on 16 March 1966.

Pertinent evaluations for the performance of Atlas Vehicle and of the target docking adapter are based on information transmitted to Lockheed by General Dynamics Convair (GDC) and by McDonnell Aircraft Corporation (MAC), respectively.

SUMMARY

The Gemini Agena Target Vehicle (GATV) Serial No. 5003 was launched from Cape Kennedy, Florida, Complex 14 at 1500:03:127 GMT, 16 March 1966. Launch, boost, and separation were excellent. After an Agena propulsion system burn of 183.37 sec, the GATV was injected into a nearly perfect circular orbit: perigee 160.75 nm, apogee 162.37, and an inclination of 28.88 deg. During the first burn a yaw c.g. offset of +5 deg occurred shortly after ignition and gradually increased throughout the burn with the c.g. shift. This offset was apparent during all the subsequent PPS burns. Corrective action has been taken for GATV 5004.

During Revolution 3 over Texas Tracking Station, the GATV position in the yaw plane was rotated 90 deg in preparation for rendezvous and docking with the Gemini VIII spacecraft. Docking was accomplished without difficulty, and the mating was exceptionally smooth. After 41 minutes of docked cruising, trouble was experienced with the spacecraft. The Gemini crew immediately undocked and, after returning the Agena to ground control, initiated emergency procedure for reentry of the spacecraft.

After undocking, the Agena quickly stabilized and remained in an attitude-stabilized condition for the remainder of its orbital life. Subsequently, the Agena underwent a series of planned maneuvers consisting of 8 additional PPS burns and 10 SPS burns, all of which were accomplished successfully. The circularization, orbit adjust, catch-up, and planar change capabilities of the Agena were successfully demonstrated through the forty-five revolutions forming the scope of this report. Further testing of the Agena command capability was conducted by the Texas Tracking Station through Revolution 122.

Data samples (time slices), received from Texas Tracking Station subsequent to Revolution 45, revealed that the temperatures, control gas supply, and voltage levels were as predicted until complete loss of power 8-1/2 days after GATV launch.

CONTENTS

ILLUSTRATIONS

TABLES

ABBREVIATIONS

ACS	Altitude Control System
AFETR	Air Force Eastern Test Range
AGE	Aerospace Ground Equipment
AVTW	Agena Vehicle Time Word
BAC	Bell Aerosystems Corporation
BECO	Booster Engine Cutoff
DRAPE	Data Reduction
EST	Eastern Standard Time
F/C	Flight Control
FCLP	Flight Control Logic Package
GAT	Gemini Agena Target orbital stage
GATV	Gemini Agena Target Vehicle second stage, including adapter section, payload firing, and other droppables
GD/C	General Dynamics/Convair
GE	General Electric Company
GG	Gas Generator
GGFSV	Gas Generator Fuel Solenoid Valve
GGOSV	Gas Generator Oxidizer Solenoid Valve
GMT	Greenwich Mean Time
H_e	Helium
H/S	Horizon Sensor
IRFNA	Inhibited Red Fuming Nitric Acid
IRP	Inertial Reference Package
LMSC	Lockheed Missiles & Space Company
LOS	Loss of Signal
LOX	Liquid Oxygen

MAP	Message Acceptance Pulse
MDF	Mild Detonating Fuse
N_2	Nitrogen
ODPS	Oxidizer Discharge Pressure Switch
OMPS	Oxidizer Manifold Pressure Switch
PAFB	Patrick Air Force Base
PCM	Pulse Code Modulation
PDT	Pacific Daylight Time
PFRT	Preliminary Flight Rating Tests
PHCV	Pyrotechnic Helium Control Valve
PIV	Propellant Isolation Valve
POSV	Pyro-Operated Solenoid Valve
PPS	Primary Propulsion System
PRF	Pulse Repetition Frequency
PTVA	Propulsion Test Vehicle Assembly
RTC	Real Time Command
SCCM	Standard Cubic Centimeters per Minute
SDP	Status Display Panel
SECO	Sustainer Engine Cutoff
SEP	Separation of the GAT from the Atlas Booster
S/N	Serial Number
SPC	Stored Program Command
SPS	Secondary Propulsion System
TCA	Thrust Chamber Assembly
TCP	Thrust Chamber Pressure
TCPS	Thrust Chamber Pressure Switch
TDA	Target Docking Adapter
TOS	Turbine Overspeed Switch
UDMH	Unsymmetrical Dimethylhydrazine
VECO	Vernier Engine Cutoff
V/M	Velocity Meter

Section 1

INTRODUCTION

Section 1
INTRODUCTION

1.1 PURPOSE AND SCOPE

This report has been prepared to provide an evaluation of the flight performance of Gemini Agena Target Vehicle 5003, which was launched from Complex 14, Cape Kennedy, Florida, on 16 March 1966.

The report documents the test objectives and the flight performance. The flight performance, conclusions, and recommendations are based on all available data from liftoff through Revolution 45. This portion of the flight included 9 PPS and SPS (16-lb thrust) burns and 2 SPS (200-lb thrust) burns for orbital position adjust. Atlas-derived data are discussed, where applicable, to the extend made known to Lockheed Missiles & Space Company (LMSC). The General Dynamics Convair (GDC) report of the Atlas performance should be consulted for detailed performance data.

In Section 2, flight performance is discussed in detail. Section 3 presents Agena Target Vehicle subsystem performance data, a description of the yaw anomaly that occurred, and an interpretation of the obtained data. Conclusions and recommendations are presented in Section 4.

Vehicle commands executed during the mission are presented in Appendix A; the tracking station contact schedule in Appendix B; and the on-orbit temperature measurements recorded by the tracking network are tabulated in Appendix C.

1.2 GATV OBJECTIVES

The objectives of the GATV 5003 were as follows:

- Provide a 5-day active orbital life

- Provide a restartable primary propulsion system capable of at least 5 starts
- Provide a secondary propulsion system which would operate with tank pressures as low as 1110 psi
- Provide a communications and command system capable of executing a minimum of 1000 commands (stored-program, real-time, or a combination of both)
- Provide a total system which would consume power at a rate not to exceed 450 watts average

1.3 COUNTDOWN

The countdown was initiated at Complex 14, 15 March 1966 at 2355 EST or 700 minutes before liftoff. Countdown proceeded without any technical holds. There were no vehicle anomalies that caused a hold in the countdown. Weather conditions and surface winds were satisfactory for launch. Liftoff (2-inch motion) occurred at 1500:03.127 GMT (1000:03.127 EST).

Section 2
FLIGHT PERFORMANCE

Section 2
FLIGHT PERFORMANCE

2.1 Launch and Ascent

The azimuth of the Gemini VIII Atlas-Agena launch was 84.36 deg east of north. Evaluations of the GATV 5003 coast ellipse derived from the received sets of AFETR radar data were closely grouped. The deviations from nominal in the coast ellipse parameters based on the 7.18 (Grand Turk) radar data were as follows:

Coast ellipse apogee radius (ft)	-661.0
Coast ellipse apogee velocity (fps)	+0.762
Coast ellipse inclination angle (deg)	-0.022
Time from SAT to apogee (sec)	-0.23

The General Electric tracking radar data provided a value of approximately 4 fps for the retrovelocity applied to the Atlas at separation.

The 7.18 tracking data were selected for the performance analysis subsequent to secondary propulsion system ignition. No propulsion anomalies were observed from the radar data analysis.

The c.g. offset, apparent in the yaw position gyro telemetry records, prevented a satisfactory estimate of the initial yaw angle or of the yaw gyro drift. The powered fit to the 7.18 radar data produced a +0.004 deg equivalent deviation from the desired horizon scanner mechanical bias.

Injection parameter deviations derived from the powered fit were as follows:

Radius (ft)	-1380.0
Velocity (fps)	-2.0
Flight path angle (deg)	-0.0041
Inclination angle (deg)	+0.012

2.1.1 System Performance Prior to SPS Ignition

Performance was determined by evaluating the coast ellipse apogee radius, apogee velocity and inclination angle, and the time of flight from start of the Agena Ascent Timer (SAT) to the coast apogee. Since the Agena target vehicle guidance system is open loop and can not detect deviation from the preflight design trajectory or make inflight corrections, it is necessary that the Agena be provided with correct conditions at the start of the powered phase at SPS ignition.

The preflight nominal values for the evaluation were obtained from the preflight reference trajectory (Enclosure A to LMSC/A794338) and are given in Table 2-1. The table also provides estimates of the actual coast ellipse obtained from the indicated data sources. The 19.18 (Merritt Island) radar data was unsatisfactory due to the low (approximately 2 deg) elevation angle and therefore is not included in Table 2-3. There was no coverage of the coast phase from the 91.18 (Antigua) radar, and no estimate could be obtained. Figure 2-1 is a plot of the apogee radius versus apogee velocity for the estimates in Table 2-1.

In comparing the preflight and postflight values, note that the coast ellipse evaluations obtained from the GE sources refer to the booster ellipse, which differs from the GATV 5003 ellipse by the retrovelocity applied to the booster at separation. All estimates of actual apogee radius and velocity are within 600 ft and 1 fps respectively, of the nominal preflight values, except for the estimate from the 3.18 (Grand Bahama Island) radar. These deviations of 1300 ft and 2 fps have not been satisfactorily explained at this time, but are not considered excessive. The coast ellipse inclination angle deviates by 0.02 deg for all the postflight estimates, except for that from the 3.18 radar where the deviation is 0.04 deg. All estimates of the SAT-to-coast-apogee time are within 0.5 sec of the preflight nominal value.

These comparisons indicate that the booster placed the GATV 5003 on an ellipse close to the desired ellipse and that the sequence timer was started at near nominal time with respect to coast apogee. It is concluded that system performance prior to SPS ignition was satisfactory and achieved its designed objectives.

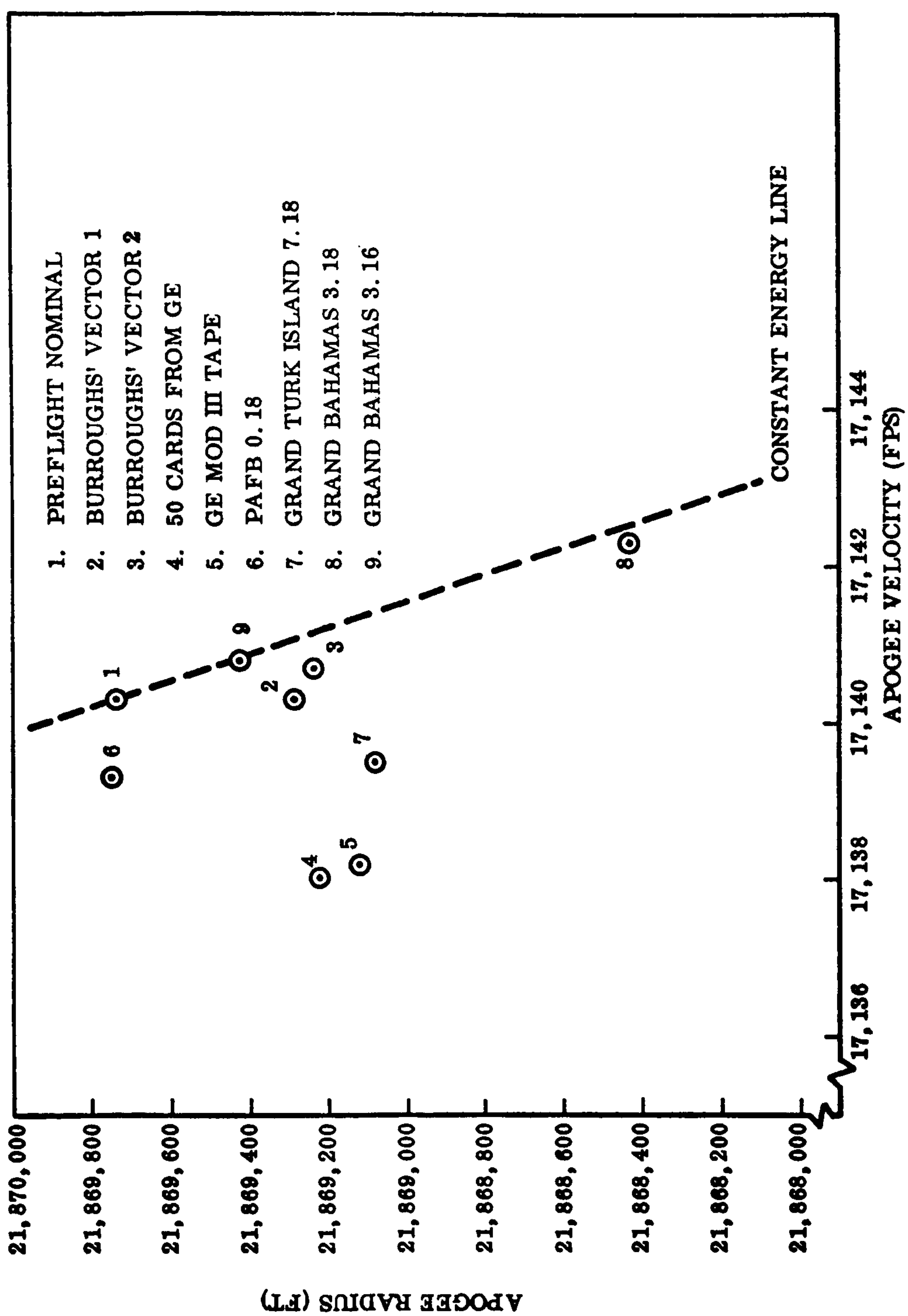

Fig. 2-1 Boost Ellipse Evaluation

Table 2-1

LAUNCH AND ASCENT VALUES, BOOSTER COAST ELLIPSE

Data Source	Apogee Radius (ft)	Apogee Velocity (fps)	Inclination (deg)	Time From SAT to Apogee (sec)
Preflight Nominal	21869742	17140.269	28.866703	197.51528
Burroughs Vectors				
1	21869298	17140.279	28.848141	197.13
2	21869340	17140.747	28.848243	197.15
50 Cards From GE	21869224	17138.038	28.844909	197.21
GE Mod III Tape	21869125	17138.193	28.844936	197.19
PAFB				
0.18	21869752	17139.302	28.847700	197.48
Grand Turk Island				
7.18	21869081	17139.507	28.844485	197.29
Grand Bahamas				
3.18	21868418	17142.327	28.825917	197.06
3.16	21869428	17140.792	28.845224	197.32

Note: GE cards and tapes reflect booster ellipse.

19.18 evaluation not included – insufficient data for satisfactory estimate.

91.18 did not provide data for coast phase.

The GE radar data provided an estimate of the retrovelocity applied to the booster at separation. In Fig. 2-2, the range rate is plotted for the period spanning separation from which the retrovelocity was approximately 4 fps.

2.1.2 System Performance After SPS Ignition

The GATV-VIII flight performance analysis is based on the data from the 7.18 (Grand Turk) radar. The 0.18 (PAFB) radar coverage did not extend to velocity-meter cutoff, and the data from the remaining radars was not received early enough for a detailed analysis of the powered phase to be performed. The results of the coast ellipse evaluations discussed in the previous section suggest that the difference would be small.

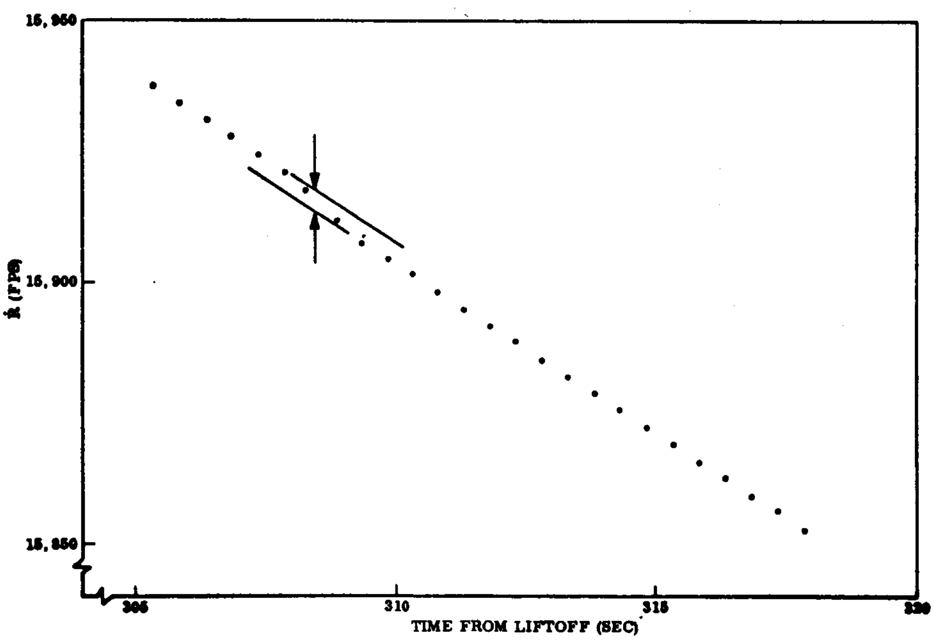

Fig. 2-2 Range Rate vs Time From Liftoff

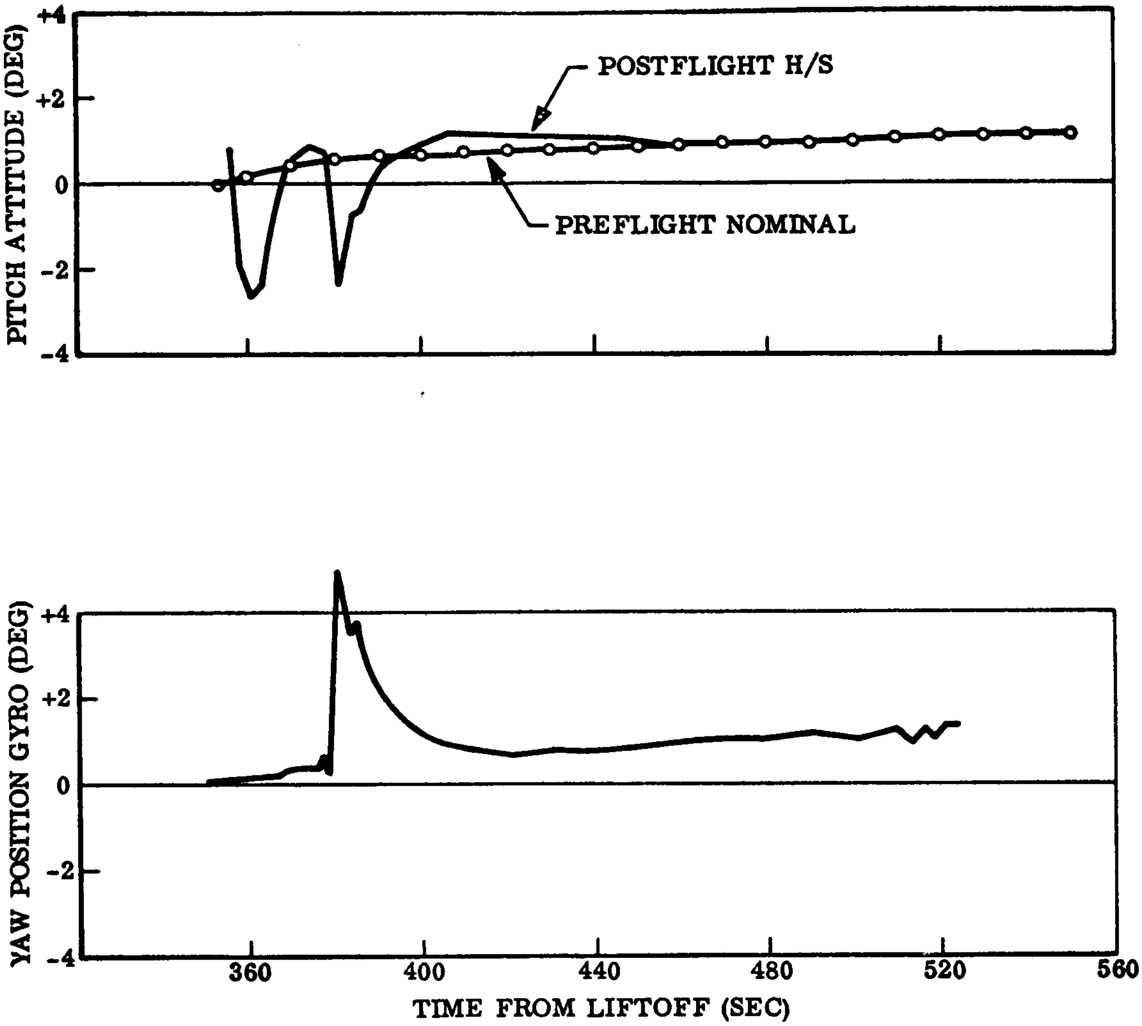

Fig. 2-3 Pitch and Yaw Attitude Histories

Trajectory reconstruction was more complicated on GATV-5003 than for similar previous Agena missions, primarily because of the unanticipated yaw offset experienced at PPS ignition, which could not be directly simulated as a yaw attitude history in the postflight radar fitting program. One analytical approach was to obtain a least-squares fit to the data for the SPS burn and the first 20 sec of the PPS burn (by which time the yaw position gyro had reached a reasonably steady-state value), then to fit the radar data for the remainder of the PPS burn. This method provided performance estimates based on the data after the yaw transient and effectively by-passed the problem area. An alternate approach was to simulate the yaw attitude history obtained from T/M by appropriate changes in the center-of-gravity history. Neither approach proved entirely satisfactory; however, adequate analysis was obtained by combining the two sets of results.

In determining performance after SPS ignition, all available sources of data were used as they became available, including the postflight sequence of events, the reduced T/M data, raw radar data, etc., pertinent to the powered phase of the ascent.

From the sequence of events (Table 2-2), the powered phase was initiated with SPS ignition at 357.98 sec after liftoff, and ended at velocity-meter cutoff 560.43 sec after liftoff. SPS burn time was 19.98 sec in comparison with a nominal 20.0 sec, whereas PPS burn time, measured from 75 percent chamber pressure to velocity-meter cutoff, was 183.35 sec in comparison with a predicted nominal of 184.20 sec. It was also determined that the sequence timer performed satisfactorily in providing the SPS and PPS ignition signals. Both occurred 0.14 sec earlier than the preflight nominal values after SAT, well within the three sigma range of ±0.54 sec.

Table 2-2

ASCENT SEQUENCE OF EVENTS

Event	Flight Time (sec) Nominal	Actual
Liftoff (1500:03.127 GMT)		0
Booster Engine Cutoff (BECO)*	131.0	129.6
Start Sequence Timer	277.4	282.1
Sustainer Engine Cutoff (SECO)*	279.9	283.7
Gyros Uncaged	300.2	303.9
Horizon Sensor Doors Jettisoned	300.2	303.9
Vernier Engine Cutoff (VECO)*	300.2	304
Atlas/GATV Separation	305.0	308.5 to
Primacord and Retros Fired		310.6
Enable ACS Pneumatics	307.5	310.6
Set Pitch Rate to -1.5°/sec	338.4	342.9
Open SPS Press. Start Valve	338.4	343.0
Pitch Program "OFF"	351.4	356.1
Geocentric Rate "ON" (3.99°/min)	351.4	356.1
Enable Velocity Meter	351.4	356.1
Open SPS 16lb Bipropellant Valves (SPS Thrust Initiate)	373.4	357.98
Close SPS Start Valve		378.0
Jettison Shroud	381.4	386.8
PPS Thrust Cutoff (V/M)**	556.1	560.43
Enable Pitch and Yaw Pneumatics	556.1	560.4
Disable Velocity Meter	589.4	595.5
Gyrocompassing On, Low Gain	589.4	595.3

*From GDC data.
**First burn duration – 183.35 seconds.

Table 2-2 (Cont.)

Event	Flight Time (sec) Nominal	Actual
Antenna Transfer Ascent to Orbit	592.4	597.5
Disable Command Destruct Receivers	592.4	597.5
ACS Press Low	696.4	701.5
Fire Horizon Sensor 0 Deg Position Squib	703.4	709.5
Sequence Timer Shutdown		709.5

A comparison of the preflight (nominal) and postflight (actual) vectors at SPS ignition, obtained by integration of the coast ellipse vectors to the corresponding times, is given in Table 2-3. At the start of the GATV-5003 powered phase, the radius was low by 500 ft, the velocity low by 1 fps, the flight path angle low by 0.004 deg and the inclination angle low by 0.02 deg.

Preflight and postflight pitch attitude histories are compared in Fig. 2-3. The postflight curve was obtained by incorporating the horizon sensor T/M data in the postflight simulation and solving for a mechanical horizon scanner bias from the radar data. The close agreement between the two profiles for the later part of the flight indicates that the mechanical bias was close to the nominal value and confirms the small deviation of +0.004 degrees obtained by the radar fit. This is satisfactorily within the anticipated tolerances.

Figure 2-3 also provides a plot of the yaw position gyro history obtained from the T/M records. The significant offset occurring at approximately 377 sec from liftoff coincides with the first acceleration due to the PPS thrust. This vehicle motion would result from a lateral center-of-gravity offset and/or a thrust vector misalignment.

The 25 sec required to return to a steady-state yaw attitude is a result of the lead-lag response of the autopilot-airframe combination in the GATV-5003 configuration. The observed yaw position gyro offset is equivalent to a +7.8 inch shift in the yaw plane c. g. at PPS ignition. As a result of the yaw attitude offset, which cannot be exactly simulated in the present version of the postflight fitting program, it was not possible to obtain satisfactory estimates of the yaw attitude at SPS ignition or of the drift in the yaw gyro.

No propulsion anomalies were observed from the radar data analysis. Steady-state average values of the PPS engine parameters are given below:

	Preflight	Postflight
Thrust (lb)	16230	16374
Flow rate (lb/sec)	55.489	55.871
ISP (sec)	292.5	293.06

The shorter burn time noted from the postflight sequence of events is consistent with these values.

The preflight and reconstructed radius histories are plotted in Fig. 2-4 for the period from VECO to velocity-meter cutoff, and the event times are indicated. The close agreement in the radii at which the GATV-VIII events occurred shows that the actual system performance was near nominal during the powered phase of the ascent. The degree of success with which the postflight fitting program reconstructed the actual trajectory is given in Fig. 2-5, which shows the residuals between the radar measurements and the calculated values of slant range, azimuth, and elevation. The effects of the yaw offset are apparent in these plots, which ideally should indicate random scatter about the zero lines.

The preflight nominal injection parameters are compared in Table 2-3 with those obtained from the least-squares fit to the ascent radar. Actual injection parameters were satisfactory and deviations from nominal preflight values are as follows:

Radius (ft)	-1380
Velocity (fps)	-2.0
Flight path angle (deg)	-0.0041
Inclination angle (deg)	+0.012

The estimate of the injection vector obtained from a fit to the on-orbit tracking data is included in Table 2-3 for comparison. The two estimates of injection are as close as can be expected considering the differences that arise from the statistical nature of the estimates and from the uncertainties in the decay properties of the GATV-VIII impulse after velocity meter cutoff.

Table 2-3

COMPARISON OF NOMINAL AND ACTUAL INJECTION PARAMETERS

	Time (sec)	Radius (ft)	Velocity (fps)	Gamma (deg)	Inclination (deg)	Azimuth (deg)	Geoc. Lat (deg)	Geoc. Lat. (deg)	Longitude (deg)	Roll (deg)	Pitch (deg)	Yaw (deg)	Weight (lbs)
SPS Ignition													
Nominal	353.38	21751510	17343.2	6.4492	28.867	88.956	28.849	29.012	-71.120	-0.0060	0.0138	-2.0746	17692
Actual	357.98	21751000	17342.2	6.4459	28.844	89.082	28.830	28.993	-70.913	0.0000	-1.7301	-1.6661	17677
PPS Ignition													
Nominal	371.88	21784790	17287.3	5.4779	28.867	89.420	28.861	29.024	-70.240	-0.0055	0.4957	-1.6126	17677
Actual	377.08	21785390	17279.7	5.4304	28.844	89.561	28.841	29.004	-70.006	0.0000	0.7746	-1.2807	17659
Shroud Ejection													
Nominal	381.38	21799760	17513.3	4.9197	28.867	89.653	28.865	29.028	-69.786	-0.0040	0.6527	-1.1397	16947
Actual	386.74	21800420	17527.7	4.8375	28.844	89.833	28.843	29.006	-69.543	0.0003	-0.3951	-0.0410	16890
V/M Cutoff													
Nominal	556.28	21890150	25366.9	0.0029	28.868	94.856	28.492	28.653	-59.644	-0.0039	1.1732	4.3108	7253
Actual	560.43	21888770	25364.9	0.0070	28.880	95.339	28.424	28.586	-59.486	0.0000	1.1439	0.6788	7245
Orbital Data Fit	560.43	21890100	25364.4	0.0041	28.884		28.429	28.583	-59.468				

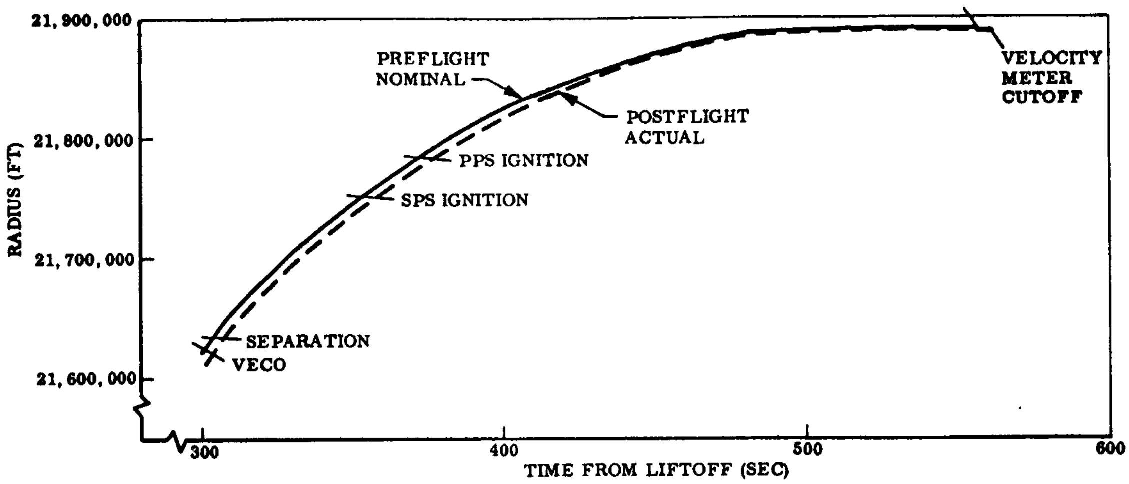

Fig. 2-4 Ascent Trajectory

2.2 ORBIT

The orbital flight performance analysis is based on radar tracking data received from the NASA Gemini rendezvous tracking network and telemetry data transmitted to ground stations from the Agena.

GATV 5003 was injected into a near nominal orbit at 15:09:23.557 GMT. The initial perigee/apogee altitude was 160.8/162.4 nm and inclination was 28.88 deg, compared to target-values of 161/161 nm and 28.87 degrees. The GATV subsequently performed eight PPS firings and two SPS unit II firings, which changed its orbital elements several times before assuming a parking orbit with a perigee/apogee altitude of 220.6/223.8 nm, compared to a planned 220/220 nm orbit. The maneuvers performed on orbit are defined in Table 2-4.

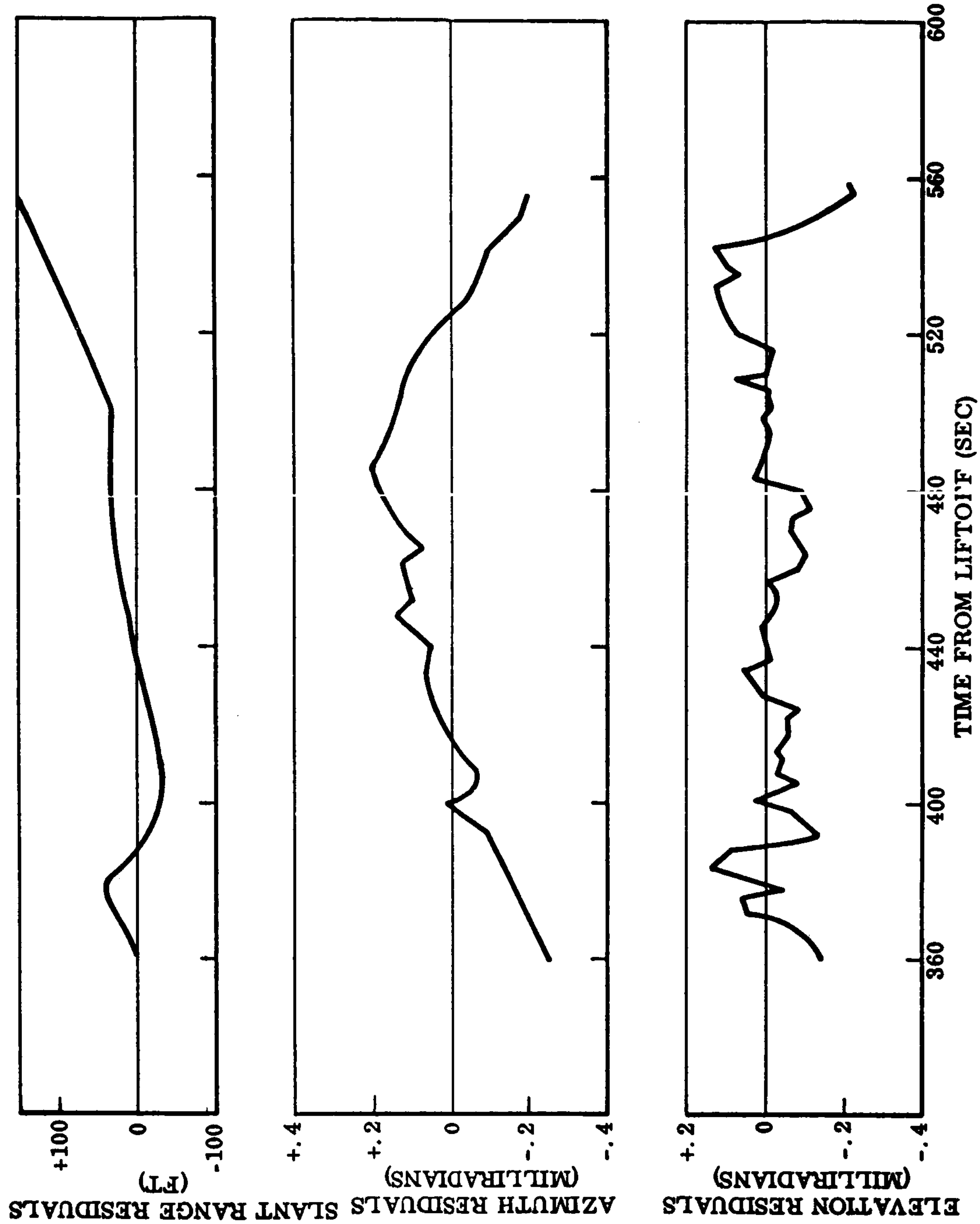

Fig. 2-5 Radar Residuals vs Time From Liftoff

Table 2-4

ORBITAL SEQUENCE OF EVENTS

	Event	Inclination (deg)	Station & Rev. No.	Event Time (GET)	Velocity ΔV (fps)
1.	90 Deg Yaw	28.90	TEX, 2	3:04:00	0
2.	Rendezvous	28.90	CRO, 5	5:07:23	0
3.	Docking	28.90	RKV, 6	6:33:16	0
4.	Undock	28.90	CSQ, 6	7:15:11	0
5.	Hohmann Transfer (PPS No. 2)	28.90	CRO, 15	21:42:31	104.4
6.	Circularize (PPS No. 3)	28.87	HAW, 18	27:03:19	106.7
7.	Plane Change (1.75 Deg) (PPS No. 4)	30.62	CYI, 26	39:16:10	1583.9
8.	Minimum Total Impulse ΔV Check (PPS No. 5)	30.62	TEX, 28	44:01:06	96.0
9.	Inclination Adjust (-1.64 Deg) (PPS No. 6)	28.98	ANT, 31	47:39:02	772
10.	Orbit Adjust (PPS No. 7)	28.93	ANT, 33	50:46:35	272.0
11.	Orbit Adjust (PPS No. 8)	28.93	TAN, 35	54:38:51	247.7
12.	Orbit Adjust (PPS No. 9)	28.93	ASC, 38	59:27:43	309.1
13.	Circularize (SPS No. 1)	28.93	CYI, 41	64:30:46	59.9
14.	Circularize (SPS No. 2)	28.89	BDA, 43	67:38:32	152.71

A complete GATV 5003 ephemeris, which is accurate to within 1500 ft, from injection to the time of the final SPS II firing was generated from the radar tracking data. The values of the instantaneous boost velocity and pitch and yaw attitudes required at the GATV maneuver times to affect the orbital changes were determined from this ephemeris. The boost velocities thus determined are shown to agree within two percent with the values recorded by the velocity meter telemetry except for the case of maneuver number 4. It is believed that the velocity meter value presented does not include the actual tail-off velocity incurred. If the velocity meter data included the tail-off velocity, the values would agree within 2 percent. The deviation in the boost velocities determined from the ephemeris data and that desired falls within the expected 3-sigma dispersions for all PPS firings except maneuver Nos. 3 and 6. The excessive velocity incurred in maneuver No. 3 is possibly due to an erroneous velocity meter input. The deviation in maneuver No. 6 is believed to be due to an error in determining the velocity meter input for the desired boost velocity.

A yaw attitude anomaly was discovered on the first orbit plane-change burn (Maneuver No. 4), which resulted in a 336.9 nm apogee altitude instead of the desired circular orbit of 220 nm. This anomaly, due to a c.g. offset from the vehicle longitudinal axis, resulted in pitch and yaw attitude deviations from nominal during all PPS engine firings.

2.2.1 Orbit Determination

In order to evaluate on-orbit maneuvers, it was first necessary to generate a high-accuracy postflight ephemeris. Since there were eleven maneuvers that appreciably change the GATV 5003 orbit, it was necessary to divide the ephemeris into eleven sections. An additional section was required to accommodate the changes in the orbit elements that occurred during the docking phase of the flight.

The LMSC closed-form ephemeris program (Ref. 2-1) was used to fit an orbit to data for each section. This program uses a least-squares minimization method to fit orbit elements to radar data. The accuracy of the fit is determined by both the in-track component of the position differences (ΔRL) and the combination of the radial and cross-track components of the position differences (ΔRR). This computer program has been used over the past three years to generate the high-accuracy postflight ephemeris for Program 241 vehicles. Typical maximum position differences for the Program 241 vehicles are 1800 ft in-track and 1300 ft cross-track and radial; typical mean-position differences are 800 ft in-track and 600 ft cross-track and radial. On the basis of these position differences, the Program 241 ephemeris is estimated to be accurate to within 2000 ft.

2.2.2 Radar Tracking Data

Analysis of the on-orbit maneuvers was based on radar tracking data received from the NASA Gemini rendezvous tracking network (Ref. 2-2) and telemetry data transmitted to ground stations from instrumentation onboard the Agena.

A summary of the tracking data obtained during the flight is presented as a station contact schedule in Table B-1. A total of 268 passes were available, of which 168 were used to determine the orbit fits. Of the passes not used in the fits, 7 were before injection, 32 were short sections of two actual data passes, 25 were either Woomera or Pt. Arguello passes, and the other 13 passes were not used because they were very close to an approximate burn time. The actual burn times were received after all the fitting was accomplished.

The quality of most of the slant range data was excellent. Experience with the Program 241 radar data has proven that the slant range data is in general of much higher quality than the azimuth and elevation angle data. Therefore, only slant range data was used to determine the orbit fits. The data used for each of the fits is identified in the station contacts schedule. During the fitting it became apparent that the data from Woomera 0, Pt. Arguello 2, and Pt. Arguello 0 would not fit with the rest of the stations. It was concluded that the Woomera 0 had radar equipment problems and that the two Pt. Arguello stations had either radar equipment problems or incorrect station locations. The Woomera 0 radar problem became apparent when, for any one pass data, some data sections would fit extremely well while others would not. The radar tracking data (magnetic tape Nos. 10205, 3796 and 7671) received from the NASA Data Reduction Center, Houston, Texas were used in the LMSC closed-form ephemeris program (Ref. 2-1) to determine the mean orbital elements of the orbit traversed by the GATV between successive engine burns. These mean elements are:

a. Inclination
b. Perigee radius
c. Eccentricity
d. Semimajor axis

e. Anomalistic period

f. Argument of perigee

g. Right ascension of the ascending node

These elements are defined as the instantaneous elements existing at a prescribed base time (a nodal crossing time) plus secular terms and terms having long period oscillations.

2.2.3 Maneuver Analysis

The program of Ref. 2-1 uses the least-squares minimization method to fit mean orbit elements to radar data. The earth model used in the fitting process is that described in Ref. 2-2, except for the zonal and tesseral coefficients. These coefficients were obtained from Ref. 2-3. Since it has been found that tesseral coefficients greatly improve the accuracy of orbit determination, a sixth order set of tesseral coefficients with its associated set of zonal coefficients was included. These coefficients have been used in high-accuracy orbit determination of many other Agena vehicles.

The mean elements of the orbits attained after each GAT engine burn are presented in the orbital maneuver summary of Table 2-4. This summary shows the times of the engine firings, the objectives sought, and the pertinent elements of the orbits actually attained. Events occurring during the docking period with the Gemini spacecraft caused a significant change in the orbit elements. This required an additional determination to be made of the mean elements for the period from undocking to initiation of the second GAT maneuver. A high-accuracy fit could not be determined after the final burn, because only one pass of data was available. All the orbits fitted are believed to be accurate to within 1500 ft.

After the determination of the mean orbital elements existing between successive engine firings, a complete ephemeris of GATV 5003 from injection into orbit on 16 March 1966 to the final SPS II firing on 19 March 1966 was generated and is available in LMSC internal documentation. The velocity vectors as determined in this ephemeris during engine firings were resolved as impulsive maneuvers to determine the effective maneuver parameters of boost velocity and pitch and yaw attitude necessary to transfer from the mean orbit existing prior to the burn to the mean orbit after the burn. A comparison of the effective maneuver parameters thus determined with those desired and those recorded in the telemetry data is shown in Table 2-5. Telemetry values for the pitch and yaw attitudes are not presented since they have not been thoroughly analyzed. However, a preliminary analysis of the time histories of pitch and yaw gyro position and pitch and yaw actuator position show sudden deviations from the nominal zero positions commencing from PPS ignition. This deviation in pitch and yaw attitude was determined to result from two factors. One is the large torque applied to the vehicle when the PPS is fired, due to a significant c. g. offset from the vehicle longitudinal axis. The second factor is the slow hydraulic response to signals requesting the engine to gimble to remove deviations in pitch and yaw attitude. This slow response is due to a change made in the autopilot network to alleviate a stability problem when the GATV and Gemini spacecraft are docked. A detailed analysis of this yaw anomaly is presented in par. 3.5. Preliminary analysis of the telemetry data does indicate that over the interval of PPS firing the average deviation in the yaw gyro and actuator position and the pitch gyro and actuator position approximately totals the deviations shown by the ephemeris data from the desired attitudes on all PPS burns.

Table 2-6 presents a comparison of the deviations in the boost velocities and pitch and yaw attitudes from the desired values as determined from the ephermeris data and telemetry. Also shown for comparison are the expected three sigma dispersions, which are determined as noted in Ref. 2-4 with the latest values of the pertinent constants. Excessive deviations in boost velocity appear for maneuver Nos. 3, 4, 6, 10 and 11. The deviation in maneuver No. 3 appears to be due to an erroneous velocity meter input as the measured tail-off velocity from velocity meter shutdown with within 2 percent of the estimated tail-off velocity. The maneuver No. 4 deviation is approximately the magnitude of the estimated tail-off. The velocity meter value listed in Table 2-5 may be only the input value without the measure tail-off added and thus may be incorrect. If this is the case, the velocity deviation listed for maneuver No. 4 in Table 2-6 may be greatly reduced. The maneuver No. 6 deviation is again the magnitude of the estimated tail-off and could either be due to the same reason stated for maneuver

Table 2-5

MANEUVER PARAMETERS

Maneuver	Boost Velocity (ft/sec)			Pitch Attitude (deg)			Yaw Attitude (deg)		
	Desired	Ephemeris	Velocity Meter	Desired	Ephemeris	Telemetry	Desired	Ephemeris	Telemetry
2	104.4	102.6	104.4	0	-.61	–	0	-3.93	–
3	104.4	108.5	106.7	0	-.96	–	0	-5.31	–
4	1600	1599.0	1583.9(2)	0	-.95	–	93.8	84.69	–
5	96	94.5	96	0	-.65	–	0	4.69	–
6	789(1)	773.1	772(2)	0	-2.5	–	101.8	72.81	–
7	272	271.7	272	0	-1.42	–	180	188.26	–
8	247.7	247.2	247.7	0	-1.38	–	0	-7.93	–
9	309.1	308.8	309.1	0	-1.17	–	180	187.72	–
10	63	61.6	58.84(3)	0	+2.01	–	90	71.17	–
11	152.7	(1)	145.5(3)	0	(4)	–	90	(1)	–

NOTES:
(1) Possible error in velocity meter load.
(2) Possible error in reading velocity meter telemetry data
(3) SPS II shutdown by stored program command.
(4) Insufficient data for evaluation at this time.

Table 2-6

MANEUVER ERROR COMPARISON

Maneuver	Boost Velocity (ft/sec)			Pitch Attitude (deg)			Yaw Attitude (deg)		
	D -E(1)	D -TM(2)	$\pm 3\sigma$(3)	D -E	D -TM	$\pm 3\sigma$	D -E	D -TM	$\pm 3\sigma$
2	-1.8	0	1.84	-.61	–	.60	-3.93	–	1.83
3	+4.1	+2.3	1.87	-.96	–	.60	-5.31	–	1.83
4	-1.0	-16.1	2.41	-.95	–	.58	-9.11	–	2.40
5	-1.5	0	2.26	-.65	–	.60	+4.69	–	1.83
6	-15.9	-17	2.74	-2.5	–	.63	-28.99	–	2.46
7	-.3	0	2.63	-1.42	–	.60	+8.26	–	1.83
8	-.5	0	2.70	-1.38	–	.60	-7.93	–	1.83
9	-.3	0	2.84	-1.17	–	.60	+7.72	–	1.83
10	-1.4	-4.16	0.21(4)	+2.01	–	.55	-18.83	–	2.39
11	–	-7.2	0.46(4)	–	–	.55	–	–	2.39

NOTES:
(1) Desired minus ephemeris determination
(2) Desired minus telemetry
(3) Expected 3σ dispersion
(4) 3σ dispersion based on velocity meter shutdown

No. 4 or to a velocity meter input erroneously determined by subtracting the estimated tail-off twice from the desired boost velocity. The SPS No. 2 shutdowns on maneuver Nos. 10 and 11 were made by stored program command, and the deviations cannot be compared with the 3-sigma value as this was determined on the basis of a velocity meter shutdown. The excessive deviations in pitch and yaw attitude are all due predominantly to the yaw anomaly discussed previously.

2.2.4 Data Residuals

During the orbit fitting process, residuals are computed which are differences between actual tracking measurements and the theoretical values computed from the orbit parameters. These measurements may represent azimuth, elevation slant range, range rate, topocentric right ascension, or declination. After the orbit has converged, the final residuals are transformed to the orbital coordinate frame, which is defined by the triad of unit vectors $\bar{e}_R$, $\bar{e}_L$, and $\bar{e}_h$. Here $\bar{e}_R$ is positive along the geocentric radius vector, $\bar{e}_h$ is positive in the direction of the satellite's angular momentum vector defined by $\bar{R} \times \bar{V}$, and $\bar{e}_L$ is then $\bar{e}_L = \bar{e}_N \times \bar{e}_R$.

For slant range data two components of the position vector difference, $\Delta\bar{R}$, between the fit orbit and the tracking data are computed from the slant range residuals for each pass. These components are ΔRL, the in-track component, and ΔRR, the component in the direction of the slant range vector $\dot{s} = o$ (a combination of radial and cross-track components).

Figures 2-6 and 2-7 present plots of the ΔRR and ΔRL vs time for the final orbit fits. The mean and maximum components of the position differences obtained from these plots are listed below:

ΔRL (1100 ft)	Maximum
ΔRR (1400 ft)	Maximum
ΔRL (300 ft)	Mean
ΔRR (300 ft)	Mean

These position differences compare very favorably with those obtained for the Program 241 vehicles. The ephemeris is estimated to be accurate to within 1500 ft and, noting that the position differences shown in Fig. 2-6 and 2-7 are generally less than 800 ft, this estimate is considered to be conservative.

2.2.5 References

2-1 "Description of a Closed Form Ephemeris Program," C. T. Warmke, LMSC/577615, Tracking Note #15, Sunnyvale, Calif., 23 September 1964.

2-2 "Directory of Station Locations for Use in Gemini and Apollo Planning Studies," NASA General Working Paper No. 10,020A, Houston, Texas, 25 February 1965.

2-3 "Physical Constants for Satellite Calculations," R. J. Mercer, Aerospace Corporation Report, TOR-469(5110-02)-2, El Segundo, Calif., January 1965.

2-4 "An Analysis of the Revised Agena Guidance and Propulsion System Errors — Gemini Program," E. Hsu/R. J. Swanson, LMSC TM 55-31-04, LMSC/577146, Sunnyvale, Calif., 13 July 1964.

2.3 POSTFLIGHT WEIGHT, PROPELLANT LOADS, AND MASS PROPERTIES DATA

The GATV 5003 weight sequence is presented in Table 2-7. The impulse propellants and gases available for maneuvers on orbit are listed in Table 2-8. The mass properties are summarized in Table 2-9.

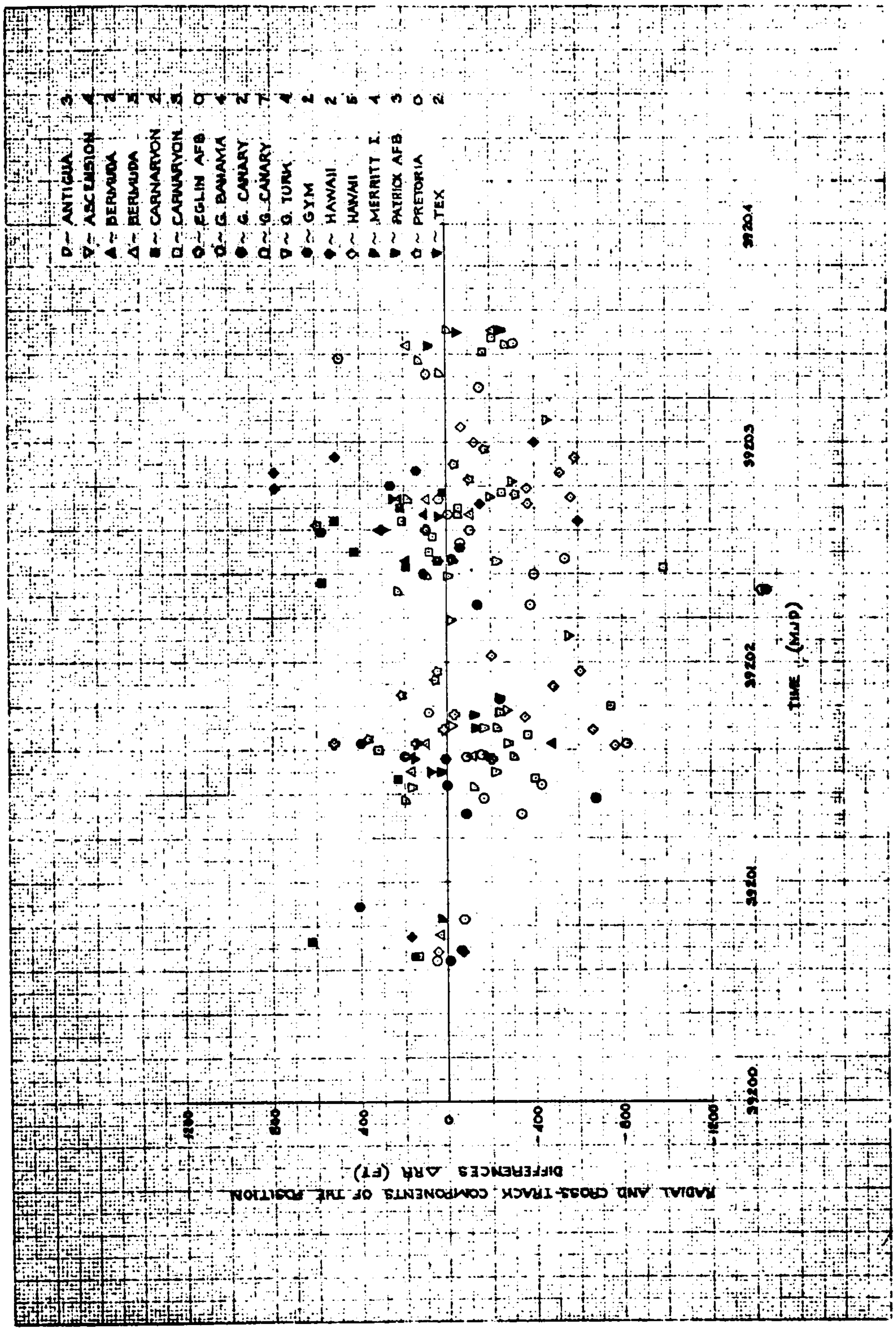

Fig. 2-6 Position Differences, ΔRR

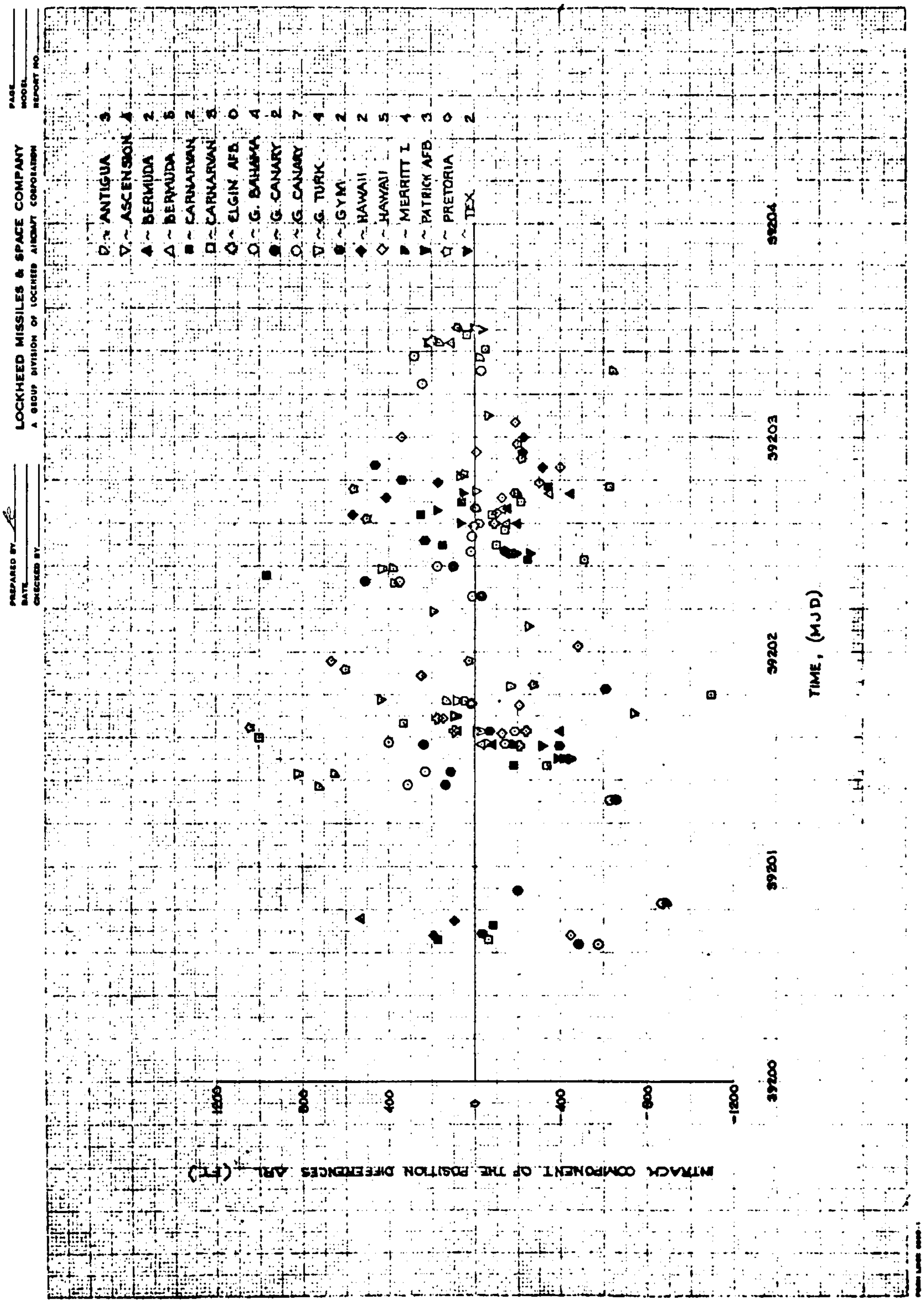

Fig. 2-7 Position Differences, ΔRL

Table 2-7

POSTFLIGHT WEIGHT DATA

		Weight (lb)
Agena/NASA Weight Empty		4085
Total Propellants and Gases Loaded		14012*
Gross Weight – Atlas Payload		18097
Less:	Booster Adapter and Extension	-382
	Self Destruct Items	-11
	Separation Detonator and Charge	-1
	Retrorockets	-10
	Horizon Sensor Fairings	-7
Separation Weight		17686
Less:	Attitude Control Gas	-3
	SPS Propellant	-3
	Propellant Preburn	-9
First Ignition Weight		17671
Less:	Nose Fairing	-260
	Impulse Propellant	-10232
	Attitude Control Gas	-2
Normal Burnout Weight		7177
Less:	Propellant Postburn	-62
Agena at Injection		7115

*Propellants and Gases Loaded

Helium – tank pressurization	3
Attitude control gas	142
PPS oxidizer loaded (IRFNA)	9702
PPS fuel loaded (UDMH)	3818
SPS oxidizer loaded (MON)	177
SPS fuel loaded (UDMH)	158
SPS nitrogen pressurization	8
PPS start tank propellants	4

Table 2-8

IMPULSE PROPELLANTS AND GASES AVAILABLE FOR MANEUVERS ON ORBIT

PPS Propellant	2474
SPS Propellant	326
Attitude Control Gas	134

NONAVAILABLE PROPELLANTS AND GASES*

PPS Propellant residuals	191
SPS Propellant residuals	6
Attitude control gas residuals	3
PPS start tank residuals	4

*Based on a 9 burn mission.

Table 2-9

POSTFLIGHT MASS PROPERTIES SUMMARY

Condition	Weight (lb)	Center of Gravity (In.) $\bar{x}$	$\bar{y}$	$\bar{z}$	Moment of Inertia (Slug-Ft^2) I_{xx}	I_{yy}	I_{zz}
Liftoff	279045	843.2	-0.5	-0.4	10450	2.67×10^6	2.67×10^6
Agena Gross Wt.	18097	339.6	0.5	0	543	13901	13918
Separation	17686	337.0	0.5	0	460	12454	12472
First Ignition	17671	337.1	0.5	0	460	12442	12460
First Burnout	7177	343.4	1.2	-0.1	418	8969	8991
Injection	7115	343.0	1.2	-0.1	417	8916	8939

Section 3

DATA ANALYSIS

Section 3
DATA ANALYSIS

The Agena subsystem performance, detailed in the following paragraphs, was evaluated from selected telemeter data sources from liftoff through revolution 45. Data processing of the selected telemeter magnetic tapes was accomplished by the Data Reduction Center, MSC Houston Texas. The data consist of time history plots and tabulations, band pass and bi-level tabulations, memory readout listings, and turbine speed, velocity meter, and vehicle time tabulations. Radar tracking data was obtained from the AFETR tracking stations for the ascent phase and from the Manned Space Flight Network for the orbital phase.

3.1 STRUCTURES

This section includes discussions of structural dynamics, launch wind environment, analyses of separation events, and evaluations of acceleration, pressure, and temperature flight data.

3.1.1 Structural Dynamics

Prior to launch of the vehicle 5003, several soundings of the ascent wind environment were analyzed to determine its effect on structural loading of the vehicle and on engine controllability. The results of these investigations are given in par. 3.1.2.

Five accelerometers were installed in vehicle 5003 for measurement of flight structural responses. These instruments – designated as A4, A5, A9, A522 and A523 – were located in the target docking adapter (TDA) and on the Agena aft rack as shown in Fig. 3-1. Table 3-1 provides data describing the functional limitations on these instruments which must be considered when interpreting the flight data.

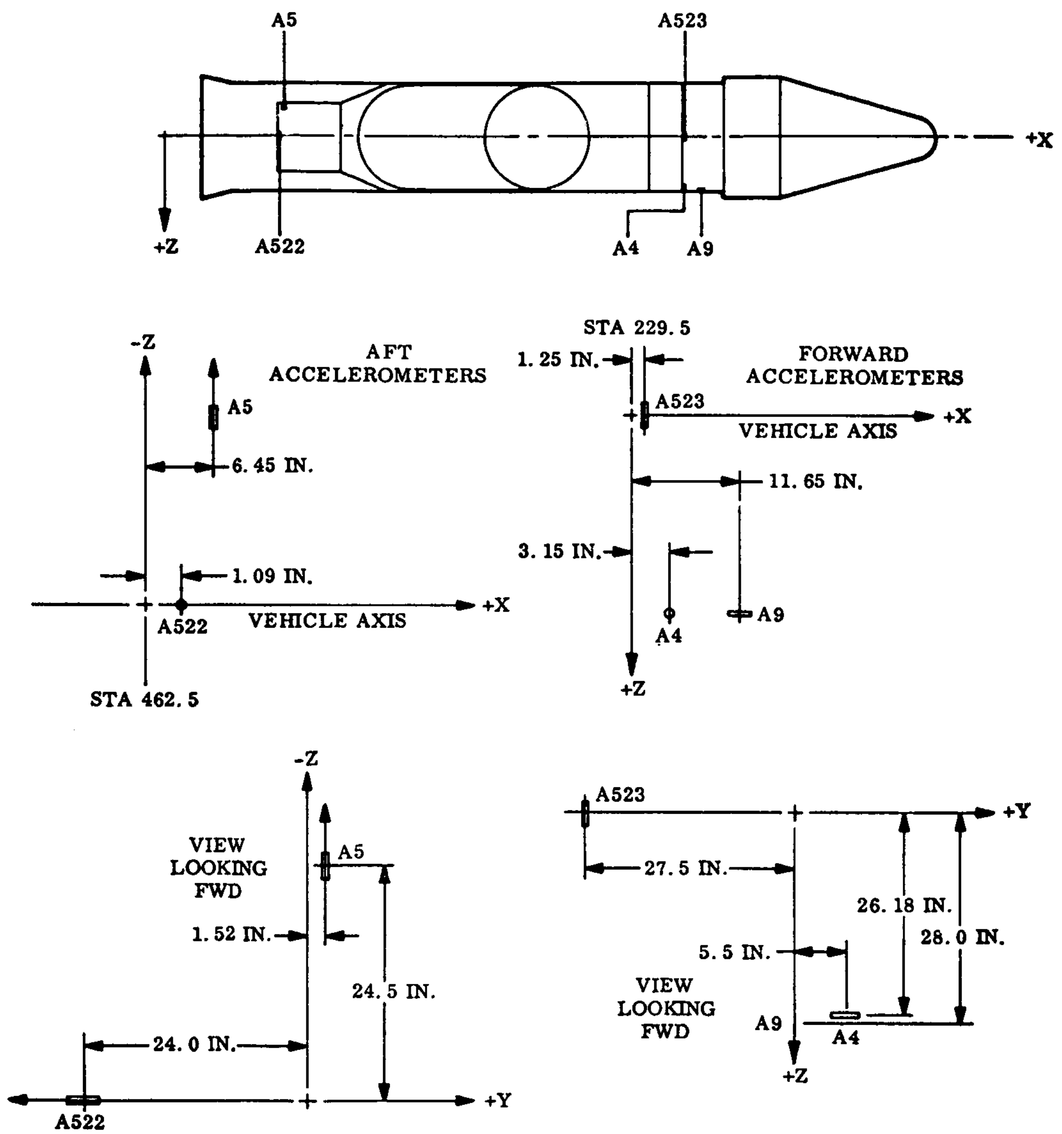

Fig. 3-1 Accelerometer Locations

Table 3-1

DESCRIPTION OF FLIGHT ACCELEROMETERS

Accelerometer Description				Associated Telemetry			Location	
					Polarity			
Transducer	Axis	Range (g)	Sensitivity* (cps)	Pulse Commutation Rate (samples/sec)	Range Limits (g)	Calibration Limits (volts)	LMSC Station	Area & Orientation
A523	Z	±1.5	0-150	32	+1.5 -1.5	5 0	228.25	TDA, Tangential
A4	Y	±1.5	0-150	32	+1.5 -1.5	5 0	226.35	TDA, Tangential
A522	Y	±5.0	0-320	64	+3.5 -3.5	0 5	461.41	Aft Rack, Lateral
A5	Z	±5.0	0-320	64	+3.5 -3.5	0 5	456.05	Aft Rack, Lateral
A9	X	±3.0	0-200	64	+3.0 -3.0	5 0	217.85	TDA, Axial

*±5% at 78° F.

Although the sensitivity of the instruments extends to more than 150 cps, the maximum readable response frequency is limited to about 6 cps and 12 cps by the telemetry sampling rates of 32 and 64 sps, respectively. This restricts the usefulness of the instrumentation to events in which rigid body motions or first body bending modes at frequencies less than 12 cps provide the dominant accelerations. Such phenomena would include on-orbit maneuvers, propellant slosh, and body bending of the docked spacecraft and Agena.

In par. 3.1.3 the flight events for which accelerometer activity was recorded are discussed in terms of (a) how the instruments performed, (b) what levels were recorded, and (c) interpretation of the data.

3.1.1.1 Launch Wind Environment. The wind environment was monitored during the Gemini VIII prelaunch period starting with a forecast for the time of launch that was made two days prior to the launch and continuing at intervals with rawinsonde wind data until the final sounding balloon was released at 1511 GMT on the day of launch. Figures 3-2 and 3-3 present three wind velocity profiles and the corresponding wind azimuths as a function of altitude; these profiles were measured by balloons released at approximately 5 hr, 3 hr, and 15 min before launch. As indicated by the relative shape of these profiles, the winds were relatively stable over this 5-hr period prior to launch.

To determine the effect of the wind environment on the structural and control capabilities of the total vehicle, each profile was used as an input to a 6 deg-of-freedom rigid body simulation of the ascent flight of the GATV. This digital computer simulation together with elastic gust contribution then defined the total vehicle response to the wind perturbations and provided a measure of the structural and control capability utilized. The winds measured by the balloon released just prior to liftoff are the most significant to the postflight analysis. The computer analysis of this profile indicated that the winds aloft would not create a loading or a control critical situation. The actual percentages of structural and control limit capability required in response to this wind were 45 and 26 percent, respectively.

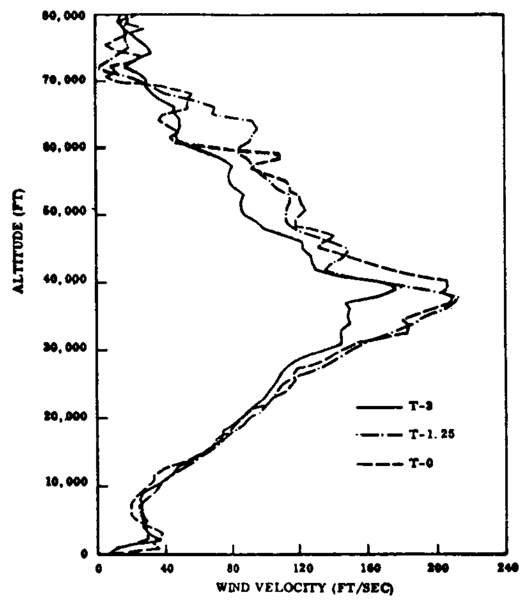

Fig. 3-2 Wind Velocity Profiles

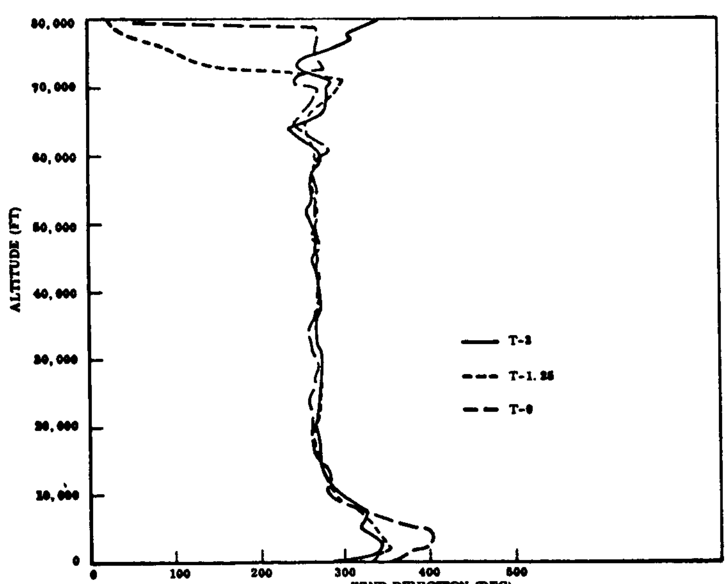

Fig. 3-3 Wind Direction Time History

3.1.1.2 Accelerometer Data. The events for which accelerometer activity was recorded and the data produced during each event are discussed below.

Ascent. The behavior of the flight accelerometers during ascent is summarized in Table 3-2. The scattering of sampled levels taken by the PCM telemetry is very similar to the ascent data of 5002. The only anomaly during this flight phase was the loss of the Z-axis (tangential) accelerometer, A523, for about one minute during the sustainer burn period. The other four transducers operated normally at this time and, when A523 recovered signal, it operated satisfactorily for the rest of the mission. No explanation for this behavior is available at this time. Much of the operation of the accelerometers is out of band during ascent, especially where the high frequency excitations are most prominent. Spike amplitudes, noted in some cases for various flight events, are not true maximum values because the sampling rate does not allow the true peak to be determined for high-frequency transients.

Agena PPS Firings. Table 3-2 provides a summary of accelerometer data for launch, ascent, and first Agena PPS burn. The average values for all nine burns are supplied in Table 3-3. The vibration levels are shown in terms of the maximum observed peaks during the burn period (max), and by the most frequently attained peaks during the burn period (avg.). The levels appear to be normal.

During Agena first burn some propellant slosh, varying in frequency from 0.7 cps to 2.0 cps, was noted. This is summarized in Fig. 3-4, which shows the estimated variation in lateral accelerations experienced due to the slosh motion. Although the g-levels are on the high side, slosh such as this has been noted before on other flights and is not considered to be an abnormality.

Docking. During the docking phase little readable activity was noted on the X-axis accelerometer A9. Some lateral pitching motion at about 1-cps frequency was noted, but was of short duration. The peak value was estimated to be about 0.2 g. This could be attributed to an unrigidized bending of the docked vehicles at the joint or some

Table 3-2

FLIGHT ACCELEROMETERS
ASCENT

Event	t Seconds From Liftoff	Transducer Performance				
		A523	A4	A522	A5	A9
Liftoff	0-5	Out of Band Vibration		Noisy But Not Out of Band		
Maximum Aerodynamic Pressures	31-74	Out of Band Vibration		Noisy But Not Out of Band		Steady Out of Band
MECO	129.8	Spike 1.0g	Spike 0.7g	Little Activity	Little Activity	Drops to Steady 1.2g
MESEP	132.8	Loss of Signal 2.0 sec	Loss of Signal 2.0 sec	Loss of Signal 2.0 sec	Loss of Signal 2.0 sec	Loss of Signal 2.0 sec
Channel Loss	140.9-201.8	Signal Went to Zero Volts	Normal	Normal	Normal	Normal
SECO	283.7	Vibration Decreases From ±0.1g to Zero	Vibration Decreases From ± 0.1g	No Activity	No Activity	Drops from Out of Band to 0.1g bias
VECO + H/S Doors	303.9	Spike Out of Band	Spike Out of Band	Spike 0.4g Peak	No Activity	Spike Out of Band
Separation	308.3	Spike 0.8g	Spike Out of Band	Spike Out of Band & Noisy	Spike Out of Band & Noisy	Spike 0.3g
Agena First Ignition	377.1	Spike 0.65g	Spike 0.6g	Slight Spike 2.3g	Spike 2.5g	Jump to 1g steady, Little O-Shoot
Shroud Separation	386.7	Spike Out of Band	Spike Out of Band	No Activity	No Activity	Spike Out of Band
Agena First Cutoff	560.4	Zero Bias	0.18g bias	-0.1g bias	Zero bias	From 2.2g Steady to Bias = +0.1g

Table 3-3

FLIGHT ACCELEROMETERS
AGENA PPS BURN

Transducer	Condition Before Burn	Vibration Excursions During Burn	Condition After Burn
A523 Z (TDA)	Bias ≈0.1g	Max* ±0.5g Nom ±0.2g Slosh: 0.1g @ 2 cps**	Same as Before Burn
A4 Y (TDA)	Bias ≈0.1g	Max ±.3 Nom ±.15 Slosh: 0.2 to 0.1g @ 2 cps	Same as Before Burn
A522 Y (AFT)	Bias ≈0.1g	Max ±3.0g Nom ±2.0g Slosh: Not readable	Same as Before Burn
A5 Z (AFT)	Bias ≈0.2g	Max ±2.0g Nom ±1.0g Slosh: Not Readable	Same as Before Burn
A9 X (TDA)	Bias ≈0.1g	Nom ±0.1g	Same as Before Burn

Values given here are averages for all nine burns. Little variation was noted from burn to burn.

---

*Max – Maximum Peaks Noted
Nom – Most Frequently Occurring Peaks
**Applies to first burn only. Some hints of low level slosh were noted during other burns but was not a pronounced response.

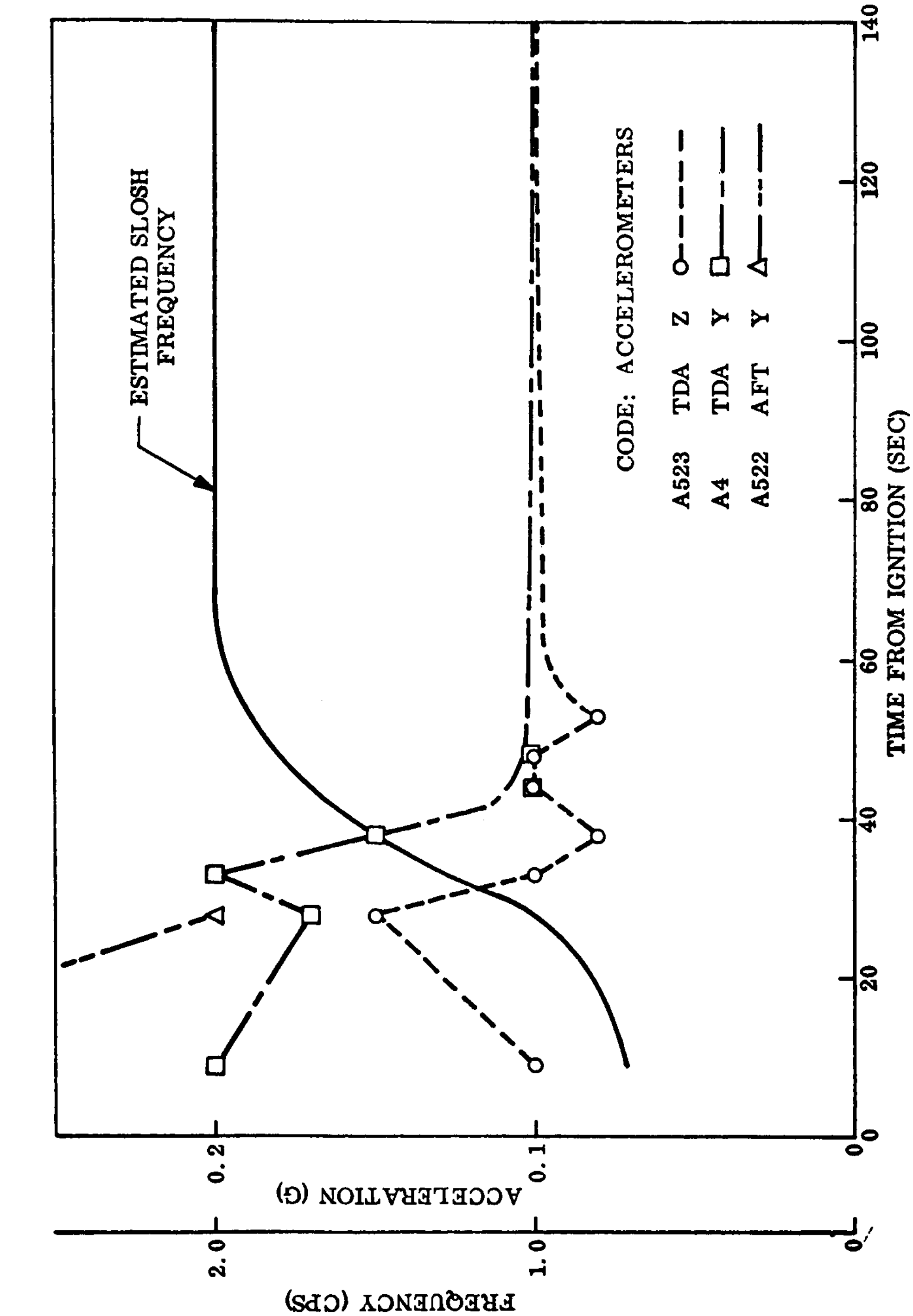

Fig. 3-4 Propellant Slosh Accelerations at Agena First Ignition and Burn (Estimated)

transient inertial loading caused by disorientation of Agena PPS propellants. After docking, no other instrument activity of significance was noted except for infrequent pips produced on aft rack instruments A5 and A522 caused by firing of the attitude control jets.

Agena SPS Firings, 200-Pound Thrusters. Vibration levels noted during the two firings of the SPS modules indicated no abnormal levels for the duration of either burn.

3.1.2 Atlas-Agena Separation and Nose Cone Separation

Both separations occurred as programmed (ref. Sequence of Events); however, uneven stepping of the Atlas/GATV separation switches was indicated on measurement A14, Atlas/Agena Separation Monitor. This same anomaly occurred on the separation of GATV 5002, and was reported as an apparent voltage problem.

The Atlas/Agena separation monitor A14 is an installation that consists of 3 tabs on the booster adapter at 216° radially. Longitudinal location is at Sta. 392.0, 422.0, and 452.0, or 30.0 inch equal spacing. The booster adapter must move 10 inches before it contacts the first switch, which is mounted at Station 462.5 on the Agena aft rack. The voltage levels should step at 1.25 volts for each of three steps to a total of 3.75 volts for the complete separation. The data showed a first step of 4.3v and the remainder went out-of-band. Subsequent examination and tests revealed that when the finger, which is mounted on the adapter, trips the switch arm, the arm oscillates and actuates the switch several times rather than once. Numerous actuaation tests were performed which substantiated the observed results.

A switch configuration change to eliminate the anomalous capacitor readings has been accomplished. A change-switch configuration change (EJA 545-40125-1 Gemini/Agena Separation Monitor Modification for vehicles 5001-5004 and up) installs a sheet metal, slotted bracket on the switch, which serves to dampen the oscillations of the long switch arm.

3.1.3 Thermodynamics

3.1.3.1 Launch and Ascent. No thermal problems were evident in the launch and ascent phase of GATV 5003. The maximum temperatures indicated by the data were in all cases lower than the corresponding design temperatures. The flight velocity and altitude data were generated from tracking data obtained from the General Electric Company. The flight data indicated the vehicle flew a trajectory with essentially the same altitudes as the reference trajectory. The data also indicated the vehicle had higher velocities than the reference trajectory through BECO, but lower velocities after BECO. The overall thermal severity of the GATV radar trajectory was less than that of the design trajectory.

The location, type, and range of the skin temperature instrumentation employed on the Agena are presented in Table 3-4. One resistance thermometer was located on the inner surface of the Agena horizon sensor fairing. Seven semiconductors were mounted on the skin of the docking adapter in order to observe the heating effects of flow separation aft of the shroud/docking adapter interface. Six resistance thermometers were mounted on the inner surface of the fiberglass shroud.

The temperature histories presented (Figs. 3-5 through 3-10) are curves faired through the data obtained from Houston MSC. Also presented in each figure is the corresponding design temperature. For all measurements, the liftoff temperatures were consistent with the accuracy of the data (Fig. 3-5).

The temperature response of measurement A210 (Fig. 3-6) was similar to that obtained in this area on other vehicles. There was a loss of signal at approximately 305 sec after liftoff, apparently due to the jettison of the fairing. The maximum temperature of 535° F indicated is lower than the Agena design temperature of 850° F for the fairing.

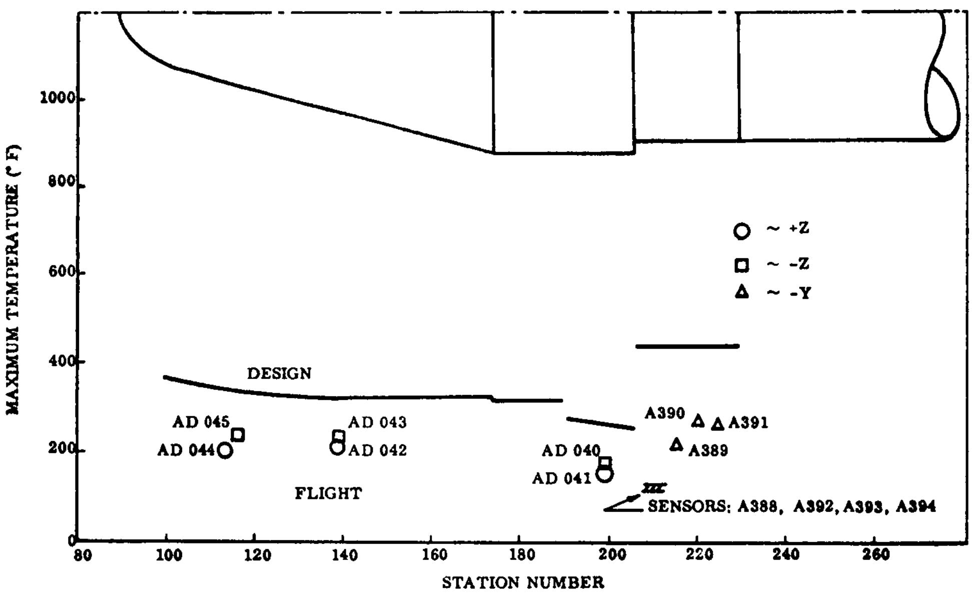

Fig. 3-5 Maximum Ascent Temperatures

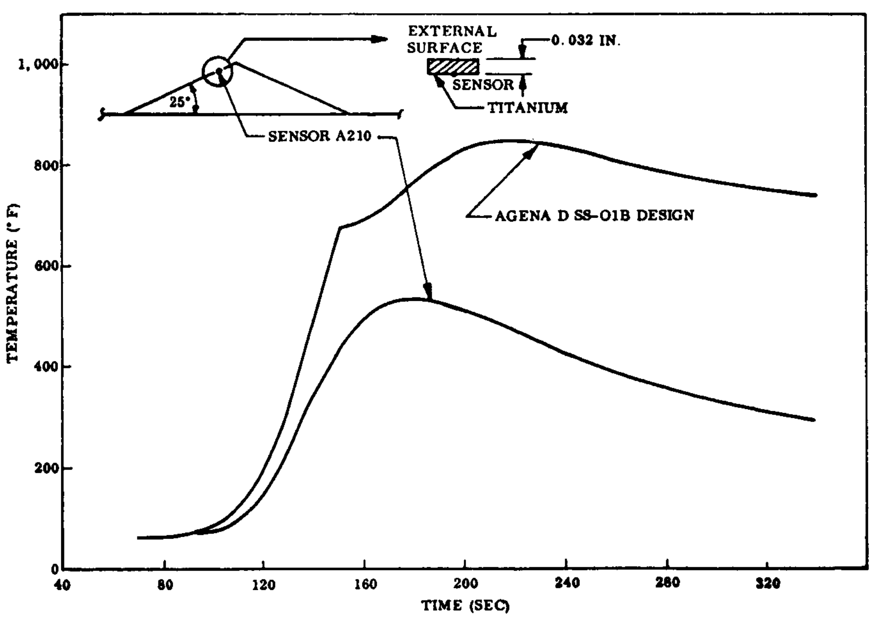

Fig. 3-6 Ascent Temperature Histories on Horizon Sensor Fairing

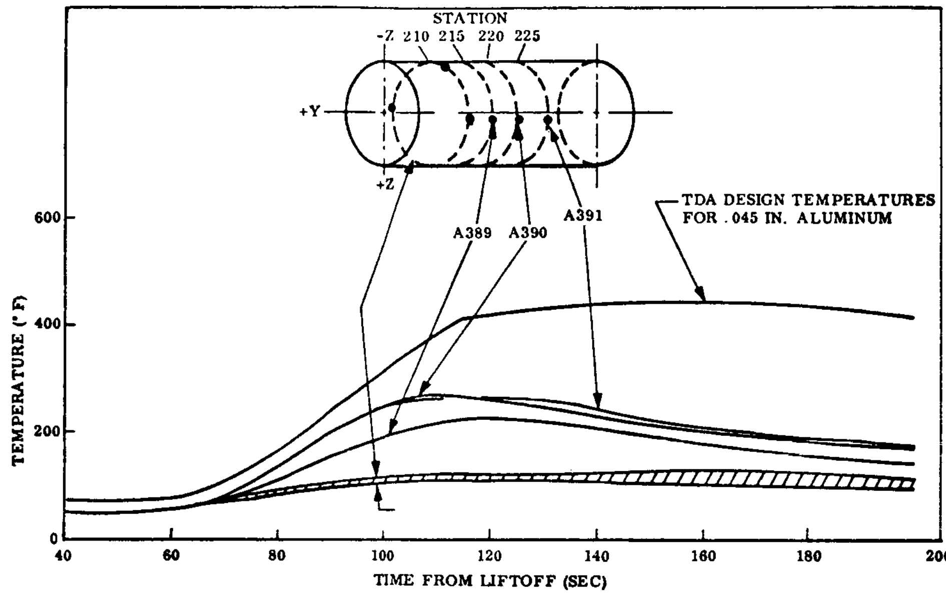

Fig. 3-7 Temperature vs. Time From Liftoff, Measurements A388 Through A394

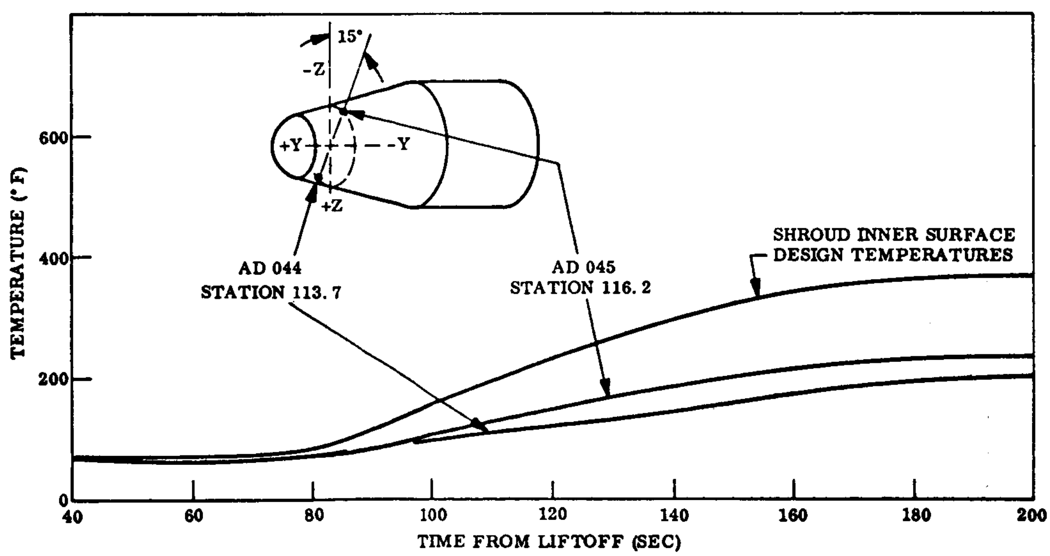

Fig. 3-8 Temperature vs. Time From Liftoff, Measurements AD044 and AD045

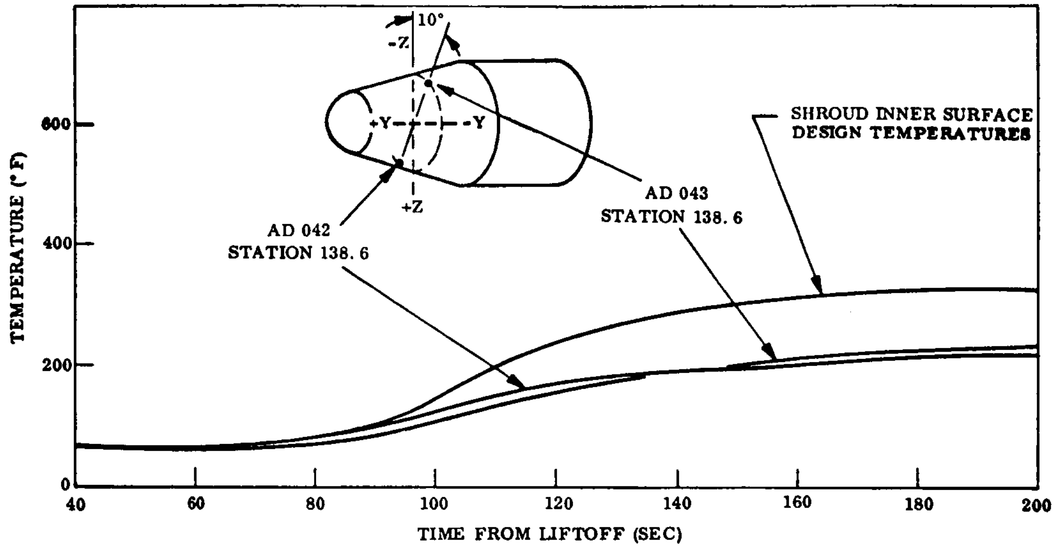

Fig. 3-9 Temperature vs. Time From Liftoff, Measurements AD042 and AD043

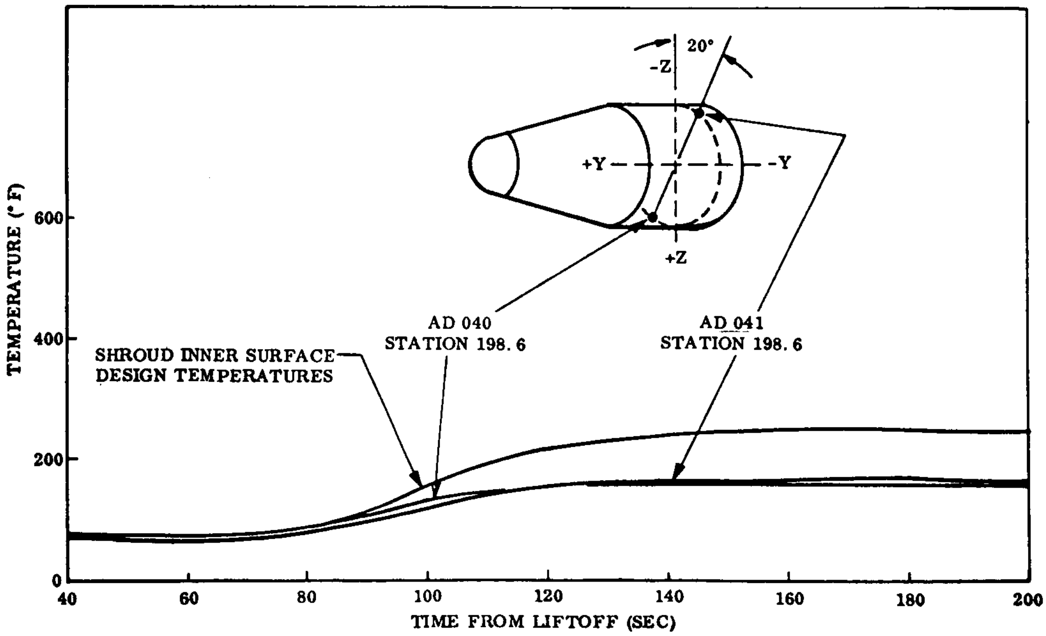

Fig. 3-10 Temperature vs. Time From Liftoff, Measurements AD040 and AD041

Table 3-4

SKIN TEMPERATURE INSTRUMENTATION

Meas. No.	Location (Sta. No.)	Type*	Range No.	Quad.	Angular Position
A210	Horizon Sensor Fairing, 260	A	+32 to +600	II	43° to +y
A388	Docking Adapter, 210	B	-100 to +500	III	13° to -y
A389	Docking Adapter, 215	B	-100 to +500	III	13° to -y
A390	Docking Adapter, 220	B	-100 to +500	III	13° to -y
A391	Docking Adapter, 225	B	-100 to +500	III	13° to -y
A392	Docking Adapter, 210	B	-100 to +500	II	17° to +z
A393	Docking Adapter, 210	B	-100 to +500	I	13° to +y
A394	Docking Adapter, 210	B	-100 to +500	IV	17° to -z
AD40	Shroud Cylinder, 198.6	A	0 to +450	II	20° to +z
AD41	Shroud Cylinder, 198.6	A	0 to +450	IV	20° to -z
AD42	Shroud Cone, 138.6	A	0 to +300	II	10° to +z
AD43	Shroud Cone, 138.6	A	0 to +300	IV	10° to -z
AD44	Shroud Cone, 113.7	A	0 to +400	II	10° to +z
AD45	Shroud Cone, 116.2	A	0 to +400	IV	10° to -z

*A – resistance thermometer
B – semiconductor

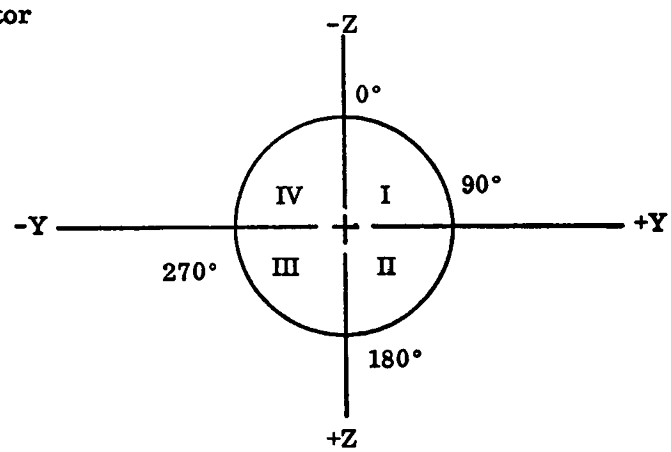

The temperature history for measurements A388, A392, A393, and A394 (Fig. 3-7) is a band faired through the MSC data. Due to boundary layer separation at the shroud/docking adapter interface, the heating to the vehicle in the area of these four sensors is less than at points downstream where the flow has reattached. The maximum temperature of 128° F indicated by the data is well below the design temperature of 440° F, based on the assumption of attached flow.

The temperature histories for measurements A389, A390, and A391 are also presented in Fig. 3-7. These three measurements are located in a line aft of the shroud/docking adapter interface. The data indicate the heating effects of flow separation and reattachment. The maximum temperature of 225° F, 270° F, and 265° F for A389, A390, and A391, respectively, are below the design temperature limit of 440° F in the area.

The temperature response of measurements AD040 through AD045 on the fiberglass shroud are presented in Figures 3-8, 3-9, and 3-10. Also presented, for comparison, are the inner surface design temperatures at the corresponding three locations. The maximum temperatures indicated by the data are in all cases lower than the design temperature.

3.1.3.2 Orbit. Flight data received through revolution 45 indicate that all critical equipment and structure remained within acceptable limits (Table C-1, Appendix C). Equipment temperatures in the two forward equipment racks were very close to those predicted, with the exception of the two transponders which were operated continuously, rather than the 28 percent duty cycle assumed for analysis. The temperature experienced by the propellant tanks also agreed with predictions. Temperatures of equipment and structure in the aft rack appeared to be in the high range of the analytical predictions, but were still well within acceptable limits. The preliminary conclusion reached, based on data received to the 45th revolution, is that the thermal effect of the PPS firings caused the aft rack equipment and structure to remain in the upper ranges of the permissible temperatures.

Forward Auxiliary Rack. All equipment located in the forward auxiliary rack remained within temperature limits, as indicated in Fig. 3-11. Also shown in Fig. 3-11 are the predicted temperature extremes for the instrumented equipment for solar incidence(β) angles of -53 deg and 0 deg. Since the first 45 revolutions of the vehicle life were spent at a β angle of approximately -20 deg, it is expected that the vehicle equipment and structural temperatures would fall between those predicted for β angles of -53 deg and 0 deg.

Comparison of temperatures shown on Fig. 3-11 indicates close agreement between flight data and predictions. The Type IC battery temperatures fell slightly below predictions, experiencing temperatures between 45° F and 73° F for the first 45 revolutions, well within the 30° F to 100° F temperature limits. Time-temperature histories for all the batteries are shown on Fig. 3-12 for the first 45 revolutions of the mission.

Temperature data for Transmitter No. 1 shows higher temperatures than predicted, because of the use of longer operating periods than were assumed in the analyses of the equipment rack. Transmitter No. 2 data shows slightly lower temperatures than predicted; a lower duty cycle was used than that assumed in the analyses. Exact duty cycles are not available at this time.

Forward Rack. The temperature data for the forward rack show all equipment remained within acceptable temperature ranges (Fig. 3-13). Type IC battery temperatures fell within the predicted ranges (Fig. 3-12). There was no indication that instrumented guidance equipment case temperatures exceeded acceptable limits, since no temperature-controlled ovens exceeded their set points. This was the first vehicle in which the velocity meter system was operated 100 percent of the time; the oven operating temperature ranges indicate an acceptable thermal design for this system.

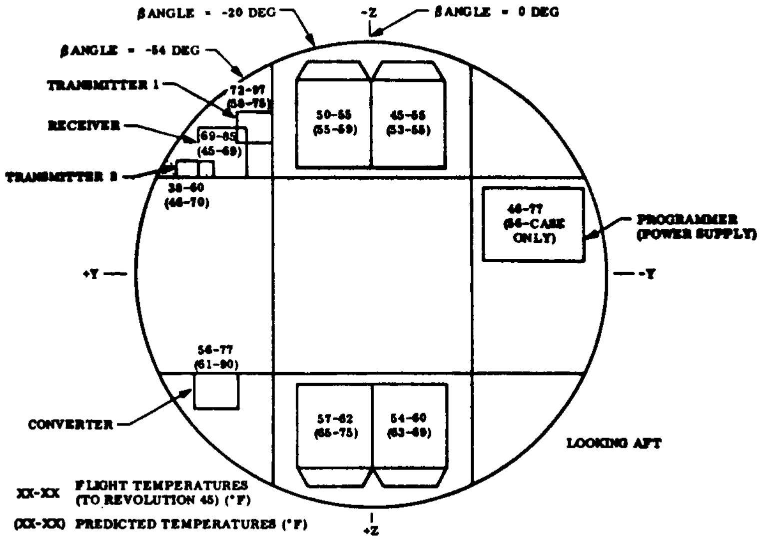

Fig. 3-11 Actual vs. Predicted Temperatures of Equipment in the Auxiliary Forward Rack

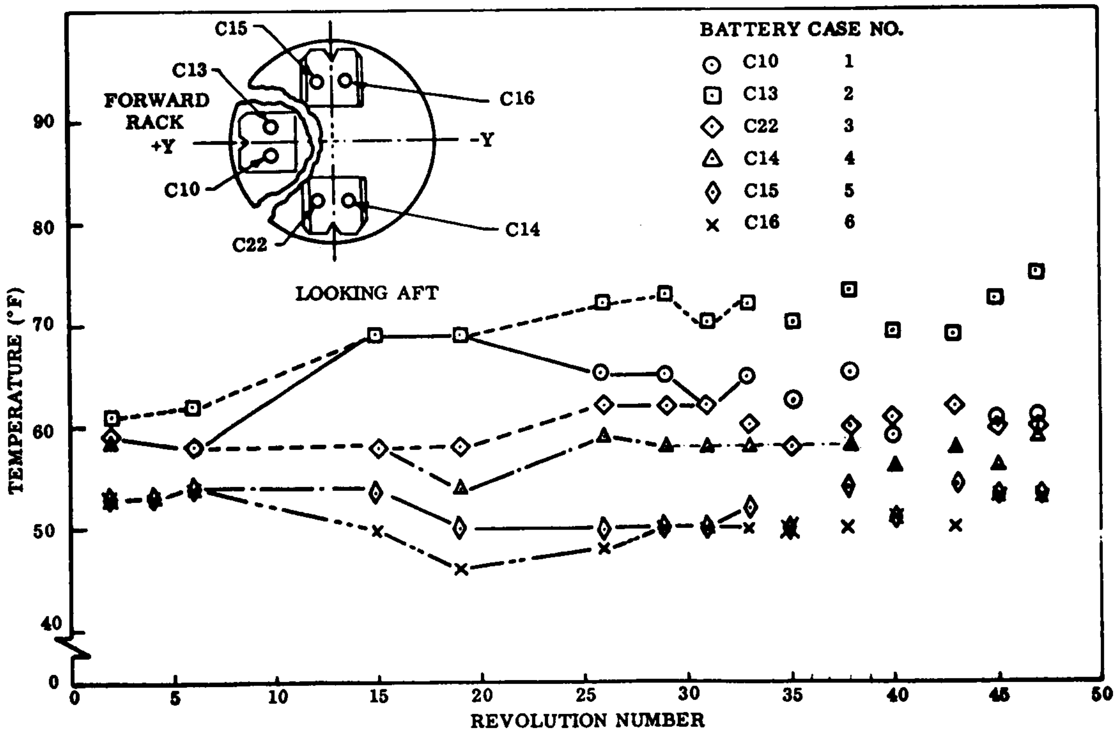

Fig. 3-12 Battery Temperature Data

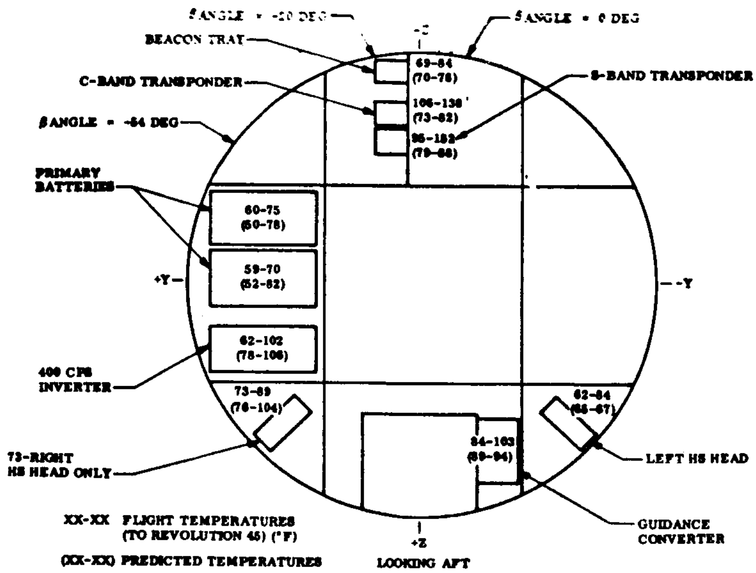

Fig. 3-13 Actual vs Predicted Temperatures of Equipment in the Forward Rack

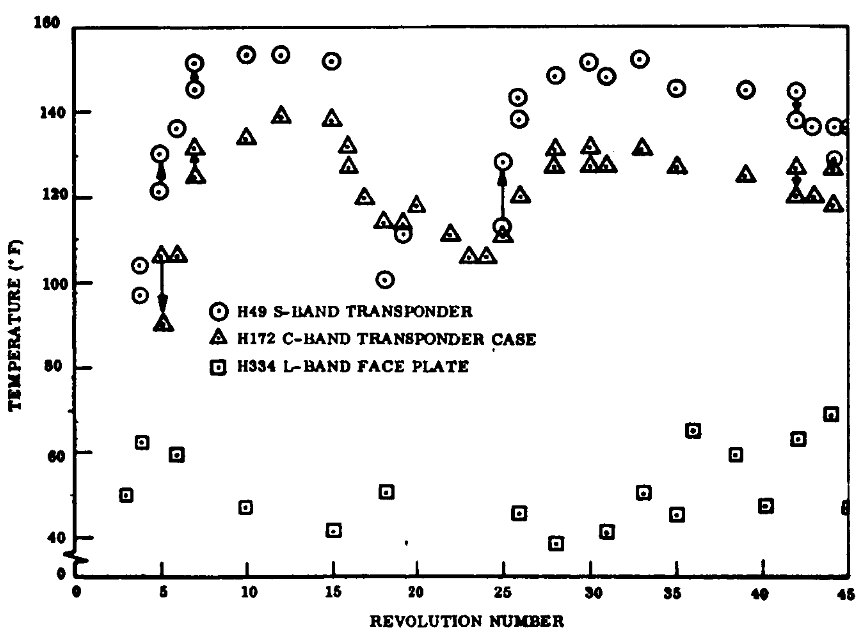

Fig. 3-14 Transponder Temperature Data

The C-band transponder and S-band transponder temperatures exceeded analytical predictions by 35° F to 60° F during the 45 revolutions (Fig. 3-14). Analytical predictions were based on a 28 percent duty cycle during each orbit for both transponders. During the mission, transponders were operated 100 percent of the time during those orbits they were turned on, causing their temperatures to rise above the predicted range. The drop in temperature near the fifteenth revolution occurred when the S-band transponder was turned off until about the twenty-fifth orbit when it was turned on. However, even with the 100-percent duty cycle, neither the transponders nor nearby equipment exceeded their temperature limits.

Propellant Tanks. Thermal flight data for the PPS propellant tanks are shown in a time-temperature history on Fig. 3-15 for the first 45 revolutions. The propellant tank temperatures ranged from 45° F to 70° F for this part of the mission. The PPS pump inlet temperatures recorded during PPS firing are also shown on Fig. 3-15. The temperatures of the propellants flowing to the engine during the PPS firings agree with the tank skin measurements in most cases. In the case of the 1.77-sec firing, the propellant flow probably was not long enough to bring the probe down to the actual propellant temperature. Furthermore, the probe was still warm from the previous firing which lasted 20 sec.

Aft Rack. Flight data received through revolution 45 indicate that all aft rack equipment and structure remained within the expected temperature ranges. Time-temperature history plots of the flight data received are shown in Figs. 3-16 through 3-22.

The data shown in Figs. 3-16 and 3-17 indicate that the SPS propellant tanks experienced temperatures near the upper limits and are above the on-orbit steady state predicted temperature ranges. However, the temperatures generally drop (Fig. 3-17) by Revolution 45. It is believed that the high temperatures result from heat soak resulting from the frequency and duration of the PPS firings during the first 45 revolutions. Other data discussed below seem to substantiate this theory. It is expected that data beyond the 45th revolution will confirm this assumption.

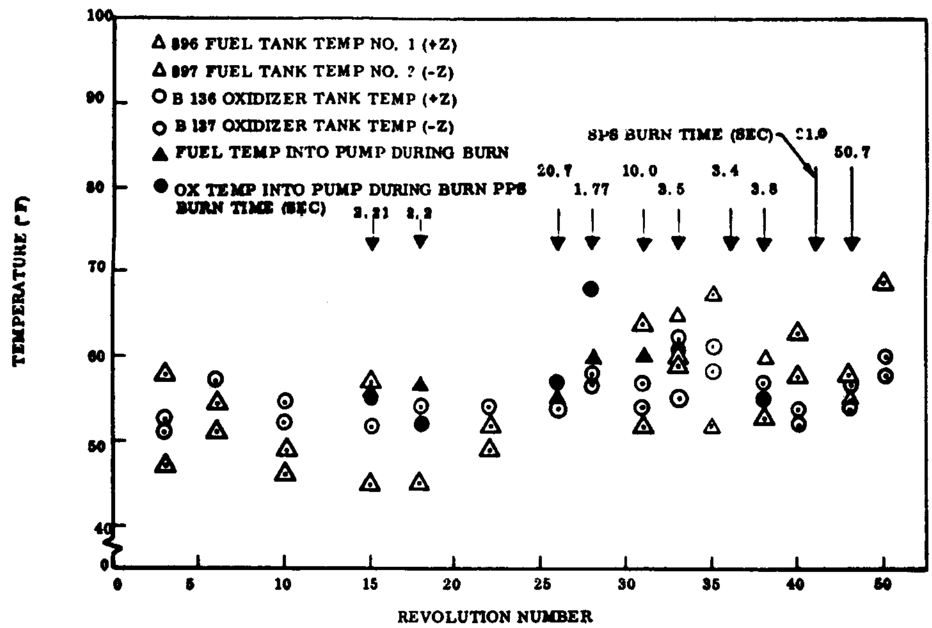

Fig. 3-15 PPS Propellant Tank Temperatures

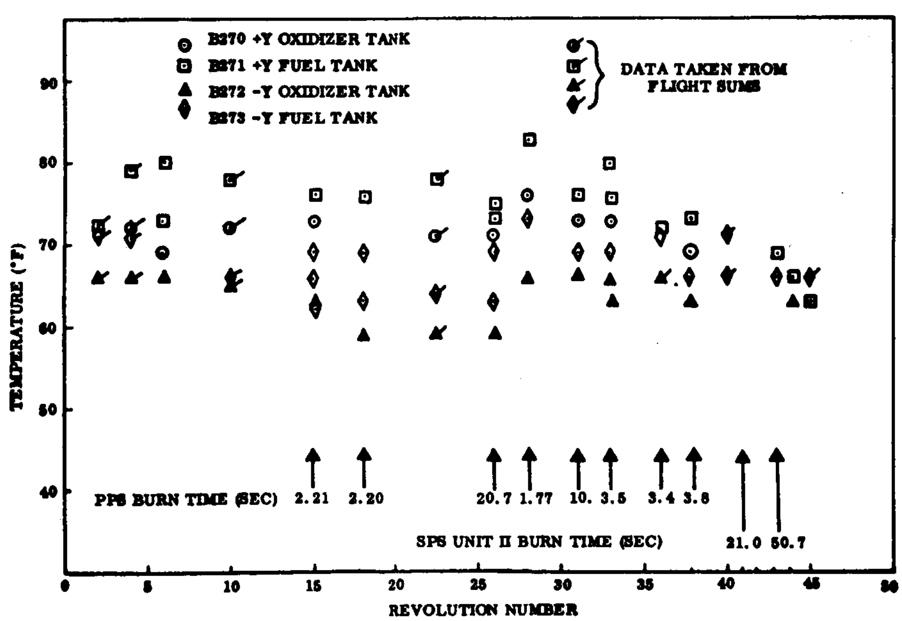

Fig. 3-16 SPS Propellant Tank Temperatures

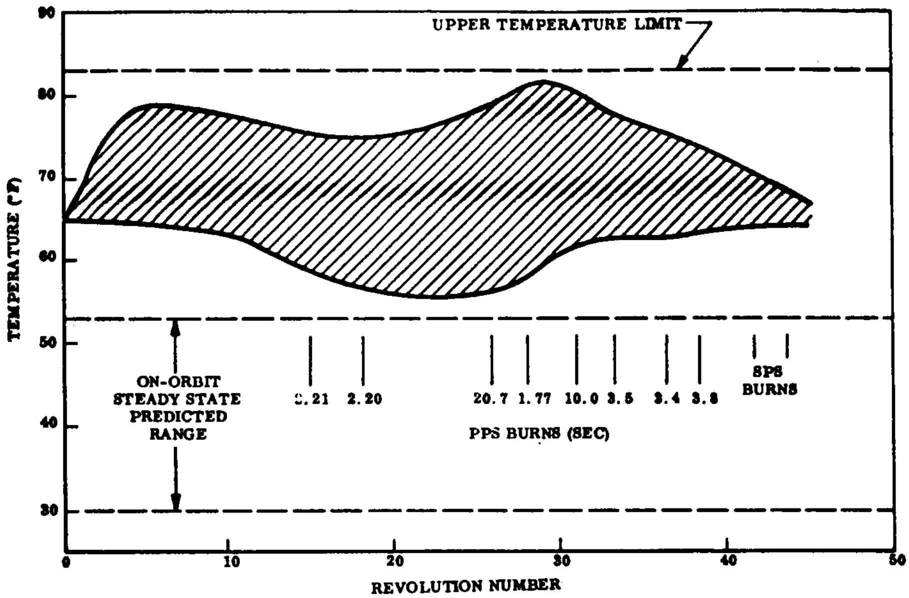

Fig. 3-17 SPS Propellant Tank Temperatures vs Steady State Predictions

Temperature data for the PPS start tanks are shown in Figs. 3-18 and 3-19. These tanks respond more rapidly to disturbing thermal influences than the SPS propellant tanks. The data show a definite correlation between temperature fluctuations and PPS engine firing time. After the ascent burn (182 sec), the PPS start tank temperatures increased due to the thermal effects of the firing and after several orbits decayed to within predicted ranges of 36°F to 47°F. This is shown most clearly in Fig. 3-19. After the 20-sec PPS firing, these temperatures again increased sharply and then fell again. The same temperature pattern occurred after the 10-sec burn, after which there were three shorter PPS firings. By the forty-fifth orbit, the temperatures had again decayed into the predicted range.

Similar time-temperature history patterns can be seen in the flight data for the SPS bipropellant valves (Fig. 3-20), for the PPS propellant pump inlet probes (Fig. 3-21). The same pattern is also seen in the shear panel temperature histories shown in Fig. 3-22.

On the basis of the above data, it can be concluded that the aft rack thermal design is satisfactory and that the SPS propellant tanks are experiencing temperatures in the upper regions of the expected temperature ranges due to the influence of the PPS firings.

When flight data are available for later portions of the flight (after the thermal effects of the PPS firings have been dissipated), it will be possible to establish the on-orbit steady state temperatures for the aft rack. These can then be compared with analytical predictions to determine the accuracy of the thermal model and to establish the effect of the PPS firing on the aft rack equipment and structural temperatures.

Attitude control system temperatures (Fig. 3-23) appear normal. During the sixth revolution, considerable quantities of gas were used to restabilize the Agena after the spacecraft anomaly. This is reflected in the very low temperatures recorded during this activity on the sixth orbit.

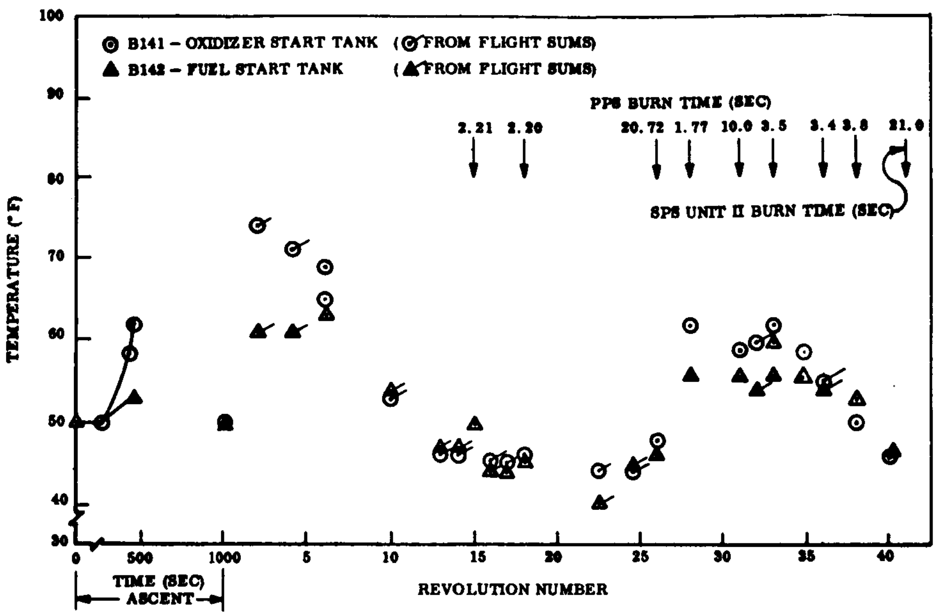

Fig. 3-18 PPS Start Tank Temperatures

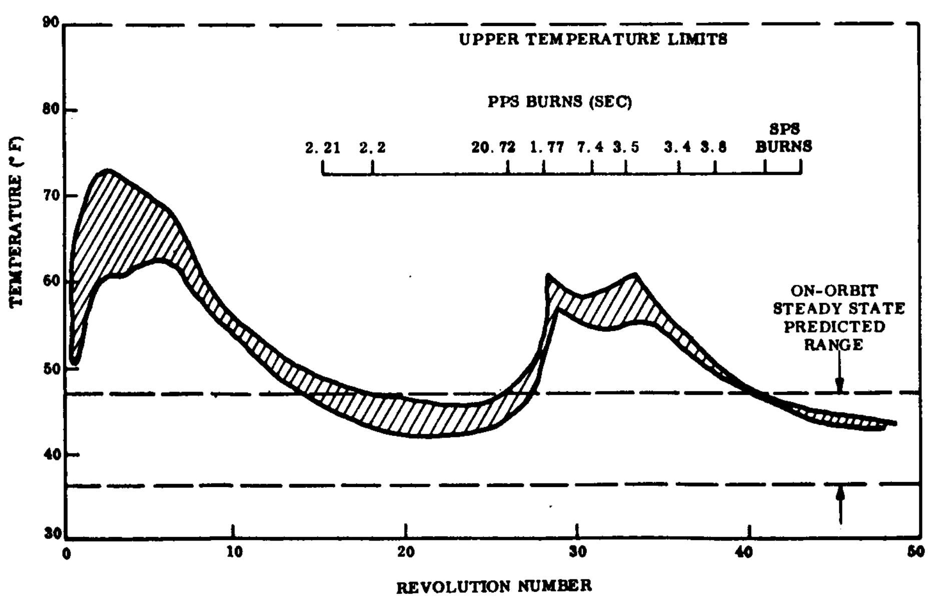

Fig. 3-19 PPS Start Tank Temperatures vs Steady State Predictions

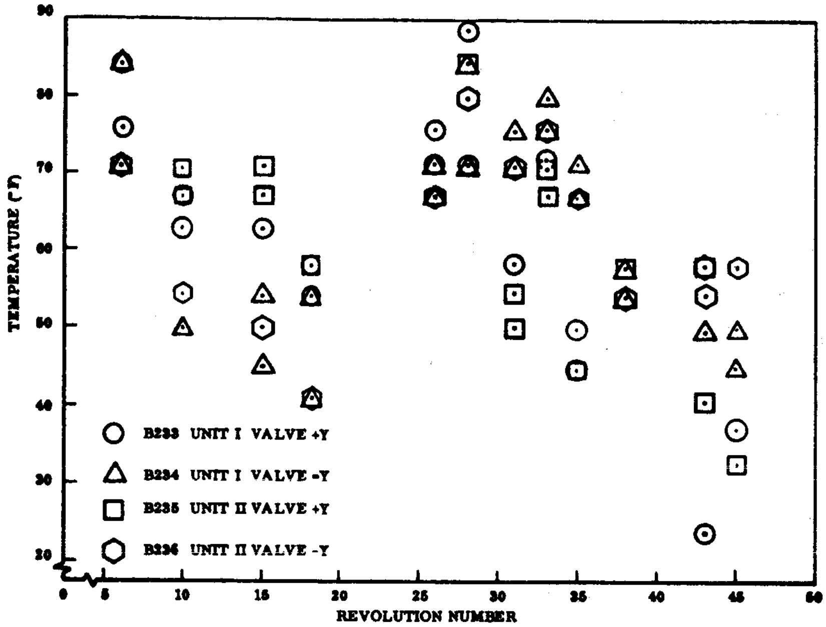

Fig. 3-20 SPS Bipropellant Valve Temperatures

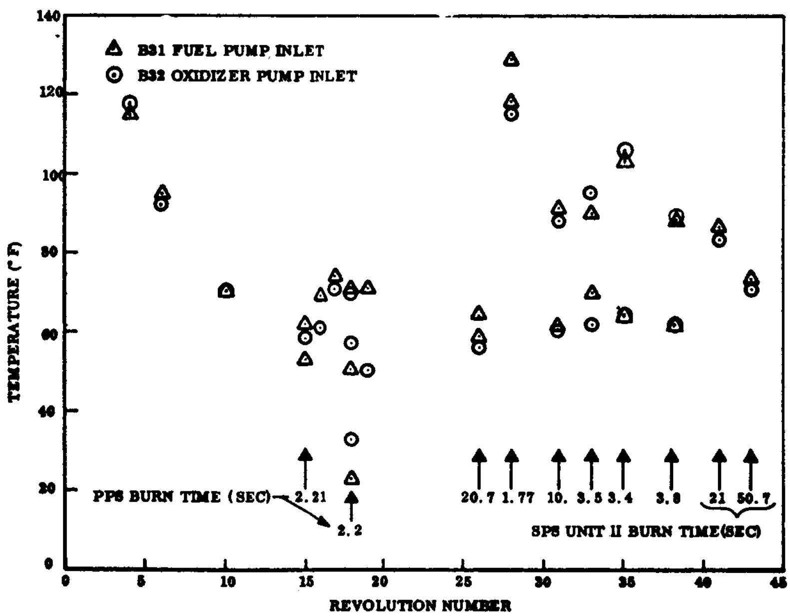

Fig. 3-21 PPS Propellant Pump Inlet Temperatures

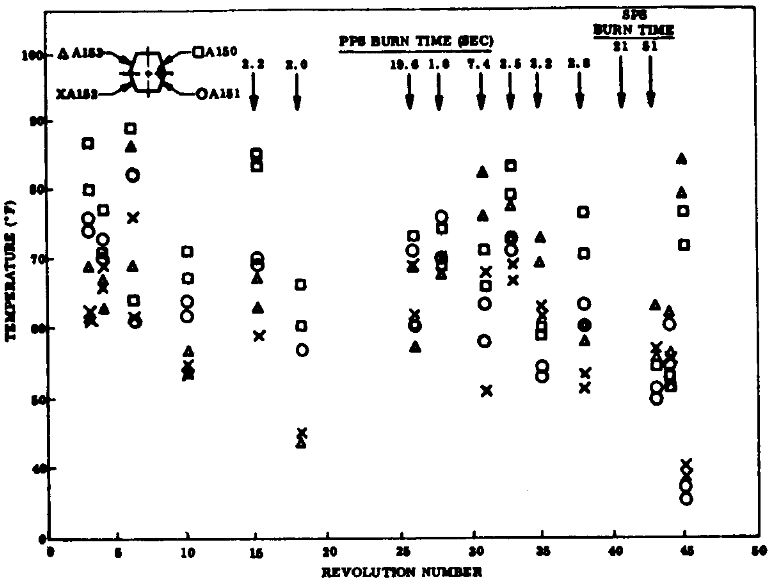

Fig. 3-22 Aft Rack Shear Panel Temperatures

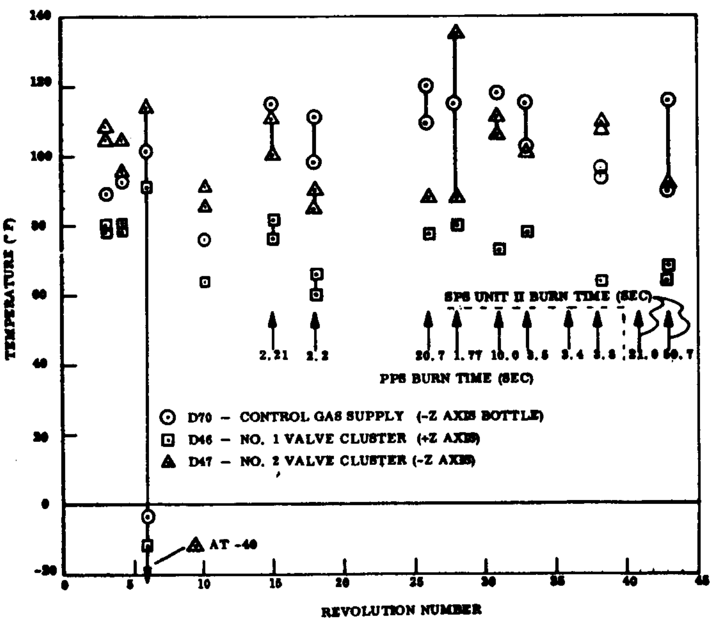

Fig. 3-23 Attitude Control System Temperatures

3.2 SECONDARY PROPULSION SYSTEM

The Model 8250 Secondary Propulsion Systems performed within specification limits, and no design or operational changes are recommended for subsequent flights.

Two operating discrepancies did occur during the flight: (1) the +Y system regulator did not lock-up prior to the Unit I TCA (thrust chamber assembly) ascent burn, and (2) the +Y system Unit II. TCA skin temperature read low on both burns. However, these discrepancies did not affect system performance. The low Unit II TCA skin temperature reading was evaluated as resulting from improper installation, and the regulator, although not locked up prior to the ascent burn, operated satisfactorily on subsequent burns. The overall system performance is summarized in Tables 3-5 and 3-6. The performance numbers presented in Table 3-6 are averages of single time-slices per burn. For the Unit I TCA the specific impulse presented is an average of all nine burns, and for the Unit II TCA it is an average of both burns.

Table 3-5

SPS PERFORMANCE SUMMARY

Number of Burns:	
Unit I	9
Unit II	2
Impulse Delivered (lb-sec)	39,000
Impulse Remaining (lb-sec)	43,000
Propellants Remaining	Approx. 52%
Nitrogen Pressurization Gas Remaining	Approx. 52% (at 2300 psia)

Table 3-6

PERFORMANCE OF SPS UNITS I AND II

Unit I Thrust Chamber Assembly

(Average of Single Time Slices Per Burn)

	+Y		-Y	
	Flight	Predicted	Flight	Predicted
Time to 90% P_C	0.252	0.270	0.226	0.224
I_{SP}	252.5	252.4	248.8	251.1
Thrust				
Ascent	16.34	16.36	16.50	16.48
Steady State Average				
(20-sec oper)	15.94	16.40	16.15	16.48
(70-sec oper)	15.55	16.13	15.79	16.19

Unit II Thrust Chamber Assembly

(Average of Single Time Slice Per Burn

	+Y		-Y	
Time to 90% P_C	0.125	0.148	0.130	0.240
I_{SP}	254.1	255.4	252.6	254.4
Thrust	194.7	196.1	194.0	195.4

The flight values are close to the predicted thrust values which were derived by calculation and an assumption of regulator operating point based on functional test data. Minor deviations between flight and predicted values are noted in the specific discussion for each burn. The two operating discrepancies already noted are discussed first.

- Regulator Lock-Up

  The data indicates that the regulator poppet was off lock-up at the time of the start-valve-on signal, thereafter reacted sluggishly, and did not lock up during the lead period, as expected. The propellant tank pressure was approximately 208 psia at the time of propellant valve opening and kept increasing throughout the burn; it was at 214 psia at shutdown. However, on all subsequent burns, where propellant tank pressure was below minimum predicted for regulator lock-up (211 psia), a pressure rise was noted during the start valve lead period. Since regulator operation data appeared normal for all subsequent operations, the discrepancy is unexplainable. No discrepancy was noted in system performance.

- Low Skin Temperature Reading

  The data indicate that the +Y Unit II TCA operated satisfactorily except for low skin temperature readings. The +Y Unit II TCA operated closer to predicted performance than the -Y TCA. However, the -Y Unit II TCA skin temperature rise followed closely previous data on the chamber, whereas the +Y Unit II TCA skin temperature rise was 200–500°F below that of previous runs on the chamber. Since the +Y Unit II TCA performance was satisfactory, it is presumed that the low skin temperature readings were due to improper installation of the thermocouple.

3.2.1 SPS Burn Number 1 Operation

Burn No. 1 was a 20-sec, Unit I TCA ullage burn prior to main engine operation during ascent. Except for the regulator discrepancy previously discussed, both systems operated satisfactorily. The -Y system had a regulator lock up of 227 psia, which was 2 psi higher than predicted but within the expected regulator operating band. Skin temperatures on both Unit I TCAs were approximately 60° F below predicted, but this is within the range expected. Figure 3-24 presents a few of the operating parameters for both systems and shows normal system reactions; except for the -Y regulator lock-up discrepancy.

3.2.2 SPS Burn Number 2 Operation

Burn No. 2 was a 70-sec Unit I TCA ullage firing (Fig. 3-25). Operation was normal, and performance was within specification limits. Neither regulator indicated a pressure rise during the start valve lead period, but this was to be expected, since propellant tank pressure for both systems was approximately 220 psia prior to start valve actuation. Propellant tank pressures decayed to values below nominal, but were approaching steady-state values. Therefore, it appears that both regulators were operating at approximately minimum expected values for Unit I flow rates.

3.2.3 SPS Burn Number 3 Operation

Burn No. 3 was a 70-sec Unit I TCA ullage firing. Operation was satisfactory, and performance was within specification limits. Both regulators approached nominal lock-up pressure during the start-valve lead period, and propellant tank pressures decayed during the firing to values slightly less than expected. Neither system blew-down sufficiently for regulation to occur. System operating parameters shown in Fig. 3-25 illustrate typical reactions for a 70-sec firing.

3.2.4 SPS Burn No. 4 Operation

Burn No. 4 was a 22-sec Unit I TCA ullage firing. Operation of both systems was satisfactory and performance was nominal. The +Y system experienced a propellant tank pressure rise during the start-valve lead period, but the rise was much less than expected. The +Y regulator appeared to approach lock-up, but the propellant tank pressure rose only to the minimum expected lock-up value, which was 11 psi less than the nominal predicted pressure of 223 psia. The regulator appeared to regulate during the last five sec of the firing, but at a value about 5 psi above the maximum expected value of 204 psia.

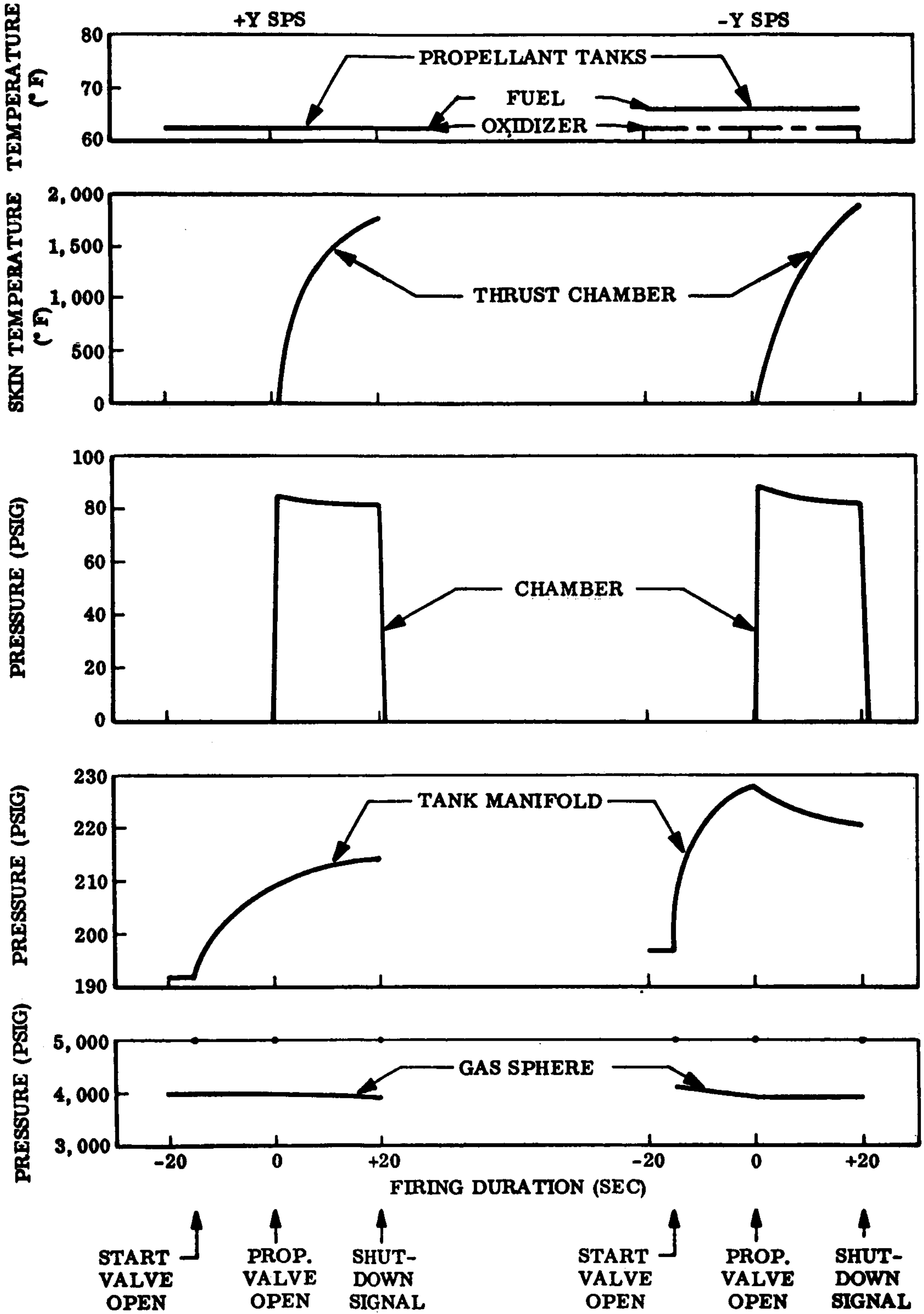

Fig. 3-24 Burn No. 1 Data, SPS Unit I

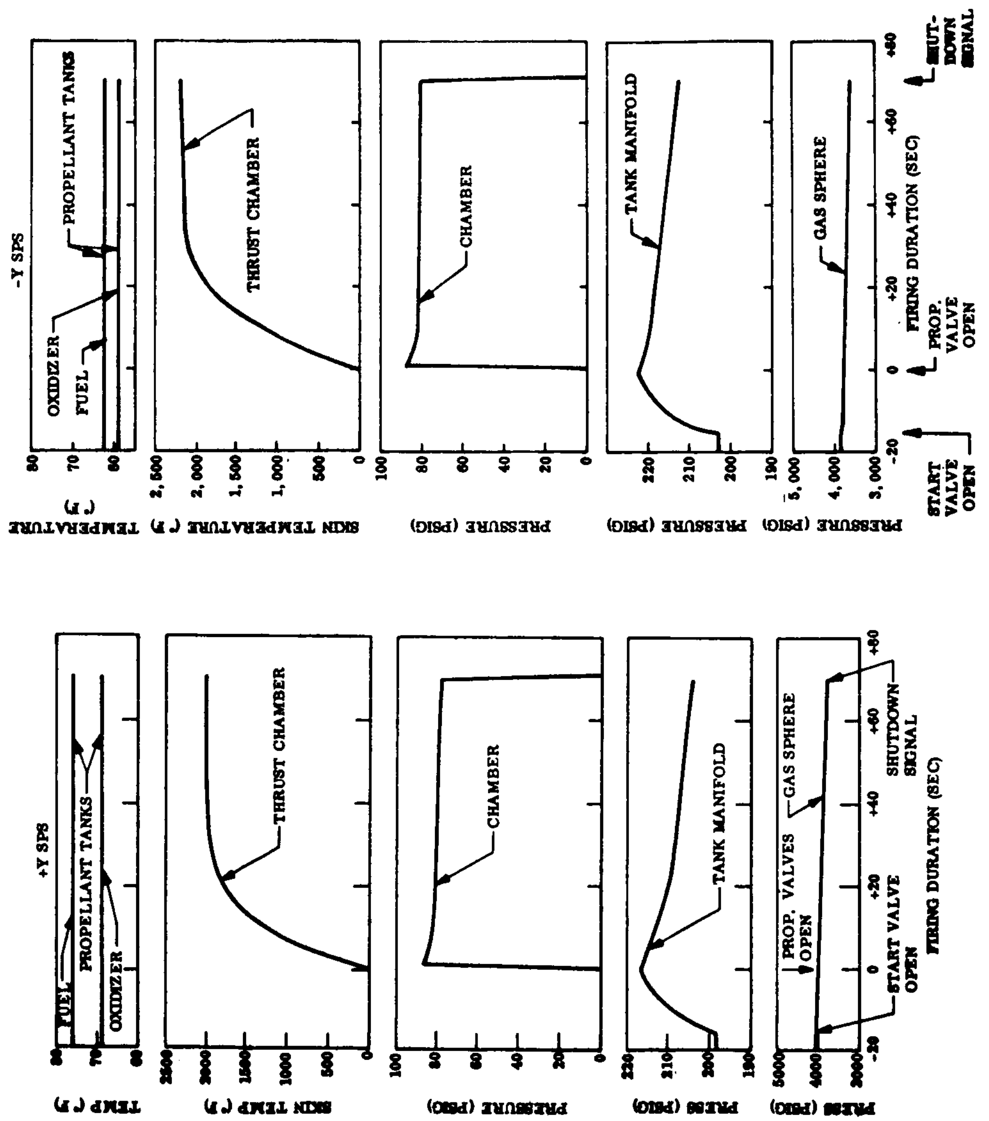

Fig. 3-25 Typical On-Orbit Ullage Burn of 70 Seconds

The -Y system propellant tank pressure did not rise during the start-valve lead period. Since the propellant tank pressure prior to start valve actuation was higher than the minimum expected lock-up pressure, the lack of a pressure rise is not considered to be abnormal.

3.2.5 SPS Burn Number 5 Operation

Burn No. 5, a 70-sec Unit I TCA ullage firing, was satisfactory. Performance data calculations indicate nominal performance. The +Y system did not experience a propellant-tank pressure rise during the start-valve lead period, and the -Y system had a slight rise. However, this is not considered an abnormal operation as propellant tank pressure prior to start valve actuation on both systems was approximately 2 psi above the expected minimum value for regulator lock-up.

3.2.6 SPS Burn Numbers 6 and 7 Operations

Both of these burns were 22-sec Unit I TCA ullage firings. Operation for both systems was satisfactory, and performance was nominal. During Burn No. 6 both systems experienced propellant-tank pressure increases to lock-up pressures within expected limits. During Burn No. 7 neither system had pressure increases during the start-valve lead period but, as mentioned previously, the operation is considered normal because the propellant tank pressures prior to start valve actuation were above expected values for minimum regulator lock-up pressure.

3.2.7 SPS Burn Number 8 Operation

Burn No. 8 was a 22-sec Unit I TCA ullage firing. While operation was satisfactory, the +Y system did indicate a condition similar to that experienced on Burn No. 1. The regulator did not reach the minimum expected lock-up pressure during the start-valve lead period. Also, propellant tank pressure during the run held at a steady 209 psia, which is approximately 5 psi above maximum-expected regulated propellant tank pressure. Data from this burn are presented in Fig. 3-26.

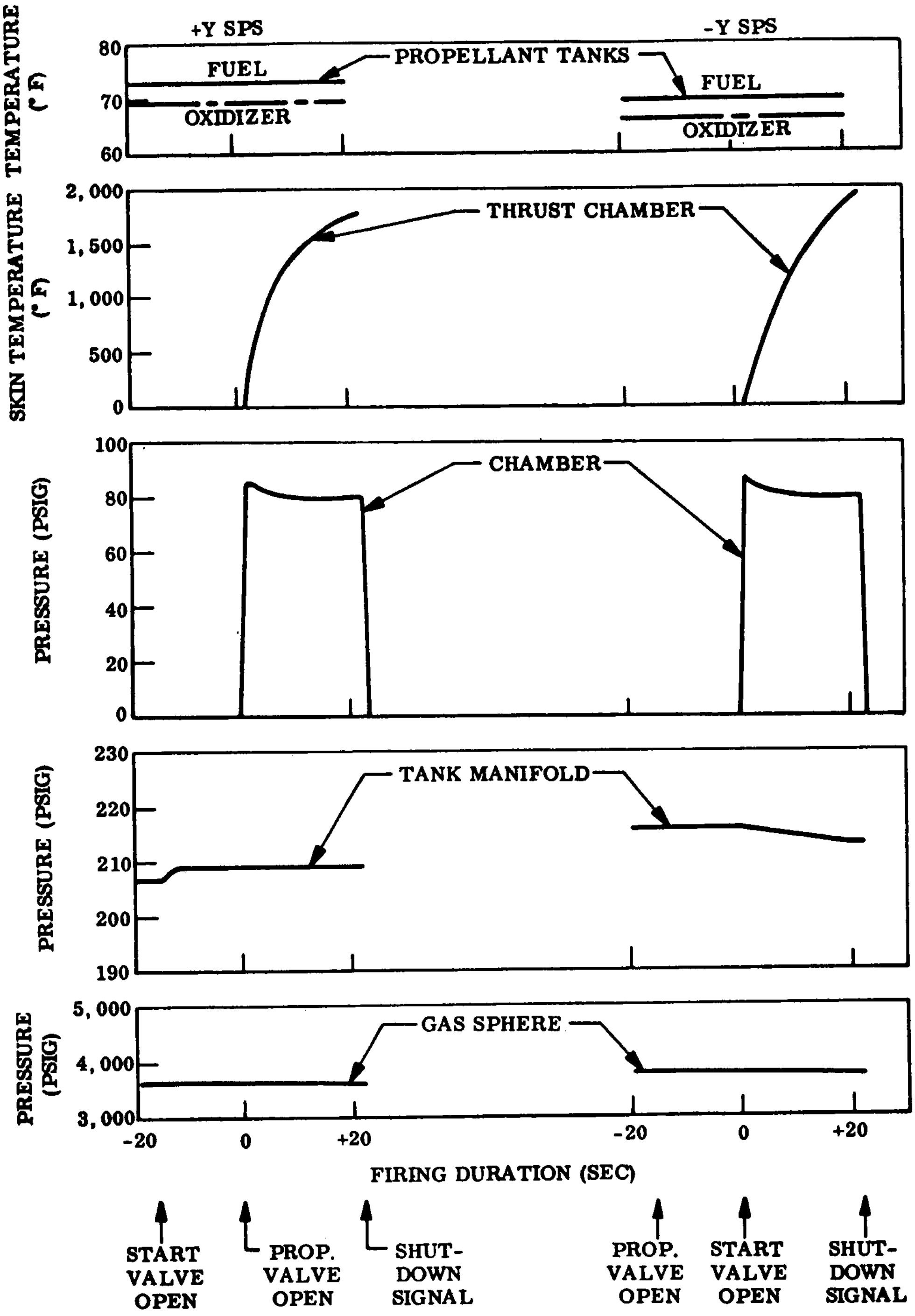

Fig. 3-26 Burn No. 8 Data, SPS Unit I

3.2.8 SPS Burn Number 9 Operation

Burn No. 9, a 22-sec Unit I TCA ullage burn, was satisfactory, and performance was nominal. Operation was very similar to previous burns in that the +Y system did not experience a pressure rise during the start-valve lead period, but since propellant tank pressures prior to start valve actuation were at the expected value for regulator minimum lock-up pressure, the operation was considered nominal.

3.2.9 SPS Burn Numbers 10 and 11 Operations

These burns were Unit II TCA firings of 21 sec and 51 sec, respectively. Operation of both systems was satisfactory, and performance was nominal. Regulator performance for both systems was satisfactory except that the +Y regulator confirmed Unit I regulator performance in that the lock-up pressure was less than predicted from functional test results. Regulated pressure during steady-state operation was within ±3 psi of the nominal values predicted from functional test data.

The low readings on the +Y system chamber skin temperature were noted during these two burns.

Figure 3-27 presents operating parameters during the 50-sec operation of the Unit II assemblies and is typical of both burns.

3.2.10 Summary of Operation

Overall performance of the secondary propulsion systems on GATV 5003 was excellent except for the minor discrepancies already discussed.

While minor variations from predicted pressures and temperature values derived from acceptance and functional test results were noted, in most cases the variations were within expected tolerances. The +Y regulator consistently locked up at pressures below nominal predicted; however, in all cases except two, the pressure was above minimum predicted lock-up pressure. The -Y regulator operated within the predicted band for regulator lock-up pressure.

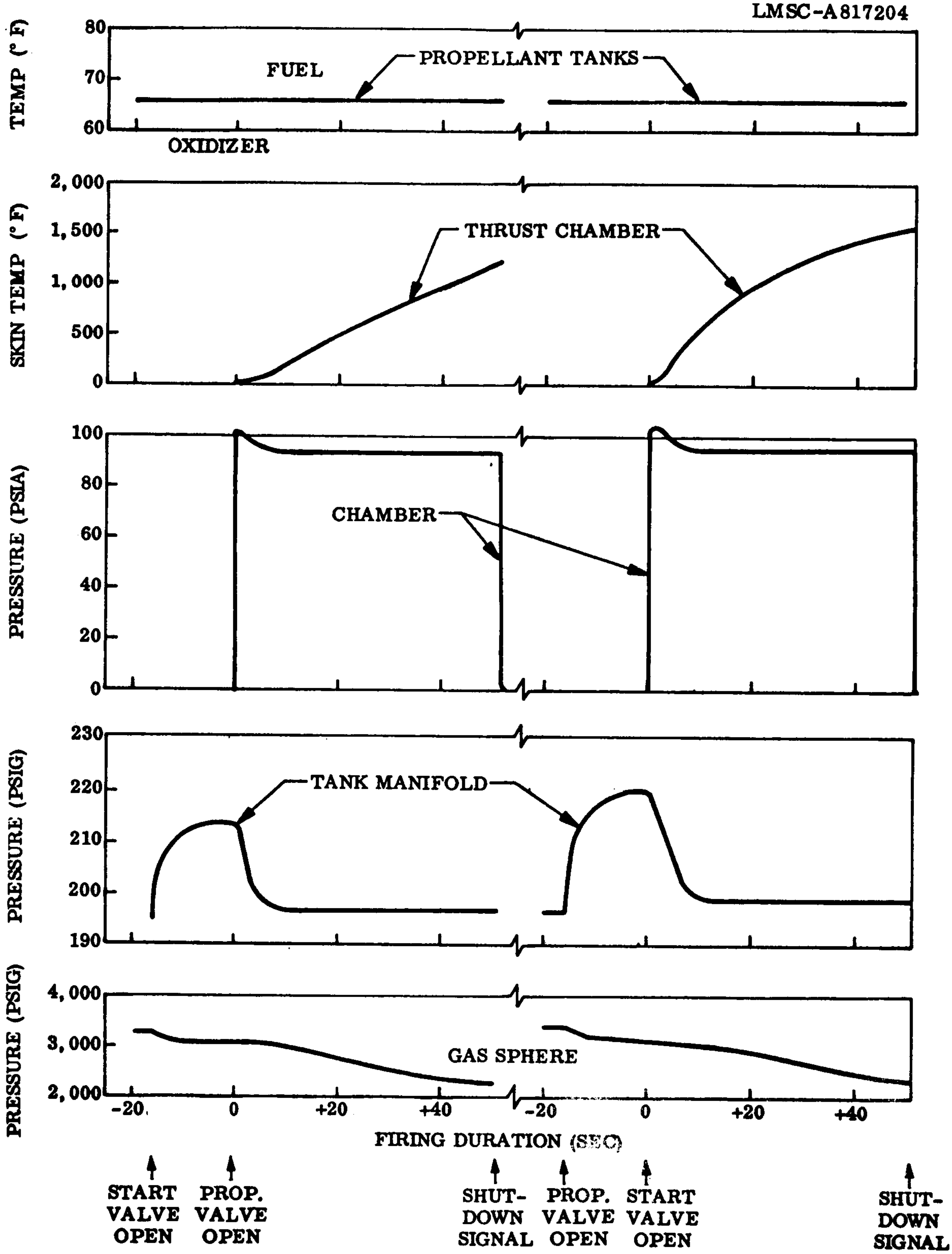

Fig. 3-27 Typical SPS Unit II Burn

The lack of a propellant tank pressure rise during some of the start-valve lead periods is not considered abnormal where the pressure prior to start valve actuation is in the band of lock-up pressures measured on ground test. Regulator functional and fire test results have shown that the regulator lock-up pressure can have a 14 to 16 psi band. Also, previous testing has shown that regulator lock-up pressure is a function of the distance the poppet is from the seat prior to lock-up, with higher lock-up pressure being associated with a larger distance from the seat. Therefore, lock-up pressure is a function of regulator outlet pressure at time of start valve actuation. In addition, when the regulator is operating in the low-flow mode (Unit I TCA operation), the poppet is only 0.003 in. from the seat; therefore, for the regulators on the systems used on GATV 5003, any time propellant tank pressure is above 207 psia the regulators would be at or very near lock-up. Because of the minute clearances involved during Unit I TCA operation, it is expected that wide ranges in regulation will occur.

3.3 PRIMARY PROPULSION SYSTEM

The objectives of the primary propulsion system (PPS) were to:

- Furnish the required impulse to place GATV 5003 into a 161-nm orbit
- Furnish the required impulse for plane change, phase adjust, and apogee and perigee corrections
- Provide a multiple restart capability
- Provide tankage, feed and load, pressurization, and engine vent systems compatible with mission requirements.

All the PPS objectives were met. The impulse required to attain orbit as well as on-orbit apogee/perigee adjust and plane changes was provided. The multiple restart capability was demonstrated by eight successful restarts on orbit, with no anomalies during any restart.

Table 3-7 summarizes the performance during the initial ascent burn of the PPS and the eight on-orbit burns. In the table, the "type of start" is a function of the SPS ullage-orientation burn time. The ascent ullage burn is controlled by the ascent sequence timer, which permits 18 sec of Unit I ullage burn and 2 sec of Unit I overlap with the PPS engine start signal. "C" starts have 68 sec of Unit I operation and 2 sec of PPS overlap. "A" starts have 20 sec of Unit I operation and 2 sec of PPS overlap. Original intentions were to use only "C" starts for orbital burns. However, loss of a large quantity of ACS gas during the Gemini-VIII anomaly made it desirable to shorten the ullage burn to conserve ACS gas. MSC made the decision to use "A" starts for the remaining burns with the exception of the fifth burn which was to be the shortest intended PPS burn duration, thus requiring maximum ullage orientation time or a "C" start.

The last column in Table 3-7 presents the time interval from application to removal of power to the rocket engine as shown on measurement B108. "Duration of thrust time" differs from "duration of power applied" only by the amount of time required for attainment of 75 percent chamber pressure during the start transient.

Table 3-8 shows prelaunch data and represents PPS configuration and status of propellants and gases at the time of liftoff.

3.3.1 Pressurization System Operation

Figure 3-28 represents the pressure time history of the pressurization system blowdown. Data loss occurred during the ascent burn between 124 and 138 sec after PPS engine start signal. The pyro-operated helium control valve (POHCV) functioned normally allowing initiation of both main propellant tank pressurization 1.480 sec after PPS engine power applied signal.

Gas load into the helium sphere was 2600 psia at 61° F. Upper and lower 3-sigma bands were calculated about the predicted blowdown curve based upon 2500 psia and 120° F. Since a greater mass quantity was actually loaded aboard vehicle 5003, the flight blowdown is, on the average, 1.5 to 1.7 psia high on the fuel tank and 0.2 to 0.4 psia high on the oxidizer tank. This higher pressure had no deleterious effect on orbital tank pressure. However, several seconds after the POHCV actuated, the fuel tank pressure transducer (B9) indicated an out-of-range overshoot to 69.5 psig. This overshoot, in no way harming the system operation, was caused by the higher load pressure and close transducer proximity to the pressure source. Sphere loads will henceforth be limited to 2500 psia maximum.

The pressure profile, although higher than predicted due to increased sphere pressure and transducer proximity, did follow the expected blowdown slope. Data received subsequent to last burn (76 hr after liftoff) indicated fuel tank pressure was 44.5 psia and oxidizer tank pressure was 23 psia. The pressurization system performed nominally throughout the GATV 5003 mission.

3.3.2 Primary Feed and Load System Operation

The feed and load system, sumps, propellant isolation valves (PIVs), and vehicle tankage performed as designed from start of countdown through loss of telemetry approximately nine days later.

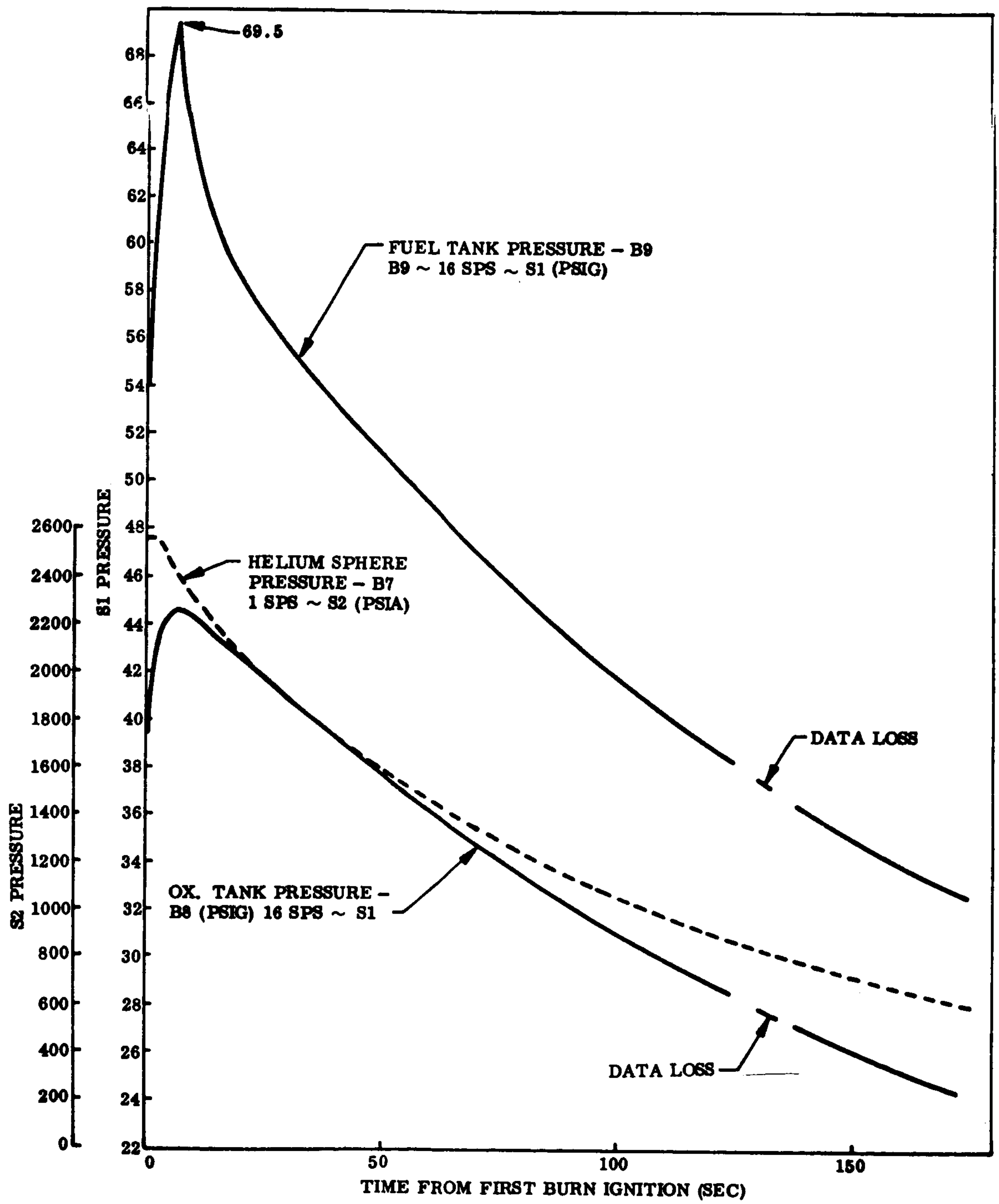

Fig. 3-28 Tank Pressure Profile During First Burn

Table 3-7

PPS GENERAL DATA

Burn No.	Agena Rev. No.	Approx. Time of Start Sequence (GMT)	Type of Start	Duration of Power Applied (sec)	Duration of Thrust Time (sec)	Reason for Burn	Orbit Obtained After Burn			Vel. Desired (ft/sec)	Vel. Obt. (ft/sec)	Act.* Tailoff (ft/sec)	Coast Time Before Next Burn (hr:min:sec)
							A (nm)	P (nm)	I (deg)				
1	0	15:06:20	Agena Timer	184.45	183.35	Ascent Burn	161.4	160.7	28.90	8234.8	8246.05	12.47	23:15:34.4
2	.5	14:31:14	C	2.16	1.16	Hohmann Transfer	219.8	160.0	28.90	104.4	104.4	12.47	5:20:45.5
3	18	19:44:15	C	2.17	1.12	Orbital Circular-ization	220.5	219.9	28.87	104.0	106.7	12.87	12:12:21.7
4	26	7:57:49	A	20.26	19.24	Orbital Plane Change	338.4	212.1	30.62	1600.0	1583.9	17.16	12:12:00.3
5	29	12:42:27	C	1.75	0.80	Minimum Total Impulse	278.9	219.9	30.66	96.0	96.0	15.46	4:45:25.0
6	31	16:20:04	A	9.09	8.06	Orbital Circular-ization	383.9	257.8	28.98	789.0	722.0	19.11	3:07:23.7
7	33	19:28:19	A	3.48	2.48	Orbit Apogee Adjust	257.6	221.7	28.93	272.0	272.0	19.24	3:52:12.4
8	36	23:59:57	A	3.17	2.15	Orbit Apogee Adjust	406.7	221.6	28.93	247.7	247.7	19.62	4:46:48.6
9	38	4:04:22	A	3.66	2.62	Orbit Circular-ization	223.1	220.1	28.93	309.1	309.1	20.66	D.N.A.

*Monitored for 60 sec only.

Table 3-8

PRELAUNCH DATA

Item	Parameter	Actual Value	Specification Limits
1	Helium Sphere Pressure	2600 psia	2150 to 2500 psia
2	Helium Sphere Temperature	61° F	50 to 120° F
3	Ox Start Tank Load	18.4 cu. in.	18.4 ±0.3 cu. in.
4	Ox Start Tank Temperature:		
	At Loading	70° F	32 to 90° F
	At Launch	46° F	32 to 90° F
5	Fuel Start Tank Load	103.2 cu. in.	103.0 ±1.1 cu. in.
6	Fuel Start Tank Temperature:		
	At Loading	70° F	35 to 115° F
	At Launch	47° F	35 to 115° F
7	Ox Start Tank Pressure:		
	At Loading	1012 psig	830 to 1155 psia
	At Launch	990 psia	830 to 1155 psia
8	Fuel Start Tank Pressure:		
	At Loading	1016 psig	825 to 1150 psia
	At Launch	1000 psia	825 to 1150 psia
9	Main Ox Tank Pressure		
	At Launch	30.0 psig	30 to 32 psig
10	Main Fuel Tank Pressure		
	At Launch	40.0 psig	38 to 40 psig
11	Main Ox Tank Temperature		
	At Launch	48° F	45 to 60° F
12	Main Fuel Tank Temperature		
	At Launch	55° F	45 to 60° F
13	Oxidizer Lip-Seal Pressure		
	At Launch	7.6 psig	2 to 20 psig
14	Propellant Specific Gravity:		
	Oxidizer	1.573 @ 60° F	None
	Fuel	0.786 @ 77° F	None
15	Propellant Loading:		
	Oxidizer	9702	9700 ±0.25%
	Fuel	3818	3818 ±0.25%

3.3.2.1 Engine Vent System Performance. Based on available data, the engine propellant vent system performance was satisfactory. The coast periods used in this flight were sufficient to insure that the subsequent start was unaffected.

The flight data was not sufficient to determine the pressure and temperature time history of the propellants remaining in the engine during engine vent cycles.

3.3.2.2 Propellant Isolation Valve Performance. PIV open and close times appear completely nominal (Figs. 3-29 and 3-30). These curves represent actual acceptance test data as well as superimposed flight data points for each burn for the PIVs flown on vehicle 5003. The plotted data points are values obtained for each burn in relation to the applied voltage at each PIV.

Table 3-9 represents all PIV functions during the 9 PPS burns. The random divergence from desired limits, shown in Item 7 of Table 3-9, is the result of variations in programming the backup shutdown signal after a velocity meter shutdown. This problem will be discussed in par 3.3.5.3. Items 4 and 8 of Table 3-9 reflect proper operation of the engine sequencer portion of the command controller.

3.3.3 PPS Engine Operation

The rocket engine operated nominally, performing one start on ascent and eight restarts on orbit. Engine transient data was highly repetitive (Table 3-10) and, for that reason, plots representing three starts and shutdown transients have been selected for presentation in this report. Figure 3-31 shows first or ascent burn transients; Fig. 3-32 shows the longest on-orbit burn (Burn No. 4) of 20.262 sec; and Figure 3-33 shows the shortest or minimum total impulse orbital burn of 1.750 sec. A detailed transient analysis follows:

Table 3-9

PROPELLANT ISOLATION VALVE OPERATION SEQUENCE

Item	Parameters	Spec Value (sec)	Burn 1 (sec)	Burn 2 (sec)	Burn 3 (sec)	Burn 4 (sec)	Burn 5 (sec)	Burn 6 (sec)	Burn 7 (sec)	Burn 8 (sec)	Burn 9 (sec)
1	From PIV Open Command to Fuel PIV Open	0.5 to 2.0	N/A*	1.119	1.181	1.119	1.182	1.150	1.150	1.182	1.119
2	From PIV Open Command to Oxidizer PIV Open	1.0 to 4.0	N/A	2.494	2.494	2.463	2.431	2.400	2.400	2.432	2.431
3	From PIV Open Command to PPS Start Signal	3.5 to 4.5	N/A	3.969	3.983	3.943	3.962	3.954	3.942	3.995	3.974
4	PIV Open Command Duration	4.5 to 5.5	N/A	4.994	4.994	4.963	4.963	4.963	4.963	4.994	4.994
5	From PIV Close Command To Fuel PIV Closed	0.5 to 2.0	0.853	0.926	0.949	0.937	0.936	0.947	0.936	0.927	0.936
6	From PIV Close Command to Oxidizer	1.0 to 4.0	2.200	2.332	2.386	2.343	2.342	2.354	2.342	2.364	2.343
7	From PPS V/M Shutdown to PIV Close Command	Orbital Burns 2.9 to 3.1	10.545	1.844	2.829	2.791	2.252	3.938	4.543	3.843	4.365
8	Close Command Duration	5.9 to 6.1	6.018	6.010	6.022	6.010	6.010	6.011	6.010	6.012	6.010

*PIVs were already open at first-burn initiate.

Table 3-10

ENGINE START TRANSIENTS FOR ALL BURNS

Item	Parameter	Burn 1	Burn 2	Burn 3	Burn 4	Burn 5	Burn 6	Burn 7	Burn 8	Burn 9	Burn Avg.	Engine A/T Value	Mod. Spec
1	Time to GGOV Actuation	.045	.034	.024	.034	.044	.044	.035	.076	.034	.041	.038	
2	Time to GGFV Actuation	.056	.045	.067	.087	.055	.065	.077	.056	.045	.061	.060	
3	Time to TMP Peak	.369	.327	.318	.328	.306	.357	.297	.307	.327	.326	.346(1)	
4	Time to MOV Open	.406	.375	.387	.386	.343	.395	.354	.375	.396	.380	.416(1)	
5	Time to OMPS Make	.906	.875	.887	.886	.843	.895	.852	.875	.896	.880	.938(1)	
6	Time to MFV Open	1.044	.939	.962	.971	.918	.959	.940	.950	.971	.962	1.015(1)	
7	MFV Opening Time	.138	.064	.075	.075	.075	.064	.086	.075	.076	.074(2)	.069	
8	Time to TC Ignition	1.073	.980	.978	.989	.947	1.010	.980	1.000	1.020	.997	1.025(1)	
9	Oxidizer Preflow to TC Ignition	7.8	5.7	5.2	5.6	5.6	5.7	6.4	6.4	6.3	6.0(2)	4.6(1)	8.5 +7.4 -4.6
10	Time to 75%F	1.103	1.002	1.034	1.031	.957	1.032	.999	1.022	1.044	1.025	1.086(1)	1.1 +.4 -.2
11	75% Pc to S/D Signal	183.371	1.165	1.143	19.241	.793	8.060	2.491	2.172	2.623			
12	Time to Pc Decay at S/D	.021	.020	.029	.021	.021	.033	.022	.032	.031	.026	.028	
13	Time to TMP decay at S/D	.130	.119	.130	.109	.109	.120	.109	.120	.088	.115	.106	
14	GGOV Closing Time	.130	.119	.130	.109	.109	.120	.109	.120	.088	.115	.106	
15	SDI(2) (lb-sec)	2775	2696	2724	3025	2660	2949	2820	2792	2793	2807(3)	(4)	3300^{+523}_{-1400}

Notes: (1) Measured on engine first start only.

(2) Based on interrogating velocity meter one minute after PPS shutdown except for Burn No. 3 when the velocity meter was interrogated two minutes after PPS shutdown.

(3) Average of burns subsequent to first burn.

(4) Cannot be measured at sea level.

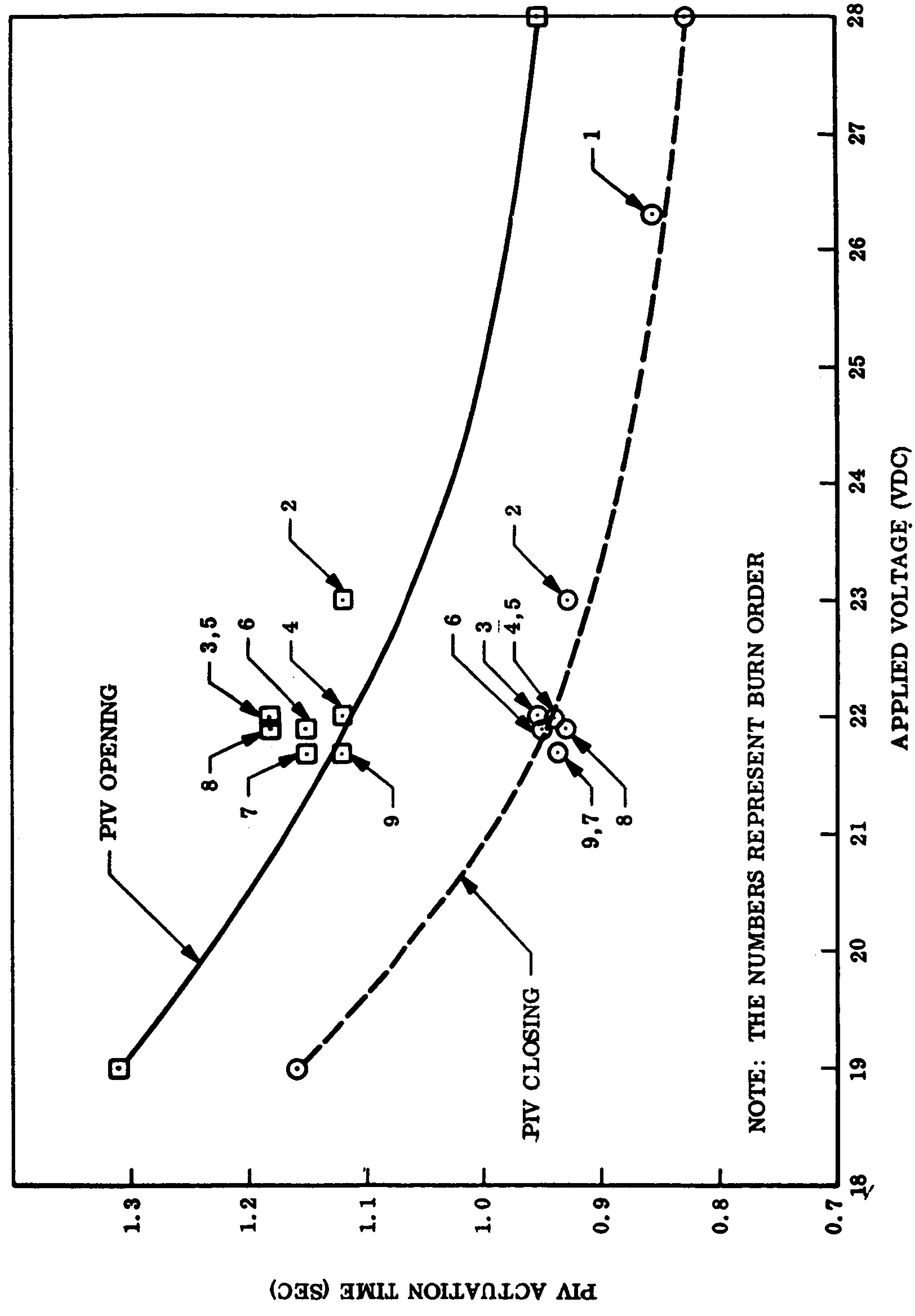

Fig. 3-29 Fuel Isolation Valve Command Signal vs Switch Actuation Times

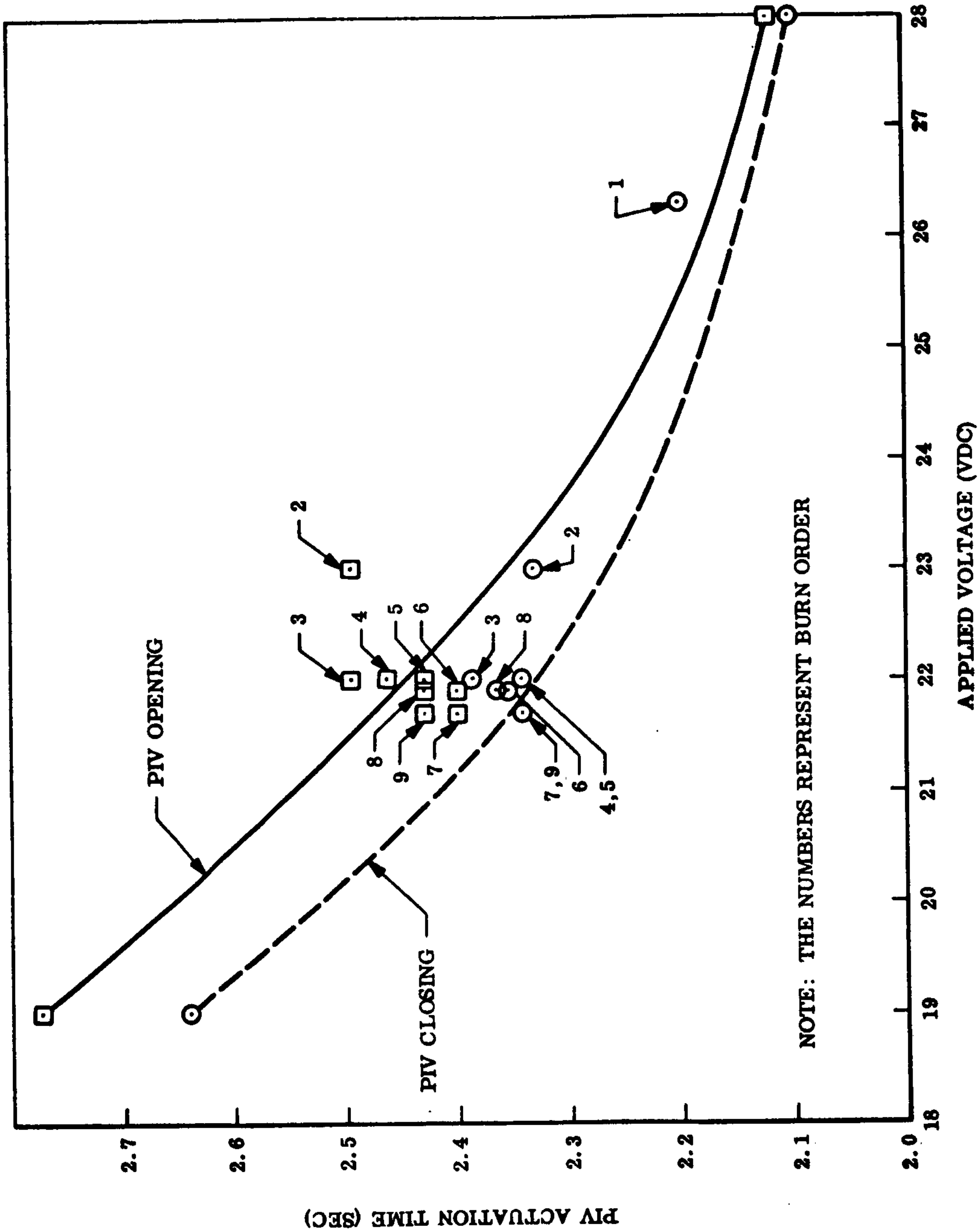

Fig. 3-30 Oxidizer Isolation Valve Command Signal vs Switch Actuation Times

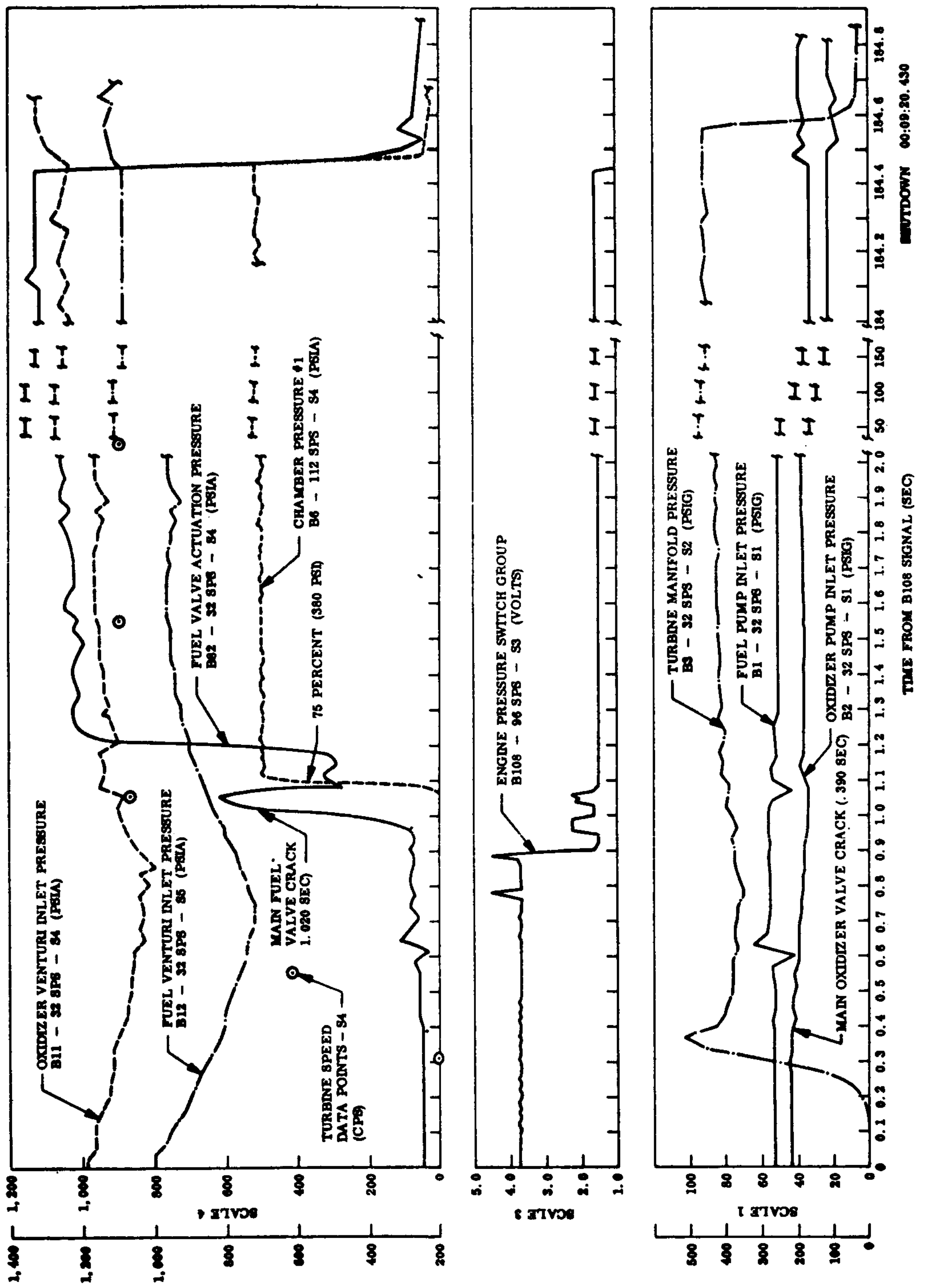

Fig. 3-31 Ascent Burn Engine Start Transients

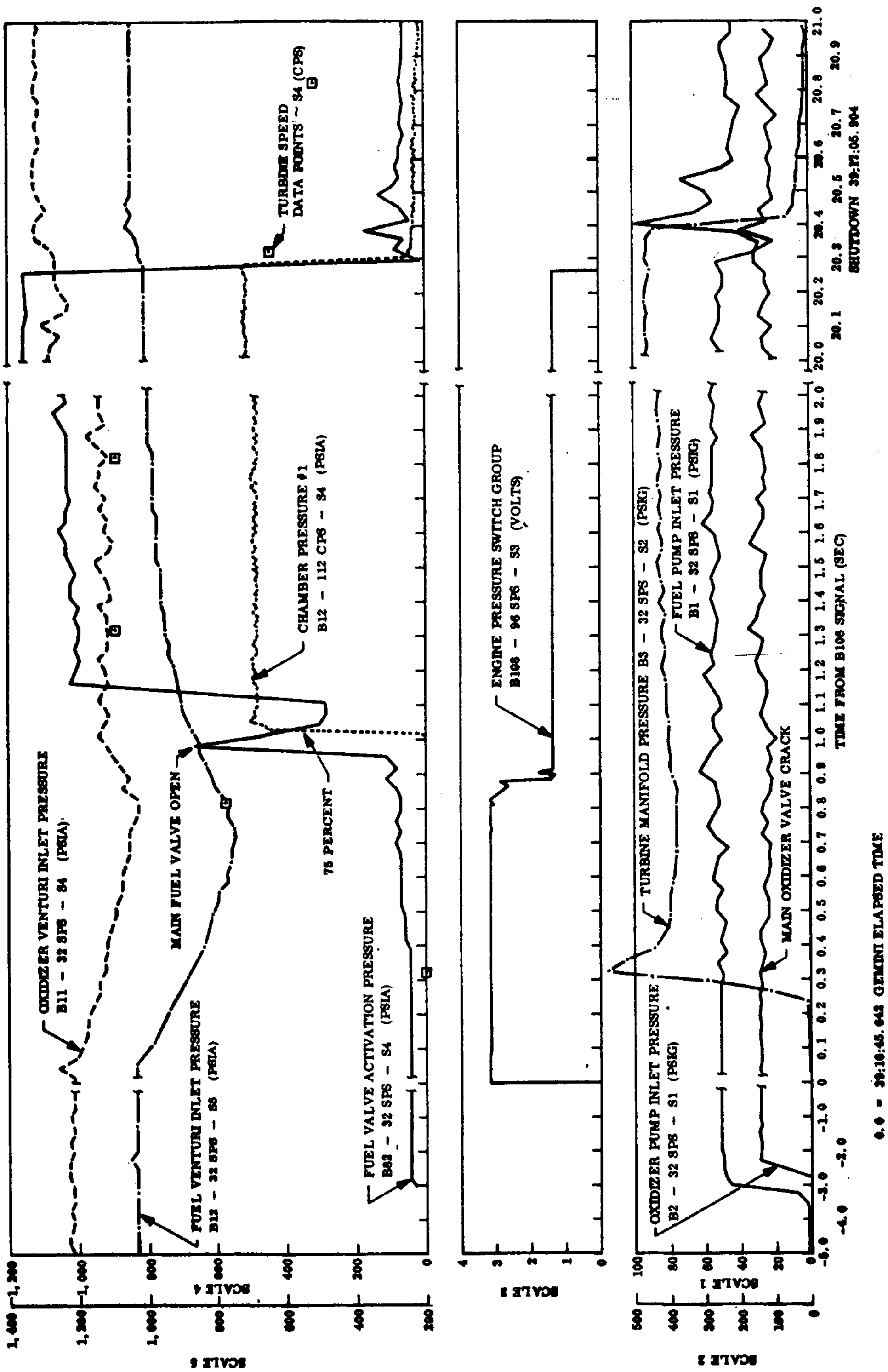

Fig. 3-32 Engine Start Transients from Burn No. 4

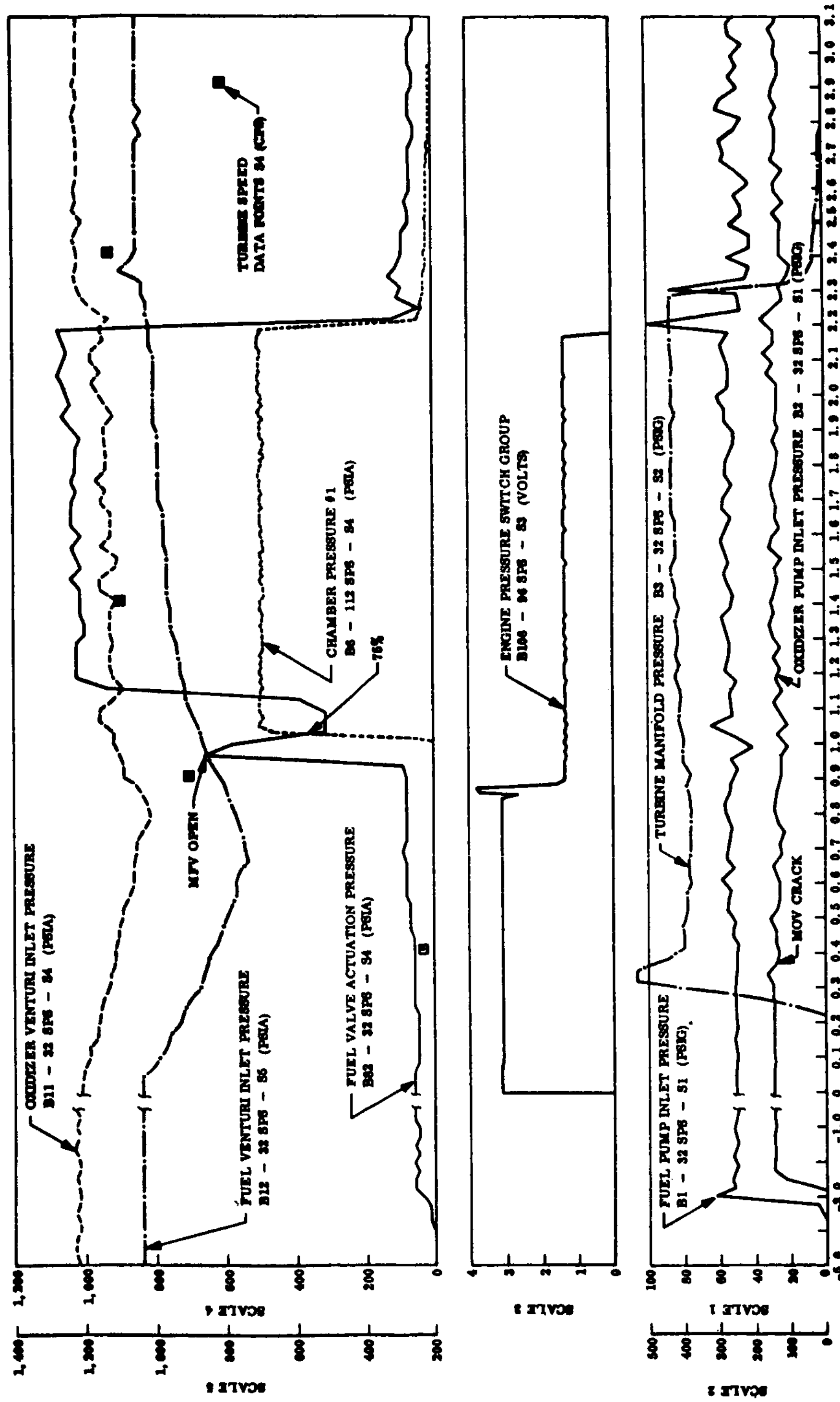

Fig. 3-33 Engine Start Transients from Burn No. 3

3.3.3.1 Transient Analysis.

Time to GGOV Actuation. The time to gas generator oxidizer valve actuation is determined by the first significant movement of the oxidizer venturi inlet pressure measurement B11. The average flight data opening time of 0.041 sec compares satisfactorily with the engine acceptance test average of 0.038 sec. The long opening time of 0.076 sec for Burn No. 8 is attributable to measurement inaccuracies which result from the data sampling rate.

Time to GGFV Actuation. The time to gas generator fuel valve actuation is determined by the first significant movement of the fuel venturi inlet measurement B12. The average flight data opening time of 0.061 sec compares satisfactorily with the engine acceptance test average of 0.060 sec.

Time to TMP Peak. Peak Turbine Manifold Pressure (TMP) which occurs 300 to 400 ms after engine start is a result of the accumulated fuel-lead propellant being ignited by the delayed entry of the oxidizer into the gas generator chamber. This pressure typically reaches 500 to 600 psia before it begins to decay to a steady state condition commensurate with the steady state flows from the bootstrap system. From the flight data, the time from start signal to Turbine Manifold Pressure (TMP) peak is selected at the highest TMP measurement (B3) during the initial rise. The TMP peak time from Burn No. 1 compares satisfactorily with Phase A start of the Engine Acceptance Test. Flight data subsequent to TMP peak times are approximately 0.040 sec faster than Burn No. 1. These faster peak times for subsequent burns have also been observed during the recent Altitude Flightworthiness Demonstration (FWD) Program of the engine and are considered typical engine operation. The significance of the TMP peak time is that it serves as an indirect measure of the gas generator valves full opening times and gas generator ignition characteristics at altitude. It was evident from Altitude FWD Program data that excessive GGFV opening times delayed the TMP peak time. Therefore, it can generally be concluded from the TMP peak times that the gas generator solenoid valves reached their full open position within a satisfactory time. During ground testing, the GGOV and GGFV opening times are obtained from their respective current traces. Since engine electrical current data for the individual solenoid valves are not available from flight data, the TMP peak and venturi inlet pressure method is employed.

Time to MOV Open. The average time of 0.380 sec for the main oxidizer valve (MOV) to open is estimated from flight data by deducting 0.500 sec from the OMPS make time. On ground tests where a high ΔP between the engine propellant supply tanks and pump inlets exists, a noticeable dip in pump inlet pressure occurs at the time of oxidizer valve open. However, the relatively small ΔP (4.4 psi) of the Agena propellant feed system does not permit a conclusive determination of the main oxidizer valve open time by the suction pressure method. For estimating purposes, the main oxidizer valve opening time is referenced to the OMPS time, since this time interval consistently exhibited 0.5 sec during the Altitude FWD Program.

Time to OMPS Make. The oxidizer manifold pressure switch (OMPS) make-time is determined from the B108 pressure switch group voltage monitor. For the particular supply voltages experienced for the mission and the resistance used in the pressure switch junction box, the OMPS make time was chosen when the T/M telltale voltage fell below 2.6 volts. The average OMPS make time from flight data of 0.88 sec agrees with Altitude FWD data; both times are shorter than those experienced during the engine sea level acceptance tests or other sea level tests. This shorter time in the vacuum is due to the faster acceleration rate of the turbine as a result of the lower turbine exhaust duct back pressure. The noticeably longer time of OMPS make time or Burn No. 1 compared to the subsequent burns is due to the slower TMP pressure rise characteristics typical of gas generator first starts. The slow rise is probably due to the gas entrapment in the gas generator feed lines as a result of the manner in which the start tanks are normally loaded. Of interest during the transient also is the Oxidizer Feed Pressure Switch chattering denoted by the B108 T/M telltale voltage fluctuations. Figure 3-31 shows that OFPS chatter occurred at 0.78, 0.88, 0.97, and 1.05 sec. This pressure switch chattering is a typical characteristic engine-start-transient.

Time to MFV Open. Opening of the main fuel valve (MFV) occurs after the pilot operated solenoid valve (POSV) closes on a signal from the OMPS. The closed POSV dead-ends the flow through the fuel valve actuation cavity and immediately causes the fuel valve activation pressure (FVAP) to rise to approximately 600 psia. As the 600 psia FVAP is reached, the pressure is high enough to begin opening the MFV, as evidenced by fuel suction pressure and flowmeter data on sea-level testing. Therefore, opening of the engine MFV is determined from the flight data by the high initial rise to approximately 600 psia in fuel valve actuation pressure measurement B82. As in the case of measuring MOV open, the opening time cannot be determined accurately from the inlet pressure measurement due to the low pressure drop in the Agena fuel feed system from the tanks to the engine. The maximum error using the above technique based on the FVAP sampling rate and evaluating sea level and Altitude FWD Program data is approximately 0.030 sec. The time from OMPS actuation (power applied to the POSV) to MFV open is defined as the MFV opening time.

MFV Opening Time. The average MFV opening time during burns subsequent to Burn No. 1 satisfactorily agrees with the average acceptance test value of 0.069 sec, and the overall average opening time of 0.073 sec for the reacceptance test of the first five modified 8247 engines. The long opening time of 0.138 sec of Burn No. 1 is attributable to the gas entrapment in the fuel valve actuation circuit, which results when loading the vehicle with propellants in the vertical position and performing no manual bleed on the fuel system. This 0.138-sec time agrees with the average MFV opening time of 0.137 sec experienced on twenty 8096 first-burn flight starts. The 8096 engine has a fuel-valve actuation circuit similar to the modified 8247 engine and is loaded with propellants for flight in the same manner as the modified 8247 engine.

From the flight data it would appear that there is no altitude effect on the opening time of the MFV.

Time to TC Ignition. The time to TC ignition is determined from the first rise in thrust chamber pressure measurement B6. The average delta time from MFV open to TC ignition was 0.035 sec from the flight compared with 0.050 sec experienced during the Altitude FWD Program, which is well within the accuracy required.

Oxidizer Preflow to TC Ignition. The oxidizer preflow for Burn No. 1 was 7.8 lb and an average of 6 lb for the subsequent burns. These values are within the specification limits of $8.5^{+7.4}_{-4.6}$ lb. These values do not compare to the engine acceptance test preflow value of 4.4 lb or the average sea level reacceptance value of 4.4 lb for all the modified 8247 engines due to the altitude effect on preflow. Based on data obtained during the Altitude FWD Program, the oxidizer preflow for flight is determined as follows.

First, the oxidizer preflow is increased at altitude conditions due to the vacuum filling of the OMPS sensing line. After oxidizer flow fills the oxidizer coolant jacket and manifolding cavities up to the TC oxidizer injector, it then establishes a pressure drop across the injector which produces a pressure upstream of the injector. This upstream pressure then becomes the mechanism which fills the OMPS sensing line to the OMPS and causes the switch to actuate.

Under sea level conditions where ambient air is present in the OMPS sensing line, it takes less liquid to cause the OMPS to actuate. This results from the liquid entering the OMPS sensing line and compressing the ambient air to approximately 3 atmospheres (the approximate OMPS actuation pressure) in 30 percent less time than it takes to completely liquid-fill the line under vacuum conditions. As a result of the longer filling time to actuate the switch under vacuum conditions, an additional 0.6 lb of oxidizer flows past the oxidizer injector during the OMPS line filling process.

Second, the time allowed for oxidizer preflow after the MFV opens is more under vacuum conditions than at ambient conditions. This time factor is a function of the thrust chamber ignition characteristics at altitude compared to sea level conditions, and the corresponding definition of the ignition point in time. This time from MFV open is normally 0.01 sec at sea level and 0.05 sec at altitude conditions. The difference of .04 sec accounts for another 1.4 lb of extra oxidizer preflow in a vacuum (.04 x 35 lb/sec = 1.4 lb).

The predicted oxidizer preflow for vehicle 5003 engine subsequent to Burn No. 1 is estimated as follows:

• Average modified 8247 engine reacceptance test preflow	4.6 lb
• Additional flow due to vacuum filling of OMPS sensing line	0.6 lb
• Additional flow due to thrust chamber ignition time under vacuum conditions	1.4 lb
• Predicted preflow based on vacuum correction factors	6.6 lb

The predicted 6.6 lb satisfactorily agrees with the 6.0 lb average from the flight data. The difference of 0.6 lb is attributable to accuracy of determination of oxidizer preflow from flight instrumentation and to the MFV opening faster in flight than observed during the sea level reacceptance test. This MFV open time is suspect due to the smaller time from MFV-open-to-TC-ignition times observed in flight compared to altitude FWD tests.

In addition, the significantly higher preflow on Burn No. 1 is attributable to the long MFV opening times, which characterize first burns due to gas entrapment as described in MFV Opening Time.

An oxidizer preflow for first burn can be predicted similarly to that done for subsequent burns.

• Average modified 8247 engine reacceptance test preflow	4.6 lb
• Additional flow due to vacuum filling of the OMPS sensing line	0.6 lb
• Additional flow due to thrust chamber ignition time under vacuum conditions	1.4 lb
• Additional flow due to gas entrapment effect on MFV initial opening time (calculated 0.061 sec x 35 lb/sec = 2.1 lb)	2.1 lb
	8.7 lb

The predicted 8.7 lb oxidizer preflow satisfactorily agrees with the Burn No. 1 preflow, and again the small difference is attributable to the faster MFV opening time (about 0.020 sec) than the FVAP measurement B82 indicates, less gas entrapment in the fuel valve actuations cavity at first burn ignition, and the accuracy of determining oxidizer preflow from flight data.

Time to 75 Percent Thrust. The time to 75 percent thrust (F) is determined by measuring the time to 75 percent of thrust chamber pressure from measurement B6. An average time to 75 percent F of 1.025 sec satisfactorily agrees with the acceptance test value of 1.086 sec and falls within the specification limits of $1.1 {}^{+.4}_{-.2}$ sec. The 0.061 sec average faster time to reach 75 percent during flight is due to the faster acceleration of the turbine pump under vacuum conditions, which causes more rapid engine sequencing. Burn No. 1, which exhibited a longer time (1.103 sec), is due to the delayed TMP peak time and slow MFV opening time that is characteristic of flight first burns (see Time to TMP Peak and MFV Opening Time.)

Time to Pc Decay at Shutdown. Thrust chamber pressure decay after shutdown signal is determined from the initial decay of thrust chamber pressure measurement B6. This parameter indicates closing of the MFV. The average closing time of 0.026 sec satisfactorily agrees with the reacceptance test average of 0.028 sec and falls within the 3-sigma limits of 0.027 ±0.007 sec to ensure the engine shutdown impulse (SDI) within specification limits.

Time to TMP Decay at Shutdown. The time to turbine manifold pressure decay following shutdown signal is determined from the initial decay of TMP measurement B3. This parameter indicates closing of one of the gas generator solenoid valves and subsequent nominal shutdown characteristics of turbine speed decay and oxidizer postflow.

GGOV Closing Time. The Gas Generator Oxidizer Valve Closing Time is determined from TMP measurement B3. Normal engine operation has demonstrated, at sea level and during the Altitude FWD Program, that GGOV closing occurs prior to GGFV closing. Consequently, the TMP decay is used to determine the GGOV closing. The average GGOV closing time of 0.115 sec (from flight data) satisfactorily agrees with the .106 sec closing time average of the reacceptance test. The closing time of the GGFV is difficult to ascertain from flight data (fuel venturi inlet pressure measurement B12), but the closing time of the GGFV is considered satisfactory due to the excellent start tank recharging characteristics noted from the flight data. The MFV closes prior to GGFV and GGOV closing, resulting in a decrease in pump HP required and causing a small increase in turbine speed until TMP decays. When TMP decays as a result of GGOV closing, the turbine speed decays as does the bootstrap pressures. The start system check valves close due to the decrease in bootstrap pressures, trapping the oxidizer in the oxidizer start tank. The fuel start tank propellants continue to discharge through the GGFV, reducing fuel start tank pressure until the GGFV closes . When the GGFV closes nominally, the locking fuel start tank pressure is higher than it was at shutdown signal.

Shutdown Impulse. The Shutdown Impulse (SDI) of the PPS results from engine steady-state thrust during the interval between SD signal and MFV closure, oxidizer postflow, and the final boil-off of the residual oxidizer in the thrust chamber coolant jacket after MOV closure. SDI is calculated from flight data based on the velocity gained during the 60-sec period immediately following PPS shutdown signal. The SDI for Burn No. 1 was 2775 lb-sec and an average of 2807 lb-sec for subsequent burns. Both values are within specifications limits of $3300 {}^{+525}_{-1400}$ lb-sec and are slightly below the mean value due to the limited velocity meter interrogation period of only one minute after shutdown.

3.3.4 System Performance

Engine I_{sp} agrees satisfactorily with the predicted value and is well within the established lower limit. The predicted engine performance values presented in Table 3-11 are based on previously experienced average I_{sp}, pump inlet temperature of +50° F, and the predicted average pump inlet pressures resulting from the main tank pressurization system. Flight data from Burn Nos. 1 and 4 show that engine thrust was well within the predicted limits established for the Gemini VIII. As expected, the average thrust for Burn No. 1 was higher than Burn No. 4 for two reasons. First,

Table 3-11
ENGINE PERFORMANCE

Parameter	Predictability Limits			Actual	
	Predicted	Minimum	Maximum	Burn No. 1	Burn No. 2
Thrust – lb	16230	(-2.6%) 15808	(+2.6%) 16652	16374	16030
Specific Impulse – sec	292.5	(-1.8%) 290.7		293.1	293.3
Mixture Ratio	2.544 (1) 2.570 (2)	(-0.8%) 2.523 2.549	(+0.8%) 2.565 2.591	2.537 (1) 2.562 (2)	2.516 (1) 2.541 (2)

(1) Calculated actuals using updated engine and vehicle tank dump data.

(2) Calculated actuals using original predicted engine flow constant data.

Burn No. 1 pump inlet pressures were higher, which produces a higher engine power level; Burn No. 1 was 183-sec duration, whereas Burn No. 4 was 19-sec duration. The average thrust for a long-duration burn reduces the effect of the lower engine-power level, which occurs for the first 15 sec of engine operation before steady state operation.

The flight instrumentation did not include propellant flowmeters. Consequently, sufficient flight data are not available for accurate determination of engine mixture ratio (MR), oxidizer post flow, or remaining propellants. However, mixture ratio is estimated for reporting purposes and deviates from the predicted values due to the difference between average predicted pump inlet for the mission and that observed for a particular burn.

Mixture ratio limits were predicted for this mission based on average pump inlet conditions and on the engine flow constraints derived from BAC data. The calculated actual MR is based on the same engine flow constants and using the observed pump inlet conditions for the specific burn. As a result, the actual MR for Burn No. 4 is slightly below the predicted limits set forth in Table 3-11, because the actual pump inlet conditions for this burn differed significantly from the predicted averages.

3.3.5 Anomalies and Problem Areas

The following anomalies or problem areas require discussion:

3.3.5.1 Oxidizer Pump Inlet Anomaly. Figure 3-34 shows a plot of B-2 oxidizer pump inlet pressure (OPIP) and B-8 oxidizer tank-top pressure (OTP). Approximately 9 sec after engine start signal, the OPIP coverages with OTP. At approximately 21 sec after start, the OPIP transducer indicates a pressure in excess of OTP by approximately 8 psi. Minor pressure perturbations are not considered abnormal; however, considering the oxidizer feed system pressure drop and vehicle acceleration pressure head at the time of the anomaly, a pump inlet pressure mean value greater than tank pressure cannot be correlated with normal operation without affecting engine performance. The flight data demonstrated nominal engine performance during the period with no adverse effects to substantiate the abnormal pump inlet pressure measurement. In addition, the OPIP transducer appeared excessively noisy prior to the 20-sec pressure spike and normal after the spike. Therefore, the most probable cause of the anomaly is a transducer rather than a propellant system problem.

Second, thrust is averaged over both burn durations. Therefore, due to the longer first burn, the decreased transient effect causes a higher average thrust value for burn No. 1.

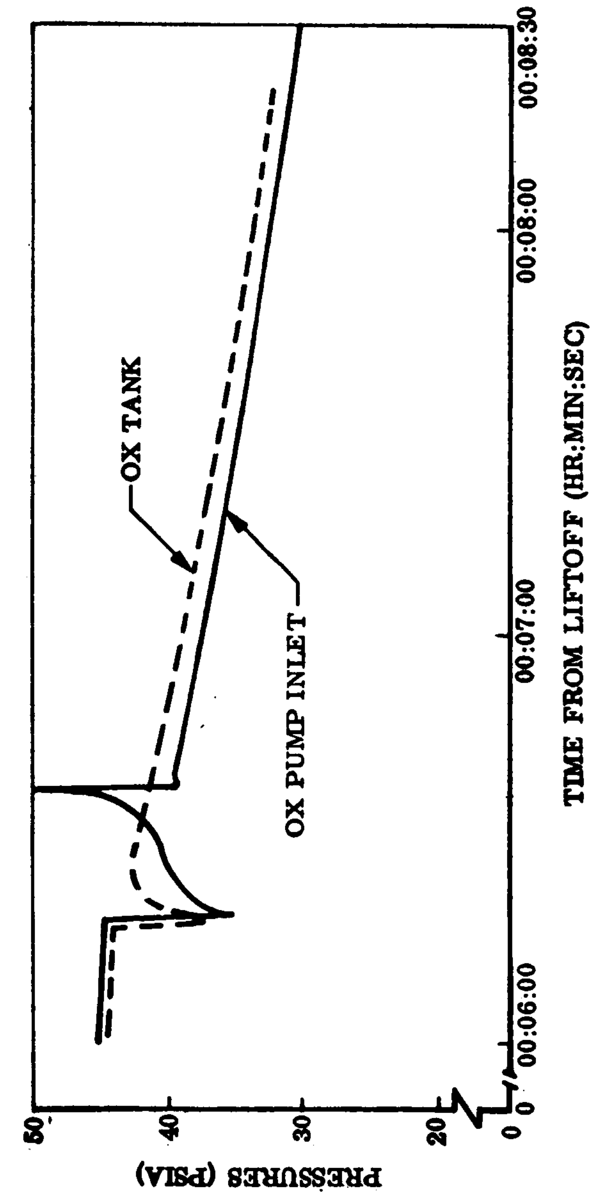

Fig. 3-34 Oxidizer Tank and Pump Inlet Pressures

3.3.5.2 Oxidizer Pump Lip Seal Anomaly. Figure 3-35 shows time-pressure histories of the oxidizer pump lip seal transducer during the first four PPS burns. Liftoff pressure in the lip seal cavity was normal at 7.6 psig. During ascent, the lip seal cavity pressure increases due to the ambient pressure decrease to the point at which the lip seal reference pressure chamber in the ACS nitrogen regulator relief valve vents. The relief valve setting is 16.5 ±1.5 psi. Ascent data indicates a maximum pressure of 17.5 psi, relieving down to 16.5 psi at the time of engine-start signal. Approximately 15 sec into the burn, lip seal pressure decreased rapidly from 15 psi to the regulated pressure of 2 psi in a period of 3 sec and remained at this level throughout the ascent burn. Lip seal pressure characteristics appear normal for the eight orbital burns.

Potential leakage and venting conditions were considered in the evaluation of the observed momentary lip seal pressure decay. Data analysis revealed no indications of erroneous instrumentation or measurement discrepancy. The ACS relief valve operation is not considered a possible cause based on analysis of pressure decay rate and considering the system configuration and subsequent flight data. A plumbing leak is not considered a possible mode due to the magnitude and momentary condition of the observed pressure decay. The oxidizer pump lip seals have the flow area and flexibility to accommodate this momentary pressure decay rate and subsequently to continue its normal seal operation. Momentary high leakage rates have been observed occasionally at BAC during engine acceptance tests with 5 to 8 psi lip seal pressure; however, these high leakage rates normally occur during the start transient turbine acceleration. This condition is not considered abnormal and is attributed to the transient dynamic loading of the lip seals and the initial seal wearing-in process. A momentary lip seal leakage is considered a possible cause of the observed pressure decay in flight; however, sufficient data are not available to conclusively demonstrate the cause or mode of the momentary venting process. The initial start transient lip seal pressure in flight is greater than during BAC acceptance test with correspondingly greater lip seal frictional and sealing forces; however, oxidizer lip seal tests have demonstrated no detrimental effects of these higher frictional forces at lip seal pressures greater than 18 psi.

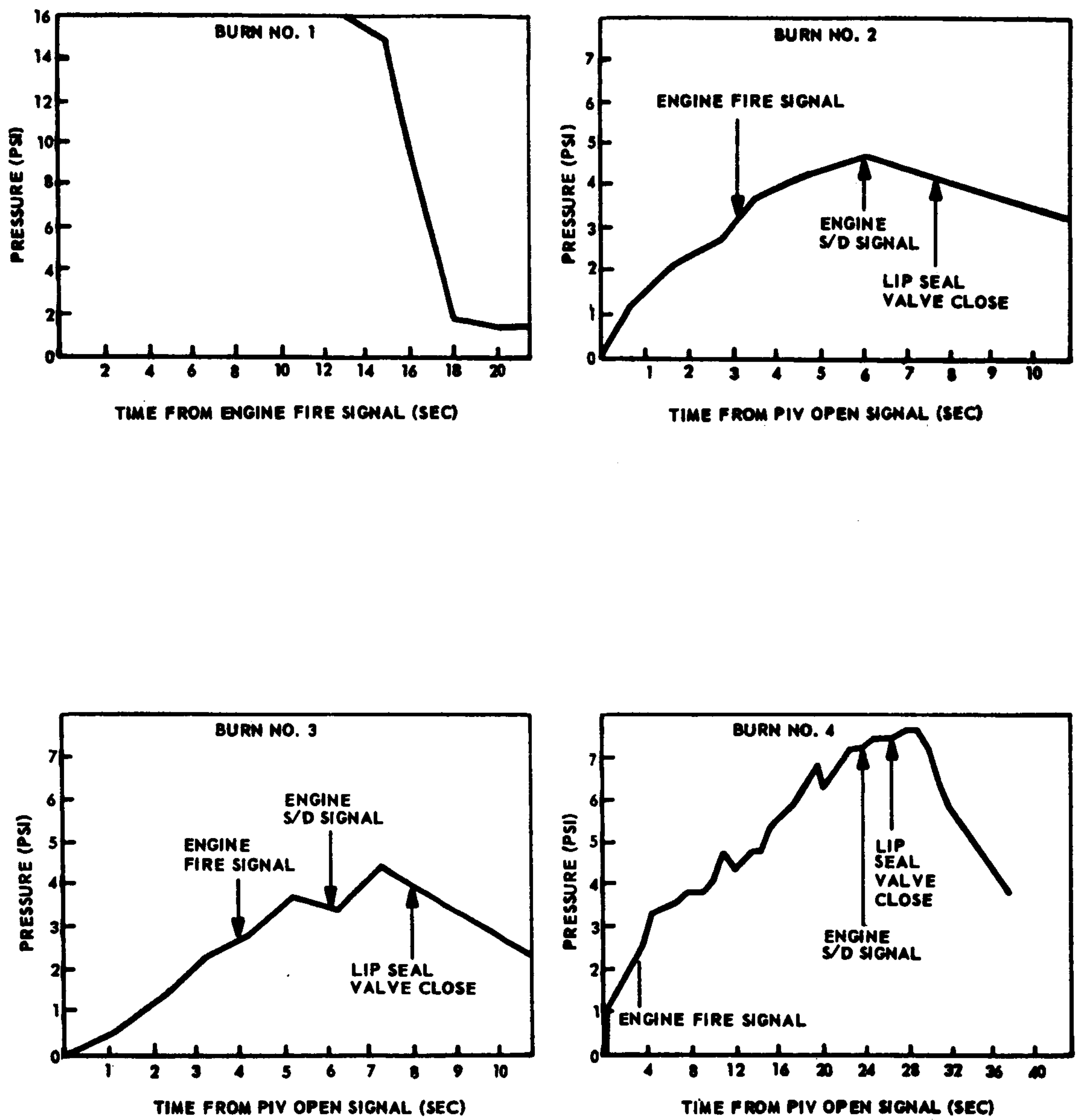

Fig. 3-35 Oxidizer Pump Lip Seal Time-Pressure History

In summary, the observed lip seal pressure decay had no apparent effect on engine operation, and momentary lip seal leakage is considered the most probable cause. This momentary leakage condition is considered acceptable, and no detrimental effects were indicated in either the flight data or the subsequent evaluation.

3.3.5.2 Thrust Chamber Extension Measurement. Figure 3-36 shows a plot of both thrust chamber extension temperature transducers B-184 and B-185. B-185 shows an expected normal temperature-time profile. The B-184 thermocouple apparently broke free from the thrust chamber extension and hung free in the vicinity of a Unit I SPS thrust chamber exhaust plume, as shown in Fig. 3-36. ETR is evaluating an improved bonding technique.

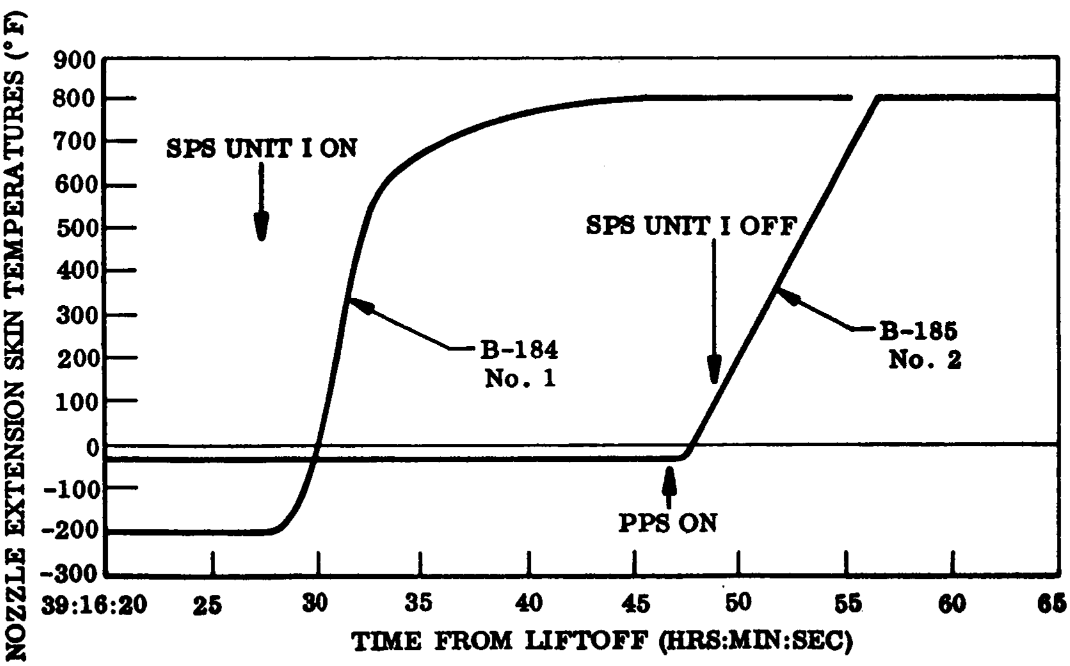

Fig. 3-36 Thrust Chamber Time-Temperature History

3.3.5.3 Backup Command Shutdown Problem. Table 3-9, item 7, indicates the time at which the Command 80 backup shutdown was sent. This may be determined by subtracting approximately 2 sec from each figure; i.e. Burn No. 4 backup shutdown was sent at 0.791 sec.

An LMSC recommended value was given to MSD/FOD of 5 percent of intended burn time or 1 sec, whichever is greater, to be added to the expected velocity meter shutdown time. However, the data presented in Table 3-9 indicate that a spread of from 0 to 2.5 sec from velocity meter shutdown to Command 80 was actually experienced on orbital burns. Furthermore, on Burn No. 2, data indicated that a Command 80 was within 10 ms of the vehicle PPS velocity meter cutoff. Command 80 must be executed within the time span recommended by LMSC.

3.4 ELECTRICAL POWER SYSTEM

Vehicle 5003 electrical system performed nominally throughout the mission and until power depletion approximately 8-1/2 days after liftoff. The system also reflected normal responses during SPS and PPS thrust operations.

Digital tabs and analog plots were available through revolution 45 or approximately 3 days. Projection of system performance beyond this period is based upon information obtained from the Texas (Corpus Christi) tracking station.

3.4.1 Bus Potentials

3.4.1.1 Main Bus Voltage. The main bus unregulated voltage followed the predicted discharge characteristics of the Type IC primary batteries. The initial high potential of 28.82 volts and the decrease and leveling-off potential of 24.40 to 24.61 volts is considered nominal (Fig. 3-37). At battery near-depletion, the rapid voltage tail-off is expected with the pyro battery influencing the main bus decay characteristics.

3.4.1.2 Pyro Bus Voltage. The pyro bus voltage, with diode isolation from the main bus, discharged as predicted. The initial high peroxide potential of 29.71 volts was anticipated and the drop-off to the 25.50 to 25.61 voltage level, imitating the main bus, is considered nominal (Fig. 3-37). At main bus near-depletion the pyro battery, then, by virtue of reserve energy retained from operating above the monoxide region, supports the main bus by operation in the steady-state monoxide region. The vehicle load dissipates this reserve relatively fast, near-depletion is reached, and rapid voltage tail-off following the main bus is as expected.

3.4.1.3 Regulated Voltages. All converter-regulated voltages were relatively steady and within specified tolerance limits. The -28vdc regulated displayed a trend change of 0.25 volts during the first two days. The voltage rose very gradually from a level of -28.48 volts to -28.73 volts (Fig. 3-38) and remained at that level for the duration. There were no appreciable load changes during this period; therefore, the change resulted from a temperature differential interacting with diverse components and circuitry in the output filter and regulator design.

3.4.1.4 400 Cps Voltages. The phase A-B and phase B-C voltages of the 3-phase a-c inverter were steady and within specified tolerance limits; the high value was 115.20 volts and the lowest value was 114.01 volts (Fig. 3-38).

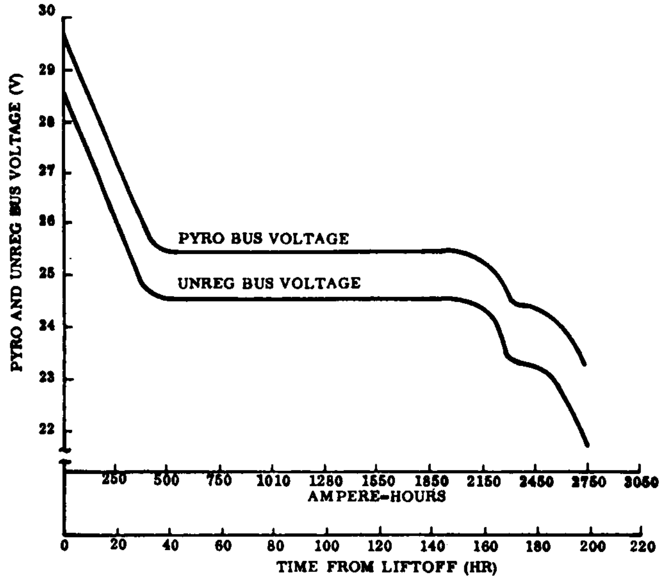

Fig. 3-37 Pyro and Unregulated Bus Voltage vs Time from Liftoff and Ampere-Hours

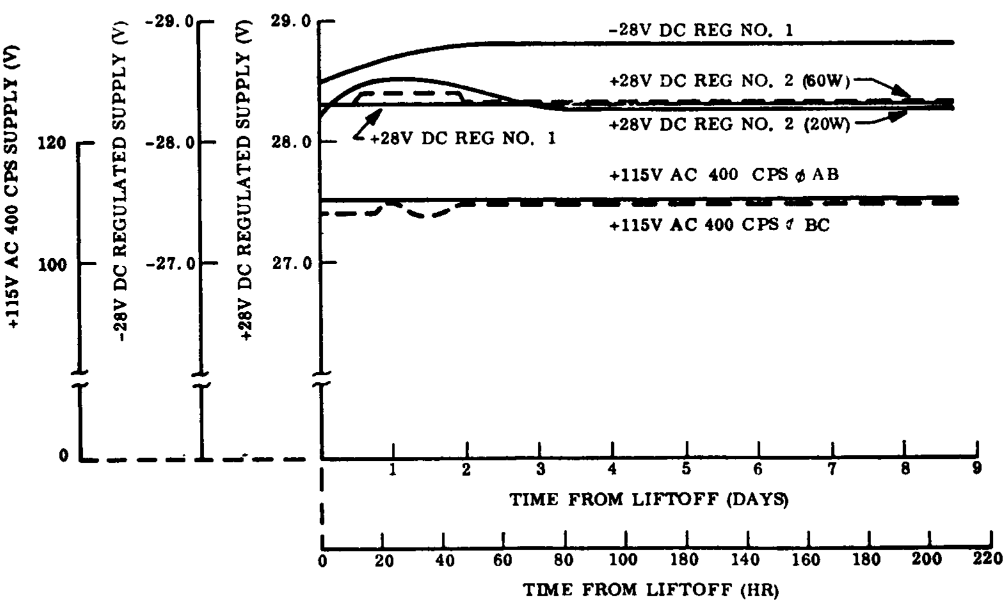

Fig. 3-38 Voltage Levels vs Time from Liftoff

3.4.2 Loads

3.4.2.1 Main Bus Current. The main bus current drain (Fig. 3-39) was nominal considering the necessity of operating the mission profile on a changed program. The average current drain for the life of the vehicle approximated 13 amperes. The lowest value observed was 9.7 amperes and the highest recorded value was 35.98 amperes. The reflected load responses were as expected and well within the capabilities of the system.

3.4.2.2 Structure Current. The indicated structure current values (Fig. 3-39) were nominal, generally ranging between 0.88 amperes and 1.75 amperes. During the docking phase (approximately 7 sec) the peak magnitude was 10.83 amperes with subsequent fluctuations and decay to around 5 amperes. During the approximately 5 sec required for undocking, the same general values were noted. Based on vehicle characteristics displayed throughout the prelaunch tests, these responses and values were anticipated.

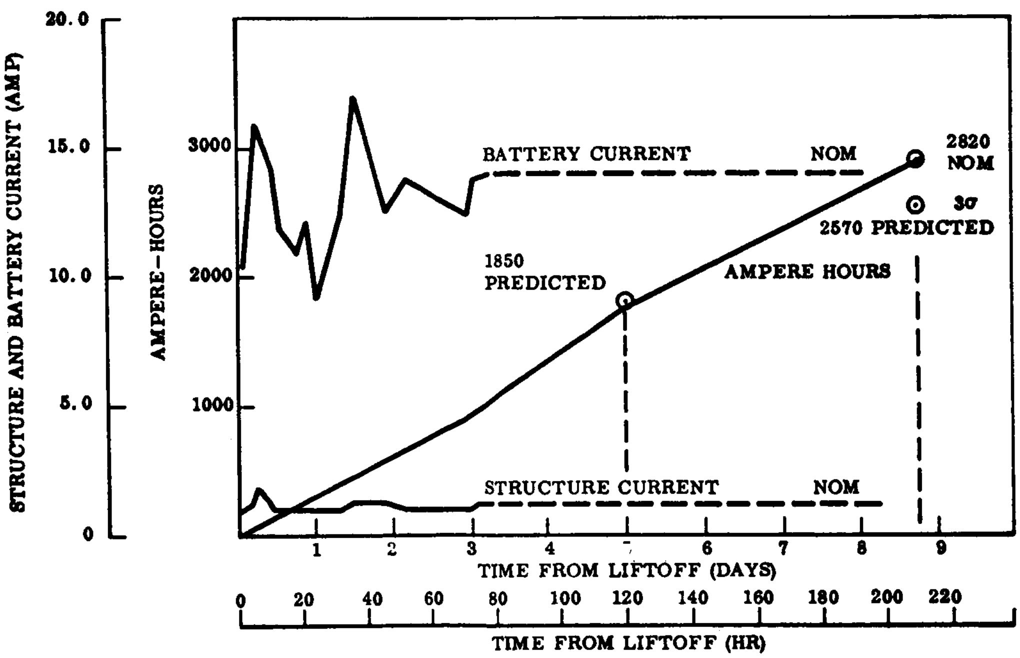

Fig. 3-39 Current and Ampere-Hours vs Time From Liftoff

3.4.2.3 Capacity. The ampere-hours consumed for the 5-day mission were close to the predicted requirements, and the ampere-hours available in the system were essentially identical to the calculated average capacity (Fig. 3-39). Vehicle life was longer than projected for the following reasons:

a. Lower 3-sigma battery capacity values are used in power summaries
b. Allocated power demands for equipment are generally conservative
c. Mission profile changed
d. Less internal system losses

3.4.3 Temperatures

3.4.3.1 Batteries. The indicated battery temperatures were within the specified tolerance limits and no change rates were excessive. The various random traces were expected insofar as variations in location and load-sharing are concerned. Battery Nos. 1 and 2, located in the forward rack, were moderately warmer and therefore contributed proportionally more to the load; the pyro battery (No. 2) followed the conditions of battery No. 1 as a result of the voltage differential across the isolating diode (Fig. 3-40). The initial temperature drops in battery Nos. 4 and 6

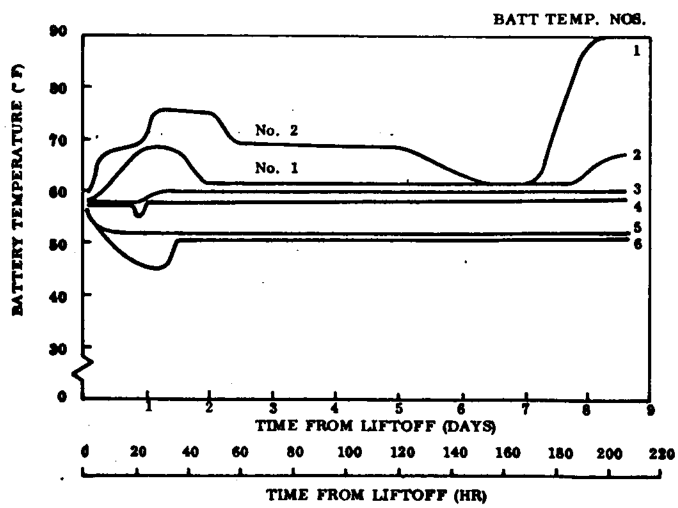

Fig. 3-40 Battery Temperature vs Time from Liftoff

indicates that these two batteries were not contributing nominally to the load. After seven days of operation, battery No. 1 had a pronounced temperature rise; this indicates that the battery was sustaining the load at tail-off.

3.4.3.2 Conversion Units. The temperature indications of the two regulators and the inverter were nominal, well within specified tolerance limits, and basically followed predicted values and trends.

3.4.4 Ascent Anomaly

During ascent a pyro-surge of 10 to 12 amperes was noted (none was expected) at approximately 386 sec and again at 535 sec. The cause was determined to be a power surge across the squib bridgewire during PPS thrust vibration levels between 377.1 and 560.4 sec. At approximately 377.4 sec the pyro voltage was impressed and maintained across the helium valve squibs (two circuits), and at approximately 386.7 sec the pyro voltage was impressed and maintained across the nose shroud squibs (eight circuits). Therefore, the first surge was in the helium valve squib circuits, whereas the second was in one of the nine remaining circuits. The first surge started at 385.96 sec and was cleared by the fusistor at 386.08 sec. The second surge started at 534.97 sec and was cleared by the fusistor at 535.78 sec. Therefore, the design proved adequate, and all operations were performed as planned.

3.5 GUIDANCE AND CONTROL SYSTEM

The guidance and control system performed satisfactorily throughout the mission. Evaluation of the flight data indicated the system performed its required functions as follows:

- Performed all inflight switching requirements and programming
- Responded properly to all commands
- Sensed and maintained vehicle attitude properly
- Reacted to attitude errors with control forces of the proper polarity
- Provided proper PPS engine cutoff through the velocity meter
- Provided proper shutdown of SPS by command
- Consumed a nominal amount of attitude control gas

The guidance and control system anomalies – excessive yaw attitude excursions during PPS engine burns and a control gas regulator pressure drop during the first commanded yaw maneuver (90 deg attitude change prior to docking) – are currently under investigation.

3.5.1 Ascent Phase

During the ascent phase, the guidance and control system performance was normal in all aspects, with the exception of yaw attitude during PPS engine burn (Figs. 3-41, 3-42, 3-43, and 3-44). The ascent sequence timer was started at 282.1 sec by a discrete command from the booster. Another booster discrete uncaged the gyros and fired the horizon sensor fairings at 303.9 sec. Separation started at 308.5 sec, with the separation switches being released at 310.6 sec (separation complete). At this point the attitude control system (ACS) was enabled, and the roll horizon sensor (H/S) was connected to the roll gyro for roll stabilization.

Rates at Atlas/Agena separation were relatively insignificant. Prior to separation there was a zero rate in roll and near zero in yaw, whereas pitch indicated a rate of approximately +0.2 deg/sec. Following separation, roll exhibited a rate of

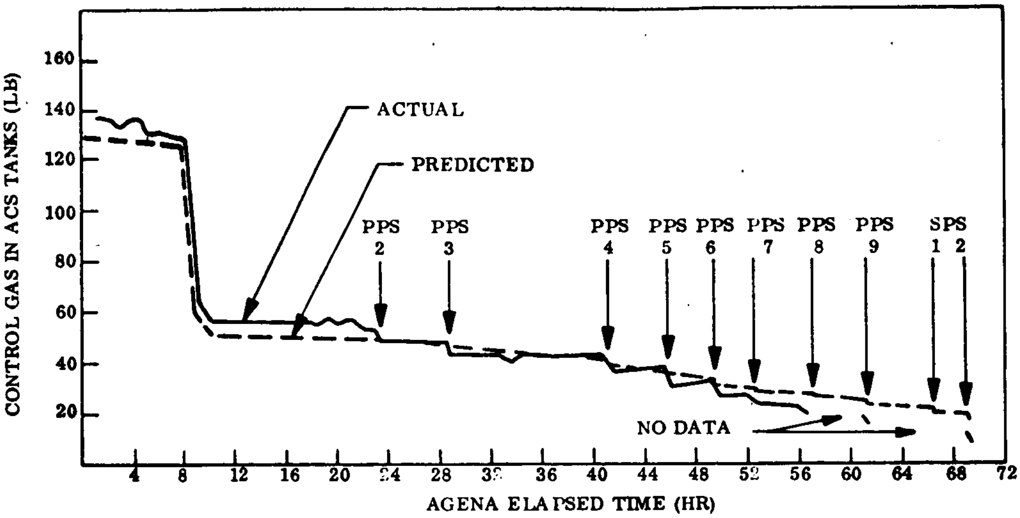

Fig. 3-41 Attitude control Gas Consumption

-0.23 deg/sec, yaw approximately zero, and pitch less than 0.2 deg/sec. Nominal residual rates at Atlas separation are approximately 0.5 deg/sec.

At 342.9 sec, the programmed pitch-down maneuver started and continued for 13 sec. At the completion of the pitch-down maneuver, the geocentric rate and the pitch H/S were connected to the pitch gyro. The rates obtained were as follows:

	Pitchdown	Geocentric
Measured	-1.6 deg/sec	-3.60 deg/sec
Required	-1.5 deg/sec ± 10%	-3.99 deg/sec ± 10%

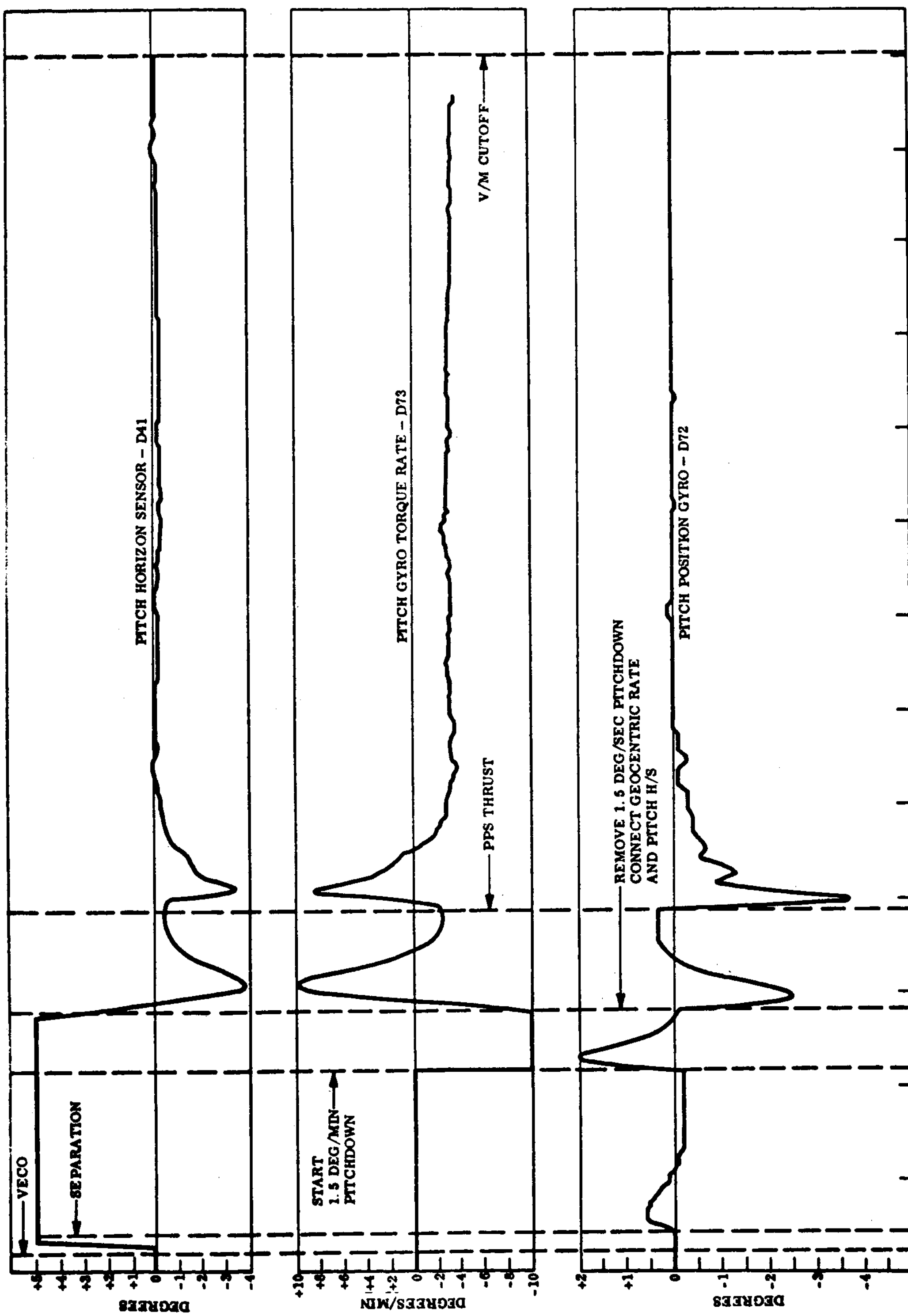

Fig. 3-42 Pitch Axis Control During Ascent

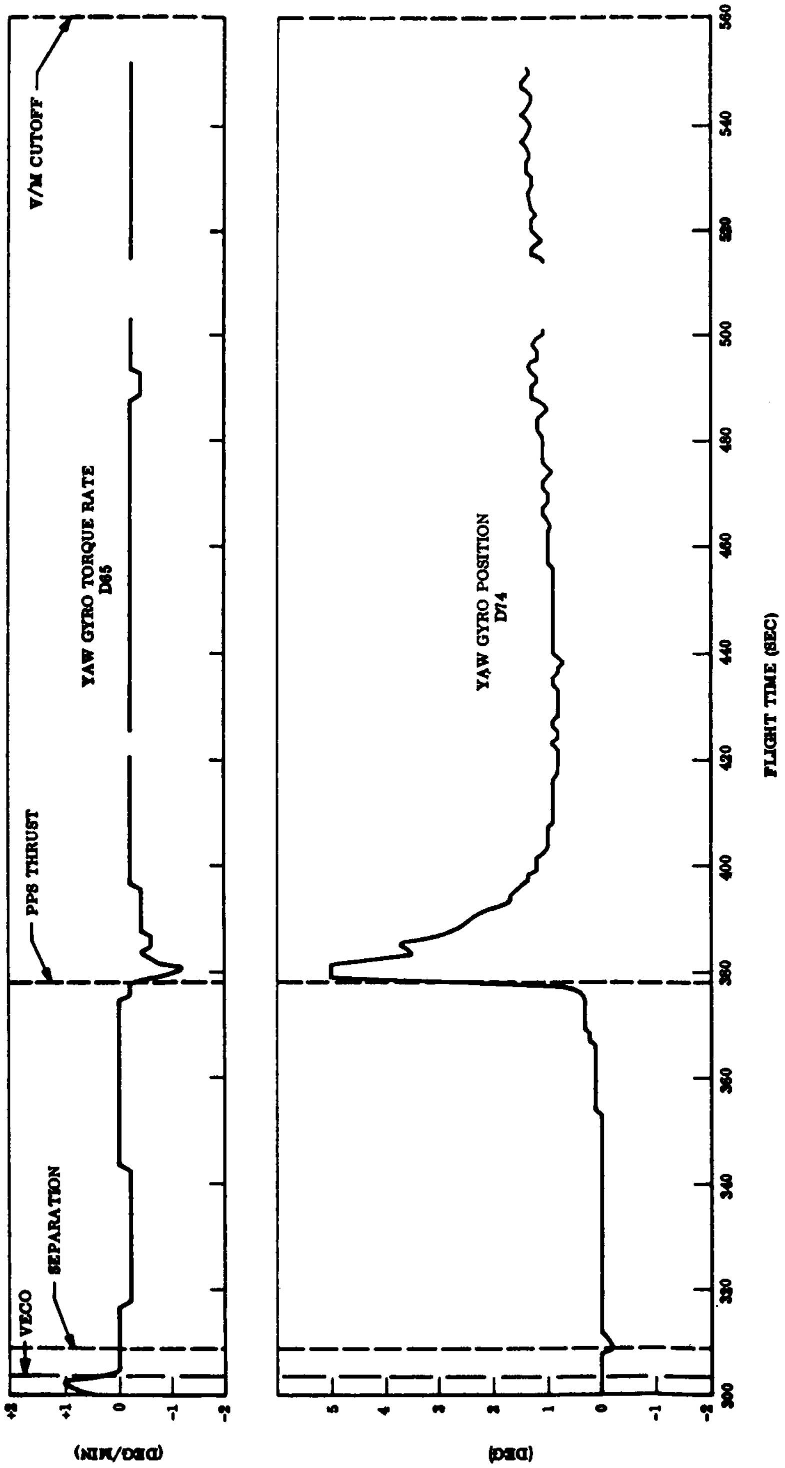

Fig. 3-43- Yaw Axis Control During Ascent

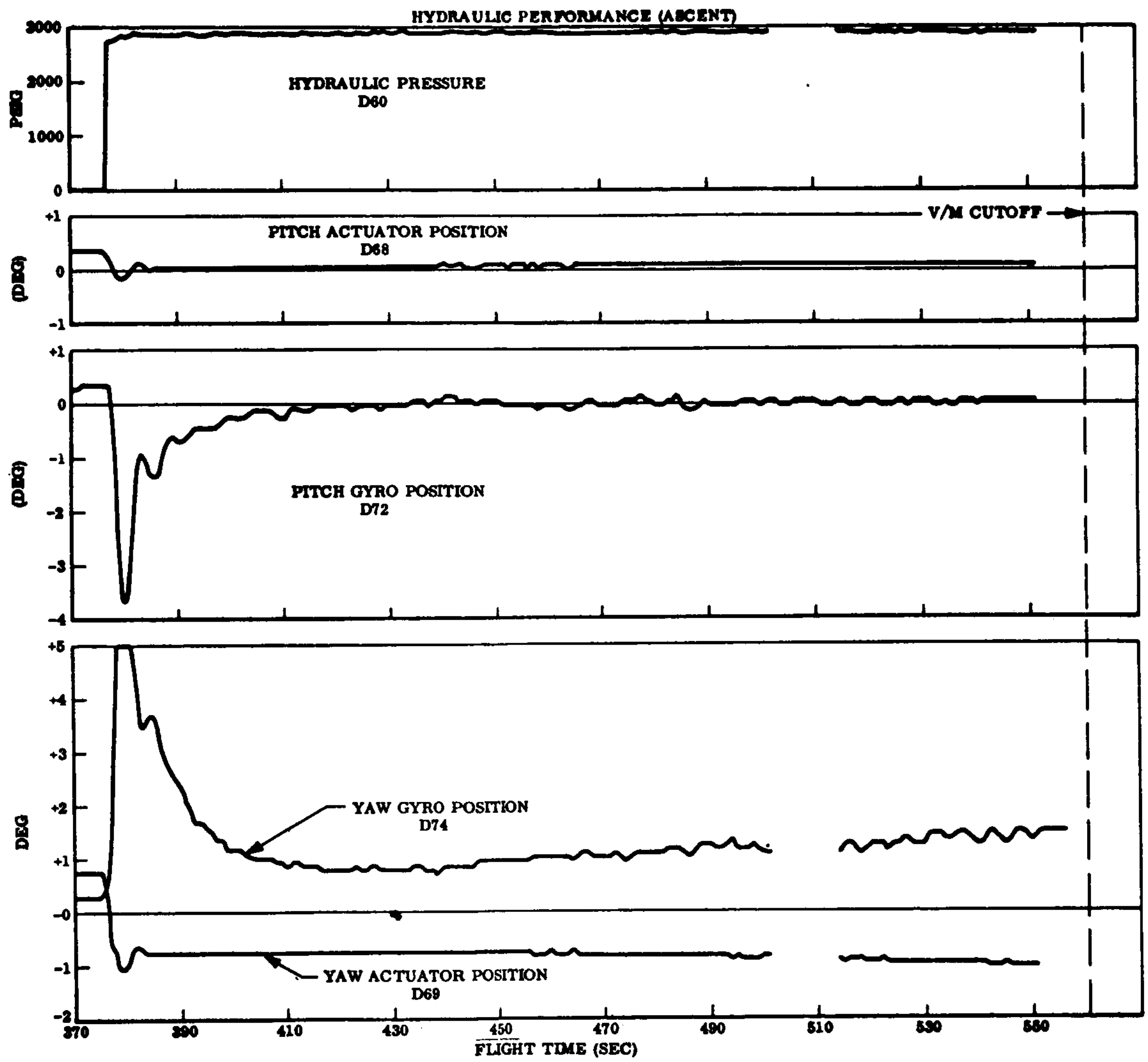

Fig. 3-44 Hydraulic System Performance During Ascent

The H/S-to-inertial-reference-package (IRP) gains were determined to be within the system requirements in the high-gain mode.

	Roll	Pitch
Measured	9.38 deg/min/deg H/S	3.48 deg/min/deg H/S
Required	9.00 deg/min/deg H/S	3.00 deg/min/deg H/S ± 20%

These gains determine the overall system time constant and the settling time of the system in response to reference errors. After connecting the pitch H/S to the IRP, the vehicle stabilized to a steady-state attitude within the allowable deadband of 0.25 ± 0.1 deg pitch, 0.80 ± 0.3 deg roll, 0.25 ± 0.1 deg yaw in approximately 15 sec (less than one time constant). Roll appeared to be within the deadband at the time the roll H/S was connected to the IRP and went immediately into limit cycle operation.

The vehicle was stabilized within the system deadbands prior to the initiation of PPS thrust. No disturbance was noted in any axds at the initiation of the SPS Unit I ullage rockets.

At the initiation of PPS thrust, the system reacted normally in the pitch and roll axes. The normal transient attitude disturbance due to turbine spin-up (1.3 deg/sec), exhaust duct misalignment, and engine gimbaling were noted. Nominal turbine spin-up rates were between 2 deg/sec and 3 deg/sec. The roll axis indicated an offset after the initial transient was dampened. This offset was due to turbine exhaust misalignment and decreased to approximately -1.0 deg when a crossover occured at 462 sec, and the vehicle moved to an offset of approximately +1.0 deg. This crossover is normal during Agena injection burns and is due to c.g. movement as PPS fuel is burned, resulting in a change in polarity of the turbine exhaust misalignment torque.

The vehicle responded normally in pitch, with the initial transient being dampened in approximately 25 sec and the pitch gyro indicating a null condition throughout the remainder of the burn.

The yaw c.g.-offset anomaly is evident during injection burn. The thrust buildup resulted in the vehicle being displaced positively in yaw (Figs. 3-43 and 3-44). The maximum displacement is greater than +5 deg (telemetry measurement is limited to ±5 deg). The displacement reached +5 deg approximately 2 sec after thrust initiation and remained greater than +5 for approximately 3 sec. The initial yaw transient was dampened and settled at +0.8 deg after approximately 30 sec. The yaw offset then greadually increased with the c.g. shift throughout burn.

The yaw hydraulic actuator responded to the yaw movement as expected and exhibited no characteristics which would indicate malfunction of the flight control electronics or the actuator itself.

This anomaly, currently under intensive study to enable corrective action prior to the flight of vehicle 5004, results from several contributing factors. The hydraulic control channel was redesigned (subsequent to 5002) to enable PPS thrust while docked, which required a slower system response time due to the introduction of low bending-mode frequencies by the TDA joint. Furthermore, the vehicle c.g. was offset along the +y axis, and the engine nozzle was aligned to the vehicle geometric x-x axis. These factors, coupled with vehicle dynamics, resulted in the initial yaw attitude excursion and the relatively long time constant. The resultant orbit (160.7/162.3 nm) was very close to the desired 161 nm circular orbit.

At the end of first burn the velocity meter (V/M) shut down the PPS engine. The V/M operation appeared nominal.

V/M scale factor at altitude	0.129974
Velocity-to-be-gained, first burn	8234.8 ft/sec
Complement of residual readout after first burn minus one pulse	24
Tailoff	12.481 ft/sec

Refer to Table 3-12 for V/M data after each burn.

Throughout the first burn, the system hydraulic pressures appeared nominal, with the high pressure running between 2850 and 2950 psi and the low pressure return maintaining 75—80 psi.

Table 3-12

AVAILABLE VELOCITY METER DATA FROM TELEMETRY

Burn	Time	V/M Word	Complement -1	Tailoff Velocity (ft/sec)
1	00:10:57.781	32742	24	12.481
2	21:45:03.198	32671	95	12.350
3	27:06:31.617	701 (V/M Load Automatic Readout)		No Data
4	31:18:27.52	32635	131	17.030
6	47:41:05.812	32620	146	18.980
9	59:19:35.114	2219 (V/M Load Automatic Readout)		No Data

Attitude control gas consumption throughout the ascent phase was less than nominal. The control gas consumption from Atlas/Agena separation to first-burn ignition was 3.0 lb; predicted consumption was 3.4 lb. The control gas consumption during the PPS burn appears unusually low at 2 lb with predicted usage of 8.5 lb. This may be due to the location of the temperature probe which did not allow a true indication of rapid temperature changes. (One probe monitors the three gas spheres.) Total gas consumption through first burn was 5 lb compared to predicted 11.9 lb.

3.5.2 Docking Maneuver

The gyro and horizon sensor data on the docking sequence indicate that the transient effect was very slight when the spacecraft and Agena made contact, latched, and rigidized. The roll horizon sensor (Fig. 3-45) showed an excursion of about 3-1/2 deg with a roll gyro torque rate dip of 2 deg/min. The roll torque rate data showed a steady +4 deg/min offset, which is the geocentric rate with the vehicle yawed to -90 deg.

The pitch horizon sensor (Fig. 3-46) dipped from +1 deg to zero and then back to +2 deg at docking. The torque rate was very low just prior to docking, about

The yaw c.g.-offset anomaly is evident during injection burn. The thrust buildup resulted in the vehicle being displaced positively in yaw (Figs. 3-43 and 3-44). The maximum displacement is greater than +5 deg (telemetry measurement is limited to ±5 deg). The displacement reached +5 deg approximately 2 sec after thrust initiation and remained greater than +5 for approximately 3 sec. The initial yaw transient was dampened and settled at +0.8 deg after approximately 30 sec. The yaw offset then greadually increased with the c.g. shift throughout burn.

The yaw hydraulic actuator responded to the yaw movement as expected and exhibited no characteristics which would indicate malfunction of the flight control electronics or the actuator itself.

This anomaly, currently under intensive study to enable corrective action prior to the flight of vehicle 5004, results from several contributing factors. The hydraulic control channel was redesigned (subsequent to 5002) to enable PPS thrust while docked, which required a slower system response time due to the introduction of low bending-mode frequencies by the TDA joint. Furthermore, the vehicle c.g. was offset along the +y axis, and the engine nozzle was aligned to the vehicle geometric x-x axis. These factors, coupled with vehicle dynamics, resulted in the initial yaw attitude excursion and the relatively long time constant. The resultant orbit (160.7/162.3 nm) was very close to the desired 161 nm circular orbit.

At the end of first burn the velocity meter (V/M) shut down the PPS engine. The V/M operation appeared nominal.

V/M scale factor at altitude	0.129974
Velocity-to-be-gained, first burn	8234.8 ft/sec
Complement of residual readout after first burn minus one pulse	24
Tailoff	12.481 ft/sec

Refer to Table 3-12 for V/M data after each burn.

Throughout the first burn, the system hydraulic pressures appeared nominal, with the high pressure running between 2850 and 2950 psi and the low pressure return maintaining 75–80 psi.

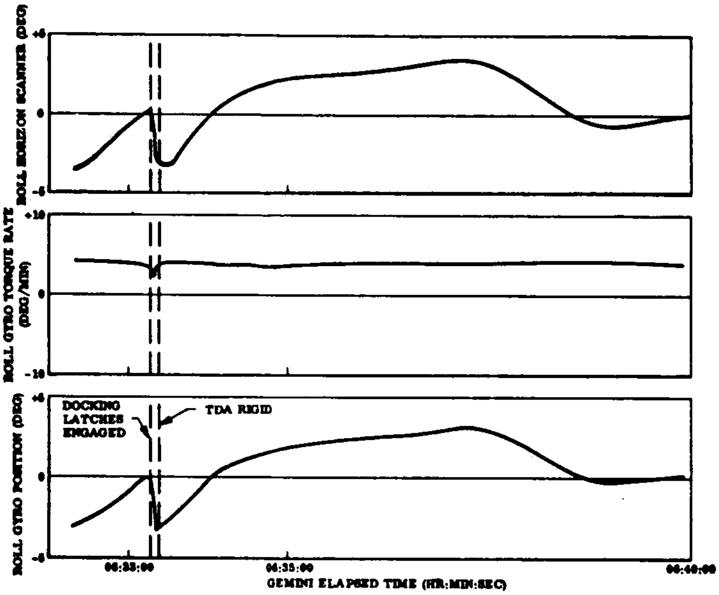

Fig. 3-45 Roll Axis Control During Docking Maneuver

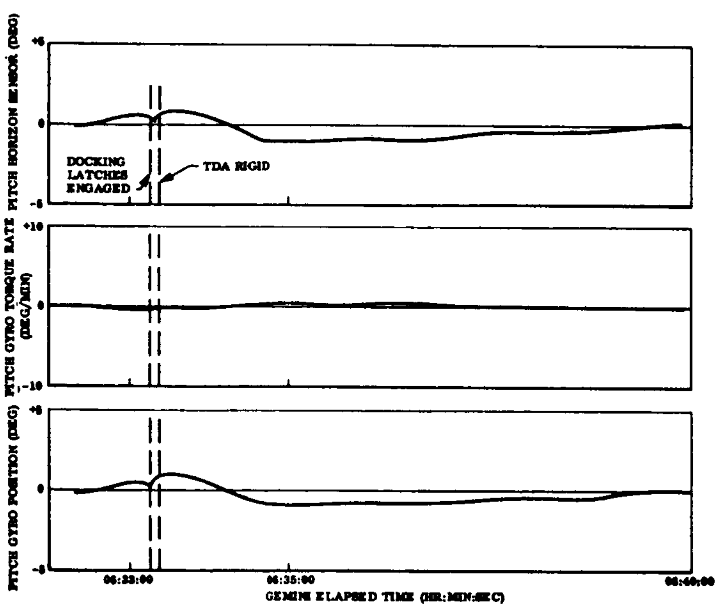

Fig. 3-46 Pitch Axis Control During Docking Maneuver

-1/3 deg/min and rose to zero at the instant of docking. The pitch gyro position followed that of the horizon sensor.

The yaw gyro position (Fig. 3-47) rose to a sharp peak of 4 deg at contact and dropped to zero deg as the TDA was rigidized. The torque rate made an abrupt change at latching from -5 deg/min to +1 deg/min and then reached -1 1/3 deg/min as the TDA was rigidized. These observations indicate satisfactory Agena control during the docking operation.

After undocking, the ACS was commanded on again, follwed by ACS-pressure-low, ACS-gain-low, and H/S-on. The deadband was in the wide mode. The roll horizon sensor was saturated (Fig. 3-48) at 5 deg and the roll gyro position was running just under 5 deg about 12 sec after ACS-on. The yaw gyro was near zero deg. The pitch horizon sensor (Fig. 3-49) was saturated at 5 deg, but the pitch gyro swung from +5 deg to -5 deg and then swung in near zero deg. A positive indication of limit cycling showing

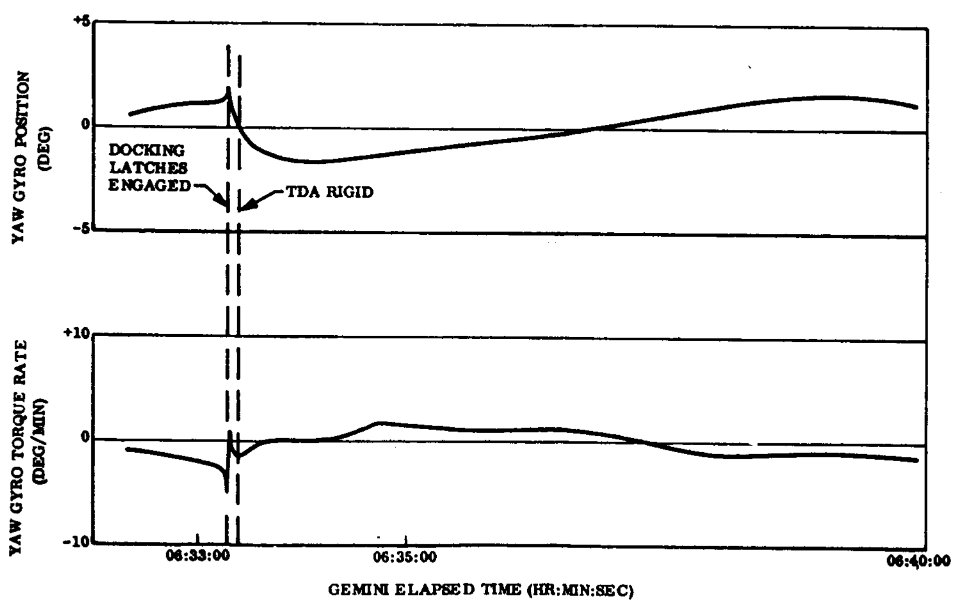

Fig. 3-47 Yaw Axis Control During Docking Maneuver

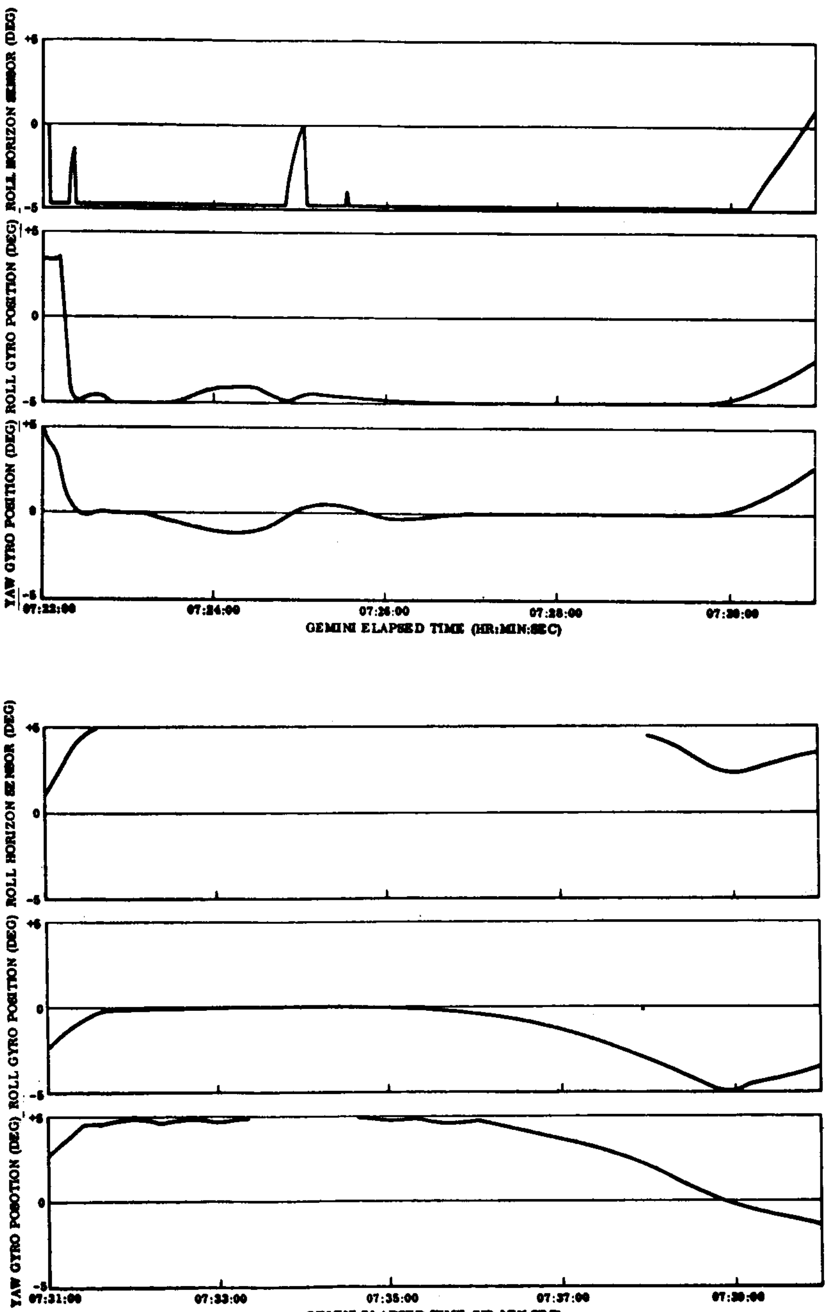

Fig. 3-48 Attitude Control Subsequent to Docking Maneuver (Roll Horizon Sensor, Roll Gyro, and Yaw Gyro)

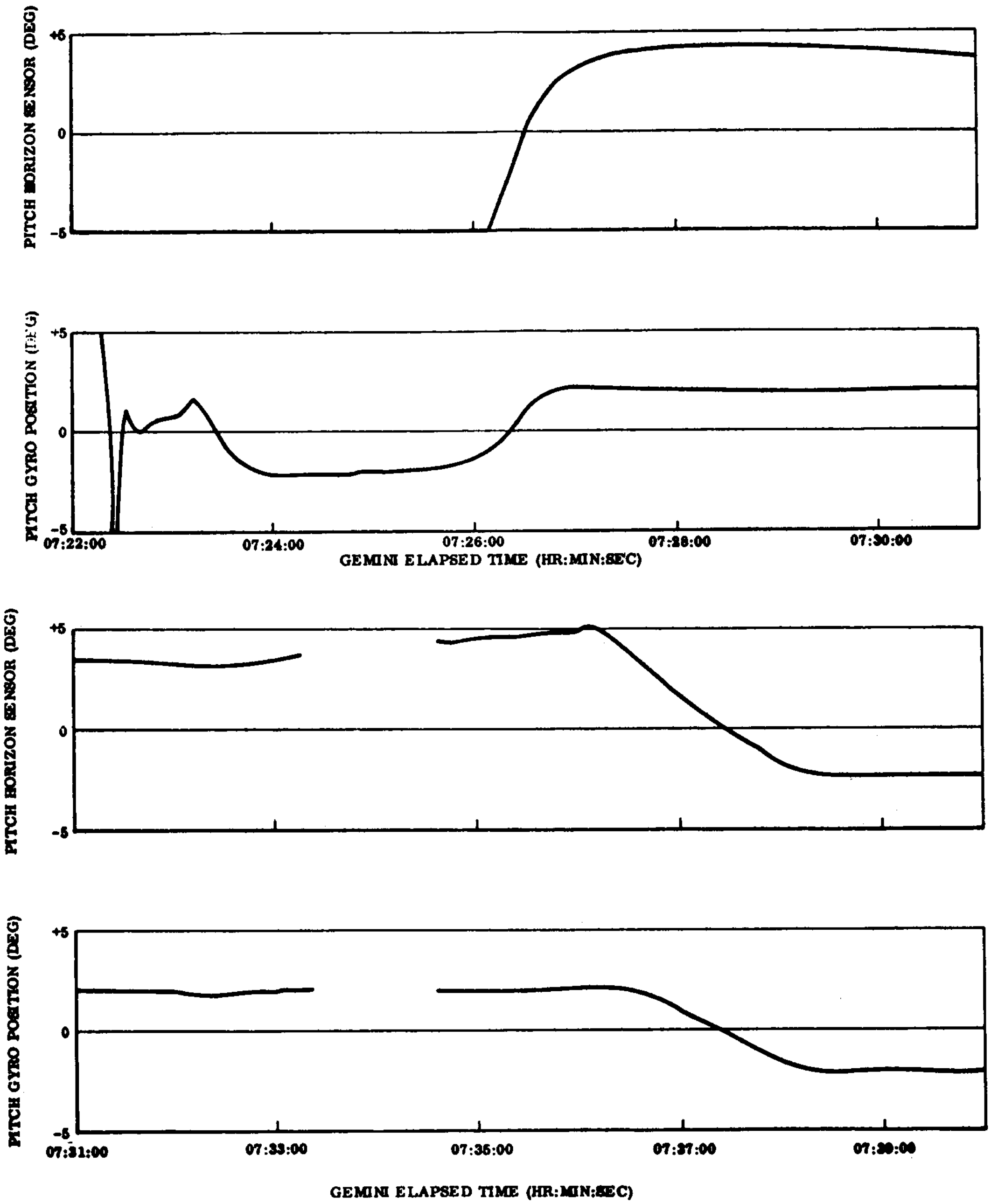

Fig. 3-49 Attitude Control Subsequent to Docking Maneuver (Pitch Horizon Sensor and Pitch Gyro)

complete control within the pitch ± 2 deg, deadband began about 4 minutes after ACS-on, as the pitch H/S came out of negative TLM saturation and went positive. The roll channel gave a positive indication of limit cycling 8 minutes after ACS-on, as the roll gyro position went from -5 deg to zero deg and the H/S went from -5 deg to +5 deg (Fig. 3-48). The changes in yaw gyro position followed the roll gyro, indicating satisfactory in-plane gyrocompassing.

3.5.3 Post Docking

This phase of the flight covers all of the flight following the recovery from the Gemini spacecraft-induced attitude excursions. At this time sufficient data are not available to allow a chronological coverage of this phase. The guidance and control events occurring during this period are repetitious and can best be discussed in the following categories.

- PPS engine burns
- SPS Unit II burns
- Yaw maneuvers
- Limit cycle operation

3.5.3.1 PPS Engine Burns. During the post-docking phase of flight, a total of 8 PPS engine firings were made. These were relatively short burns, the longest being of 19.25 seconds duration. These burns were utilized for plane change maneuvers, height adjustments, inclination adjustments, and final circularization of the orbit. As illustrated in Figs. 3-50 through 3-61, the same anomaly noted in the ascent PPS burn is evident in all of these burns. The yaw gyro indicated an attitude excursion in excess of +5 deg in each burn, the amount of excursion varying with c.g. location.

The most significant result of this anomaly is the reduction in orbital accuracy that was achieved during out-of-phase burns. In this type of burn the vehicle is yawed 90 deg prior to thrust initiation such that a velocity increment is created perpendicular to the original plane of orbit, resulting in a new plane of orbit (plane change). The yaw attitude error excursions are of sufficient magnitude and length to create an in-plane

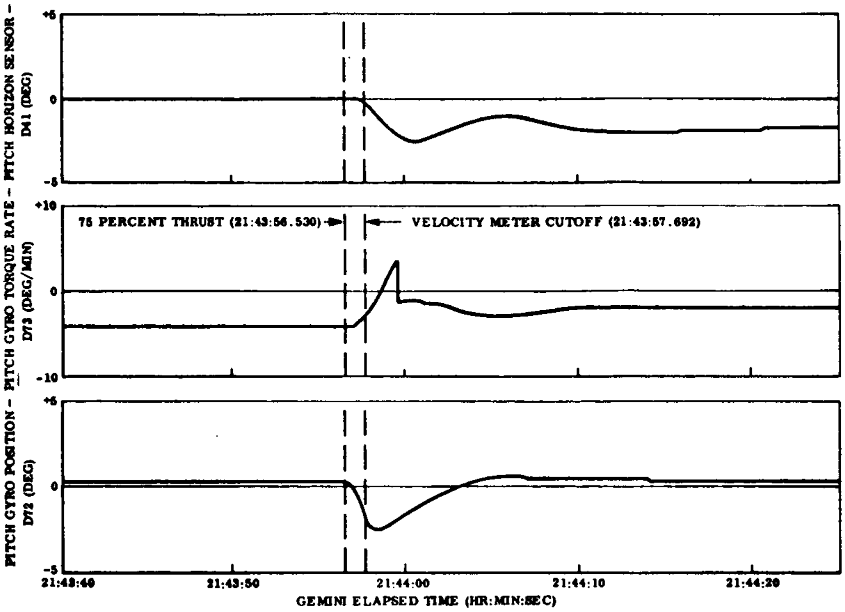

Fig. 3-50 Pitch Axis Control, Burn No. 2

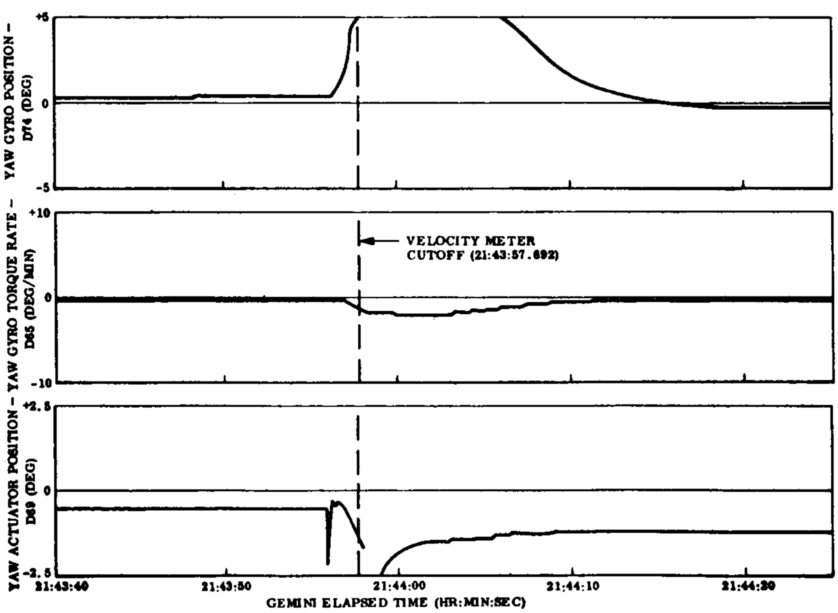

Fig. 3-51 Yaw Axis Control, Burn No. 2

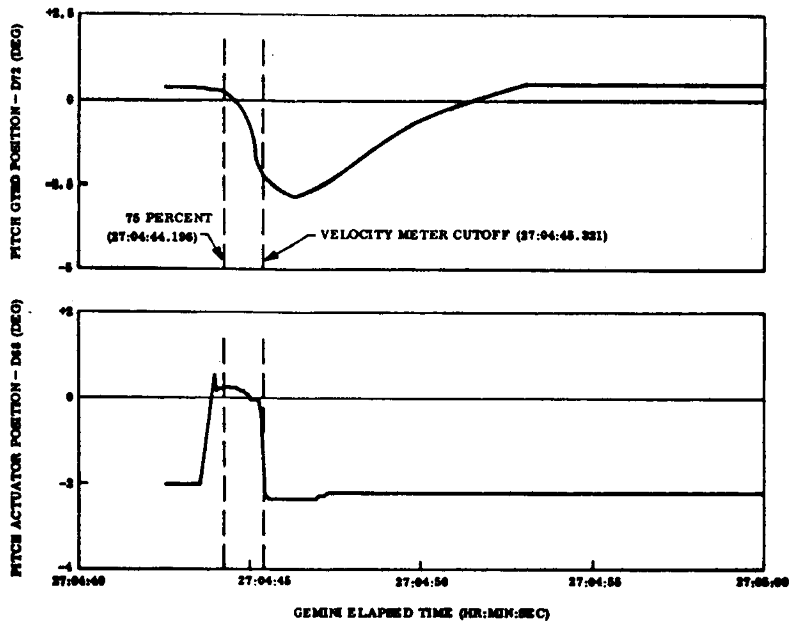

Fig. 3-52 Pitch Axis Control, Burn No. 3

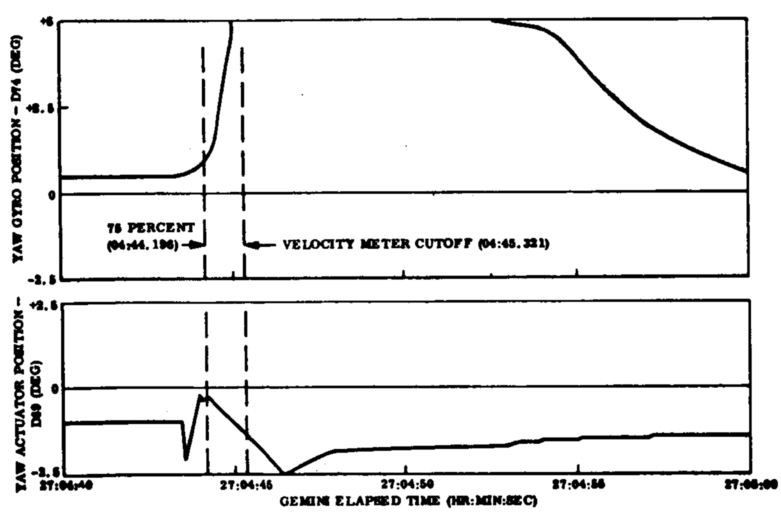

Fig. 3-53 Yaw Axis Control, Burn No. 3

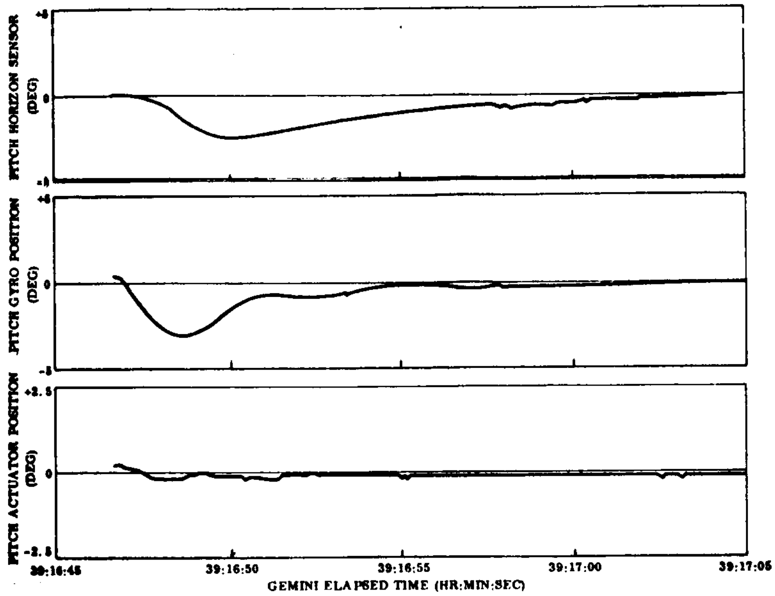

Fig. 3-54 Pitch Axis Control, Burn No. 4

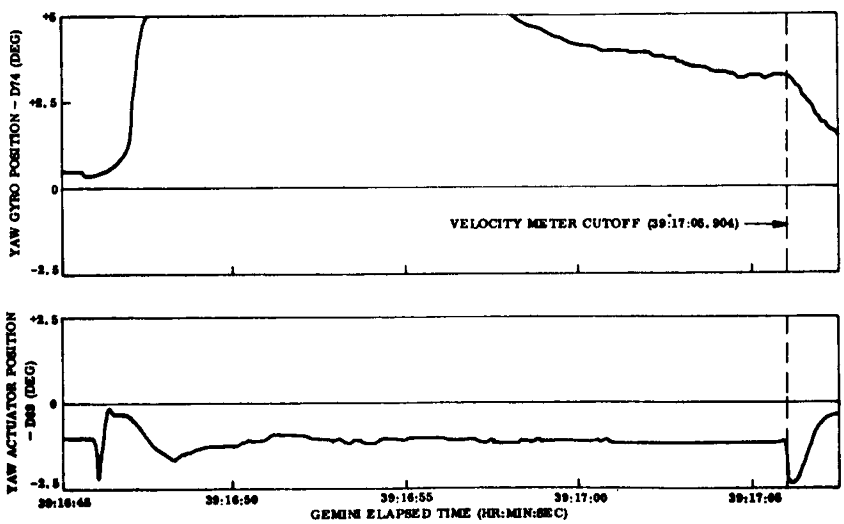

Fig. 3-55 Yaw Axis Control, Burn No. 4

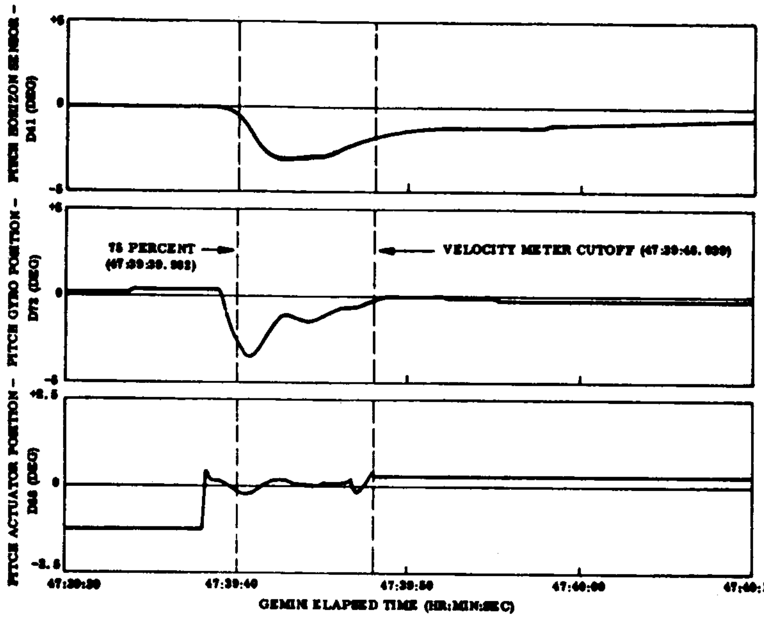

Fig. 3-56 Pitch Axis Control, Burn No. 6

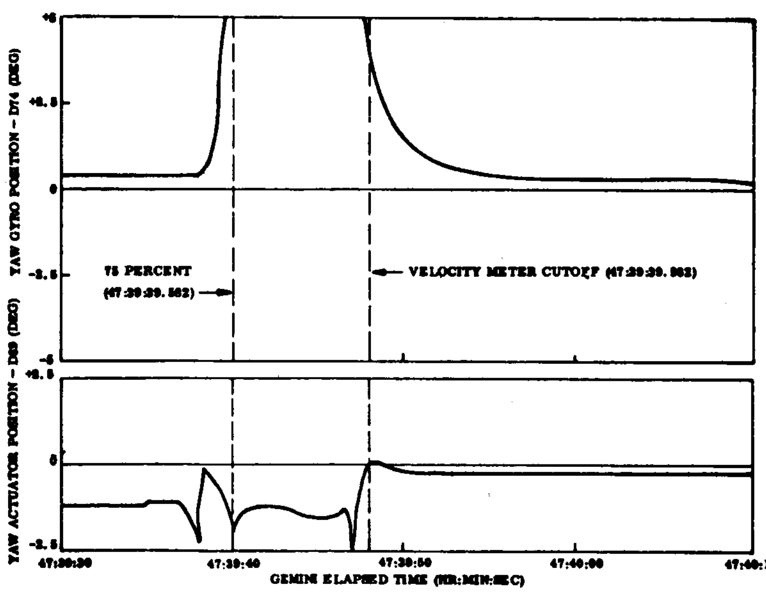

Fig. 3-57 Yaw Axis Control, Burn No. 6

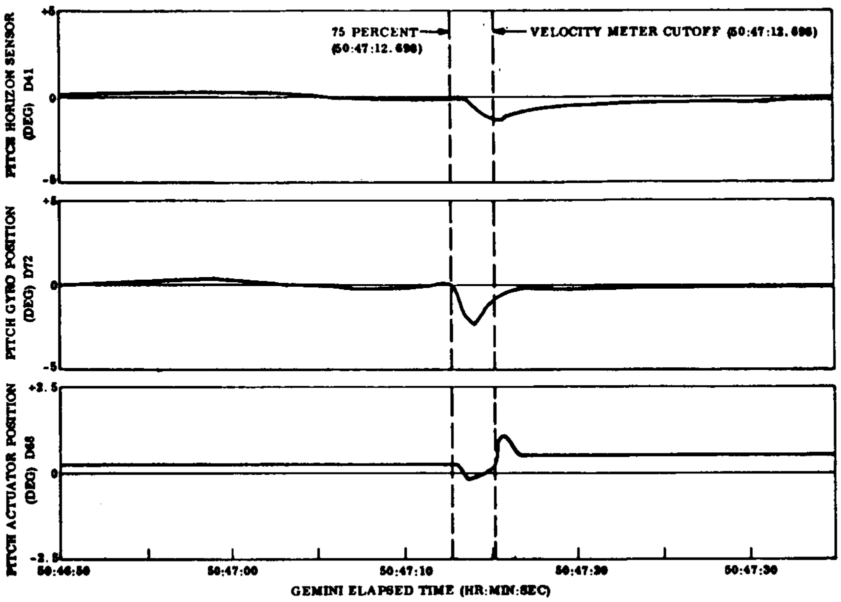

Fig. 3-58 Pitch Axis Control, Burn No. 7

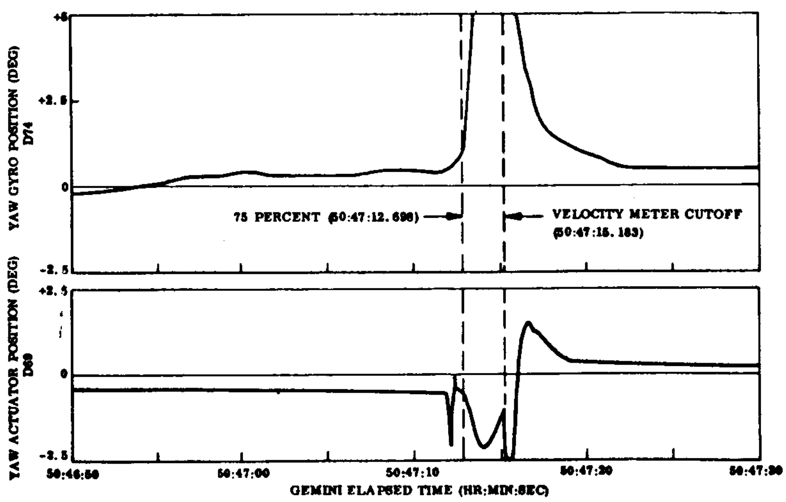

Fig. 3-59 Yaw Axis Control, Burn No. 7

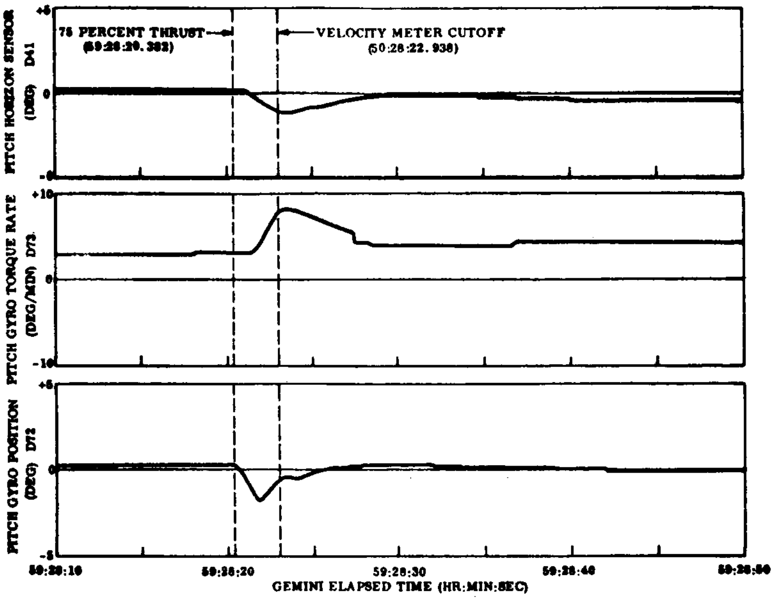

Fig. 3-60 Pitch Axis Control, Burn No. 9

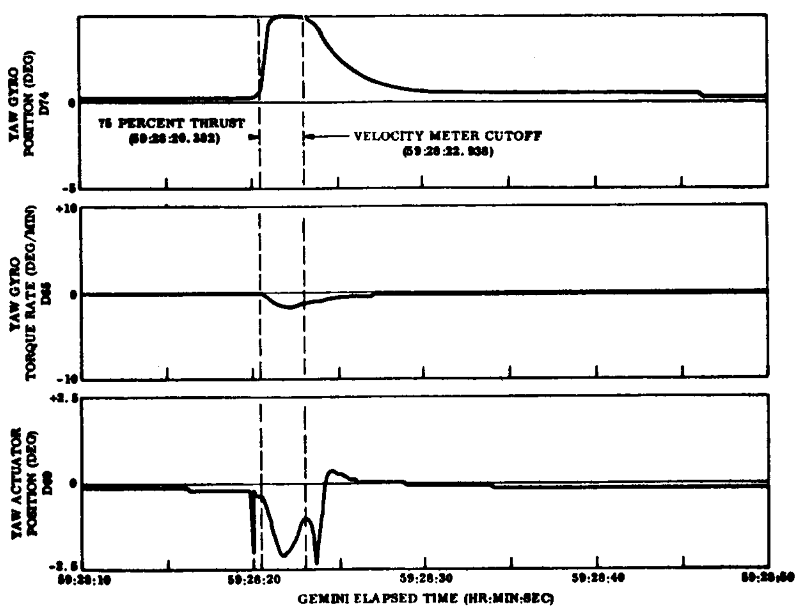

Fig. 3-61 Yaw Axis Control, Burn No. 9

velocity error and thereby reduce the accuracy of the achieved orbit. This is true only when PPS burns are used for out-of-plane maneuvers.

The second effect of this problem is the increased control gas consumption evidenced during and after the PPS burns. This was not noticeable during the ascent burn; however, with the short burns later in the flight it is quite evident (Fig. 3-41). The initial yaw excursion is normally removed or dampened by the hydraulic control system through movements of the hydraulic actuator such that the yaw error is removed and a steady-state condition is established with the actuator directing the line of thrust through the c.g. When the slow system response was combined with the short PPS burns, the hydraulic system was unable to overcome the transient and settle into a steady-state condition before the hydraulics were disabled at PPS cutoff. Therefore, the ACS was enabled with the yaw attitude and in some instances with the pitch attitudes off of the null position actuating the gas valves to return the vehicle to the attitude deadband. The amount of gas valve actuation was proportional to the attitude errors at time of ACS-enable.

An example of this is the second PPS burn (Figs. 3-50 and 3-51), which had a duration of approximately 1.2 sec. At ACS-enable the vehicle had a pitch attitude of -1.5 deg and a yaw attitude of +4.8 deg, and both were increasing. Combining these attitudes with roll, which is affected by turbine spin-down, resulted in approximately 7 sec of saturated gas valve activity with all axes being stable within their deadbands by 17 sec after PPS cutoff. The total gas usage from SPS Unit I firing to steady-state flight following PPS cutoff was 5 lb compared to a predicted 1 lb. Of this total 3.5 lb was consumed after PPS cutoff. This effect is apparent in varying degrees in the last eight PPS burns.

All other guidance parameters appeared nominal throughout the PPS burns.

3.5.3.2 SPS Unit II Burns. Two SPS Unit II burns were executed upon completion of the PPS burns. At this time data had not been received for the period covering the first SPS burn. From information received from MSC it is understood that this operation was nominal from the control standpoint and for control gas usage.

The second SPS operation appeared nominal as far as vehicle control is concerned (Fig. 3-62). The maximum attitude excursions indicated were approximately -0.9 deg in roll, -0.2 deg in pitch, and no offset in yaw. This indicates that the SPS alignment was nominal in pitch and yaw, but was apparently providing a roll torque. The control gas usage was 3 lb against a predicted 2 lb, and the excess usage, although relatively small, is probably the result of the roll torque due to SPS alignments. This again could be the result of c.g. location. The SPS operations were planned for execution with the PPS propellants depleted, and the units are aligned for this condition. The operations were conducted with approximately 6 sec of PPS propellants remaining, which would affect the thrust to c.g. alignment.

The overall operation of the guidance and control system during SPS thrusting was nominal.

3.5.3.3 Yaw Maneuver. Throughout the flight 14 yaw maneuvers were executed to reorient the vehicle. Performance of the guidance and control system during these maneuvers was nominal, with one exception: a drop in control gas regulator pressure during the first yaw maneuver.

Although all of the data on the yaw maneuvers have not yet been analyzed, it appears that the yaw maneuvers were executed at the low rate (1.5 deg/sec) in both the positive and negative directions. The maneuver executed during revolution 38, prior to the final PPS burn, has been evaluated and indicates an initial rate of 1.55 deg/sec, and a final rate of 1.65 deg/sec. During this maneuver, 1.5 lb of control gas was consumed compared to a predicted nominal usage of 1 lb. This operation was very close to nominal in all respects.

The single exception to nominal performance was noted during the first programmed Agena 90 deg yaw maneuver at GET 3:3:58.8. The ACS pressure was switched from low-mode to high-mode at 3:3:46.8 and should have remained in high-mode until 3:5:3.8, when ACS-low command was transmitted. However, when the yaw maneuver was initiated at 3:3:58.8, the ACS regulated pressure data indicated that the regulator

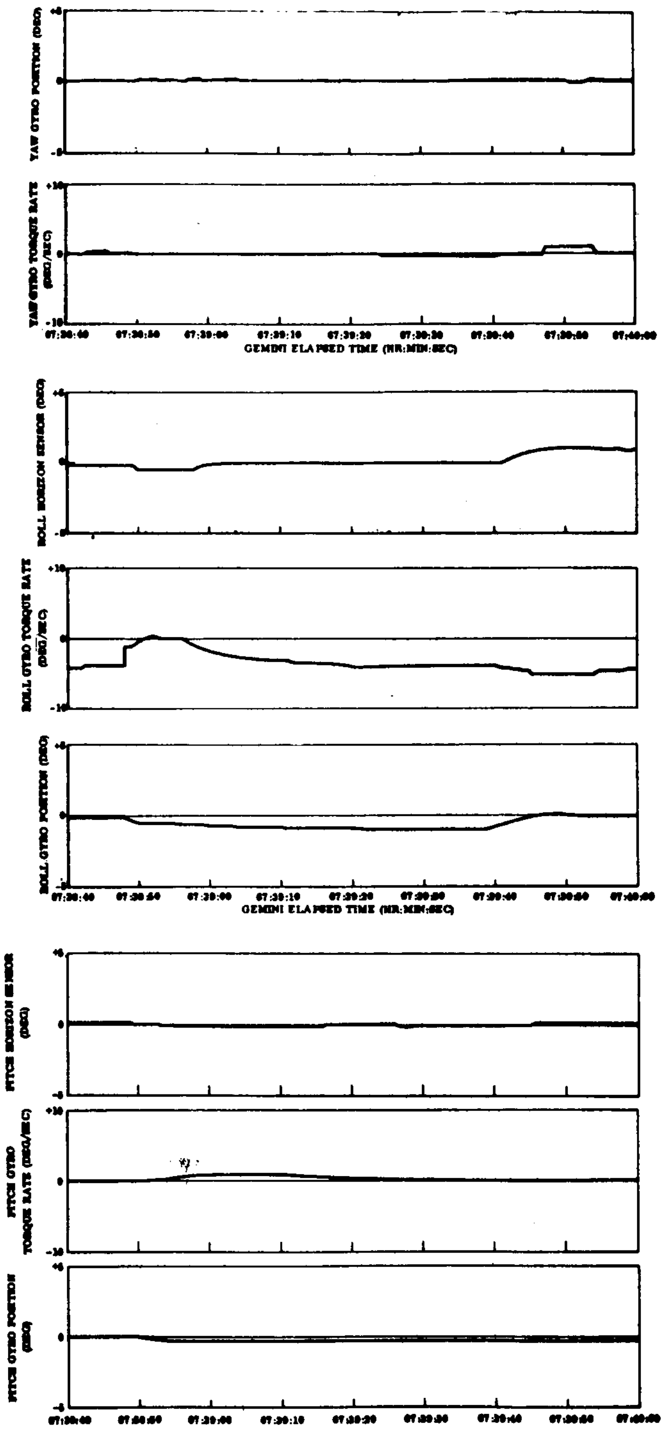

Fig. 3-62 SPS Burn No. 2, Revolution 43

was switched from high-mode to low-mode. Figure 3-63 presents programmed activity and regulator performance during the maneuver.

In an effort to explain the yaw maneuver anomaly, a failure mode investigation was initiated to determine what would cause the pneumatic regulator to switch from the high-pressure mode to the low-pressure mode in an unscheduled manner.

Results of the analysis show the following probable causes, in order of probability:

a. Electrical malfunction
b. Particle contamination
c. Mechanical malfunction

An electrical malfunction appears to be the most probable cause. Telemetered data of the regulator output supports this postulation; the pressure trace is typical of a normal high-to-low-mode pressure switching operation during a period of extensive gas valve activity.

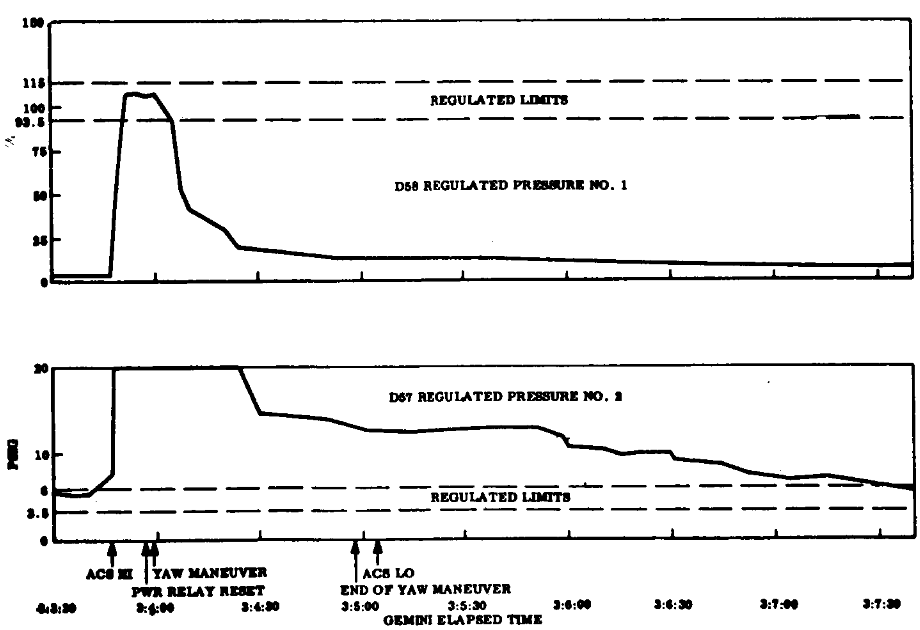

Fig. 3-63 ACS Pressure Regulator Performance During the 90-Deg Yaw Maneuver, Revolution 3

Particle contamination is a possibility, because of the presence of 5-micron filters assembled in series within the control passageways of the regulator. However, data do not substantiate performance parameters that would indicate a contaminated condition.

A mechanical malfunction in the mode switching mechanism is deemed the least probable. Without an electrical signal, it would require a force in excess of 4.5 lb to mechanically switch from high to low pressure; furthermore, subsequent data do not support this. The possibility of a coil spring failure is ruled out on the basis of satisfactory switching performance throughout the remainder of the flight. Bi-level event data during this phase of operation indicate that all commands given were correct and that no commands were given that would switch the regulator from high to low mode.

Conclusive evidence for the cause of the anomaly cannot be presented. A test, already completed on Vehicle 5004, duplicated the conditions of the inflight anomaly noted on Vehicle 5003. The vehicle was conditioned to the exact status of 5003 at the time of the anomaly, using the same commands and the same attitude control mode of operation. All resulting data indicated normal operation. It was impossible to duplicate the above anomaly. Furthermore, a review of test data over the past four years, including vendor qualification and acceptance tests, does not reveal any similar performance anomaly.

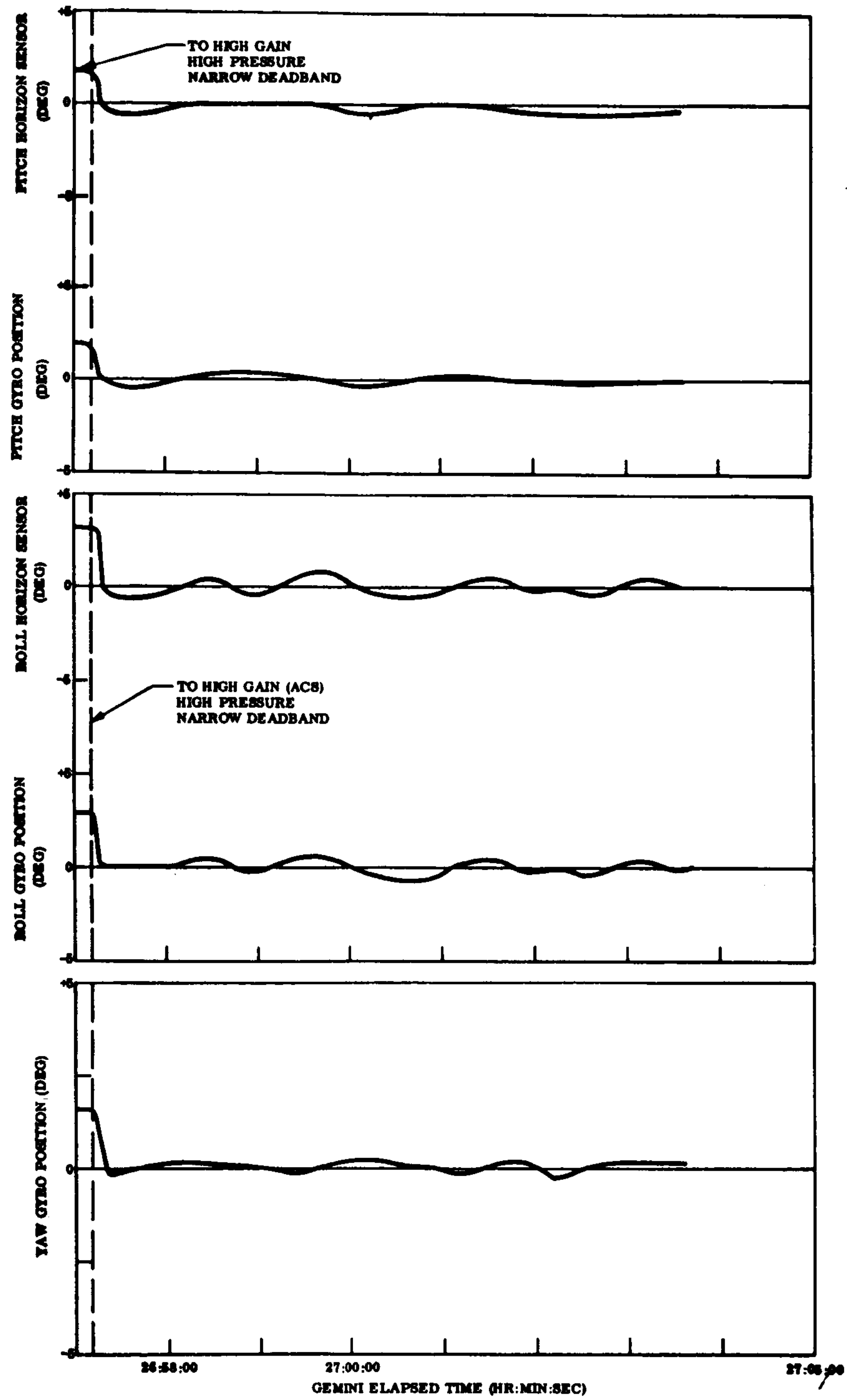

Fig. 3-64 Limit Cycles, Revolution 18

3.6 COMMUNICATIONS AND CONTROL SYSTEM

3.6.1 Launch and Ascent Performance

All C&C equipment performed properly and within specification during the launch and ascent phase. Excellent data was received from GATV 5003 from liftoff through loss-of-signal, which facilitated the quick look analysis prior to launching the Gemini spacecraft.

3.6.2 On-Orbit Performance

3.6.2.1 Telemetry. The telemeter performed perfectly for the entire life of the vehicle. All data (except for those data source anomalies discussed under Instrumentation) were of excellent quality and completely usable in the MCC data system. Acquisition was available at 5-deg antenna elevation at all locations. A typical pass signal strength plot is shown in Fig. 3-65. Prior to mission completion, an experiment was conducted during which it was shown that acquisition and ground station lock were available even when transmitting through the ascent antenna for approximately 2-1/2 hr with only a slight signal strength reduction at all sites. The telemeter was operated at a duty cycle of approximately 90 percent for the entire life of the vehicle. This is far in excess of the design expectation of a duty cycle in which continuous telemetering would be provided for the first three orbits and at 50 percent thereafter. Telemetry data acquisition during a 2-1/2-hr duration in the mod bus reverse configuration was found to be flawless. No problems were encountered with the vehicle or the ground station sites during the transition from Link 1 to Link 2.

3.6.2.2 Tape Recorder. A total of about 50 hr of tape recordings were obtained with excellent data quality. During the period of the spacecraft anomaly (Revolution 6), the tape recorder was operating. However, the tape recorder was not turned off in time to preserve all the data during this period, and only the last 3-1/2 min of

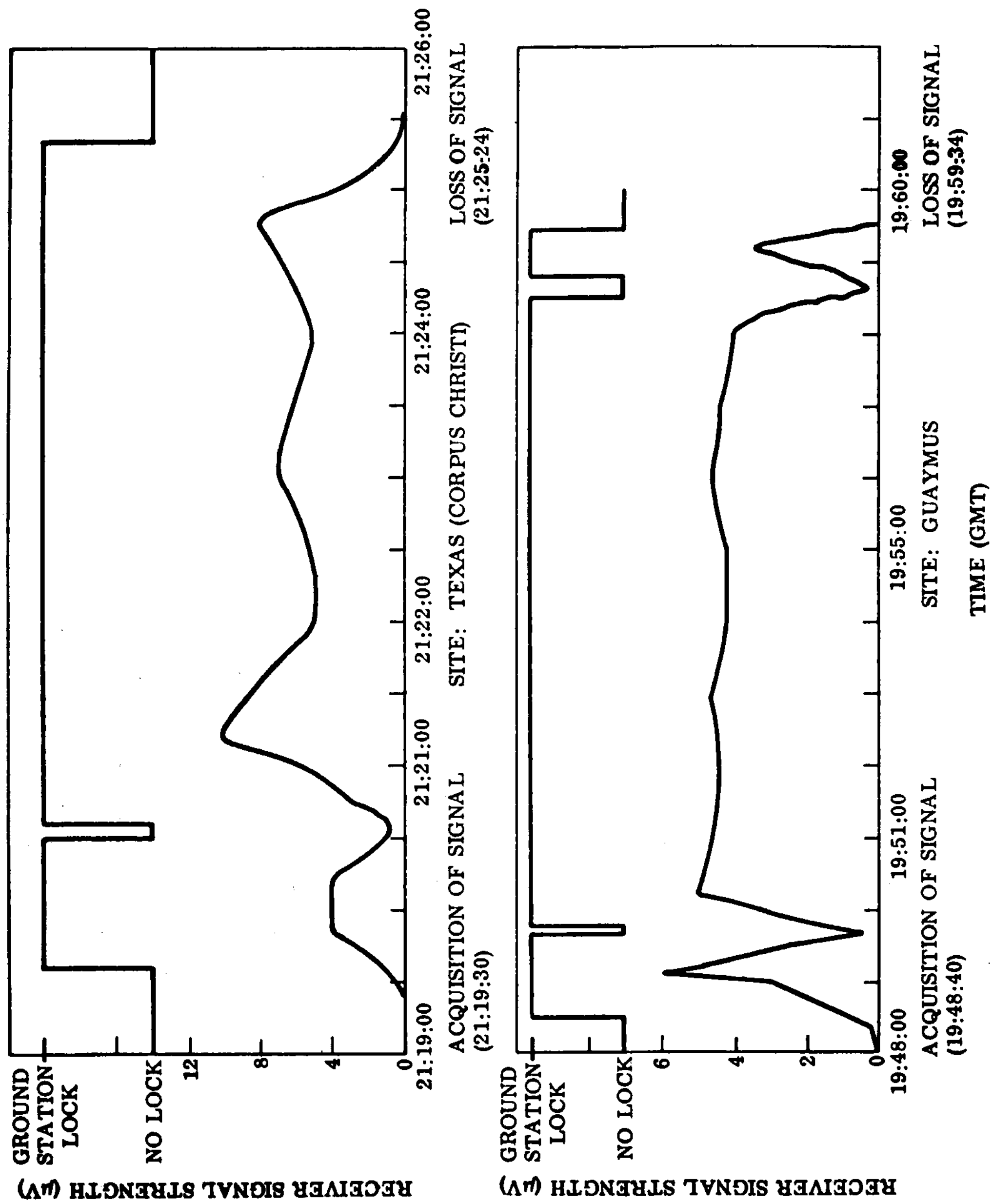

Fig. 3-65 Typical Telemetry Acquisition

data before undocking are available. This was sufficient, however, to show that GATV 5003 was behaving in a nominal manner considering the circumstances. Figure 3-66 shows the C&C activity during the period from approximately 3-1/2 min before undock. Due to the spacecraft roll and position there were intermittent periods when the spacecraft radar could not lock the decoder of the Agena transponder. During these periods of nonacquisition by the spacecraft, all ground commands transmitted were received and executed. After undocking, the vehicle was not in a stable condition because the attitude control system and horizon sensors were turned off. The tape recorder data do show the rapid return to a stable attitude after ACS and horizon sensors were commanded on.

3.6.2.3 Command System. A total of 5,439 commands were transmitted and accepted by GATV 5003 during the life of the vehicle. When the commands were properly transmitted by the source, there were no occasions when a command had to be retransmitted. Early in the mission, the MCC transmission rate exceeded the specified maximum of 1050 sub-bits per second, and retransmission was necessary. The commands transmitted and executed during the mission are summarized in Table 3-13. The types and sources of command are listed in Appendix A. During the life of the vehicle there were no spurious or erroneous executions. Furthermore, there were no spurious message acceptance pulses. All command modes – spacecraft L-band and hardline commands, ground RTCs and SPCs – were successfully employed. All commands were used at least once in the mission, except for the following:

CMD	
69	Pitch/Yaw High Rate
70	Pitch Rate Off
71	Pitch Rate On
83	PPS Start B
88	V/M to Mode IV Off
91	SPS 16-lb Thrust Initiate

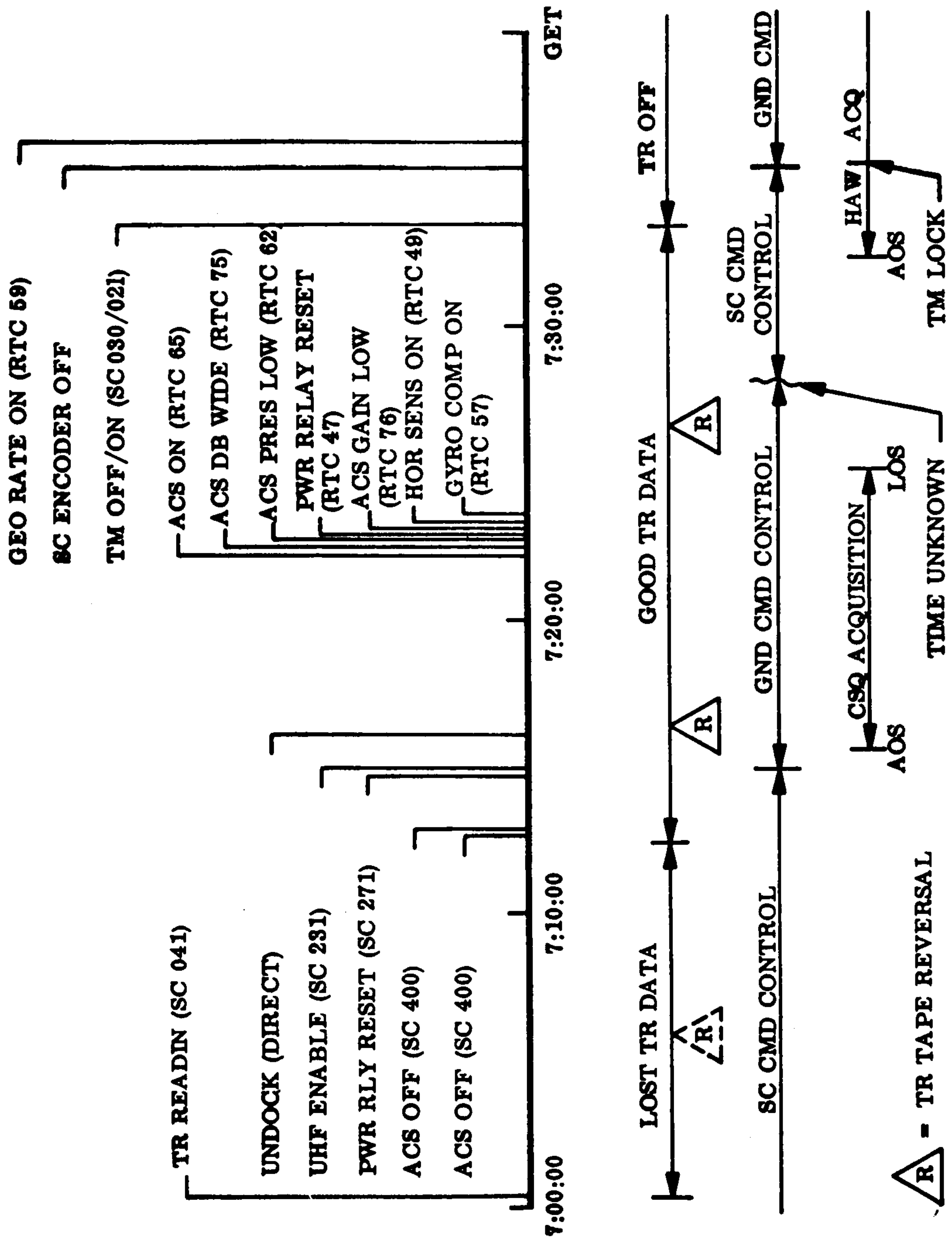

Fig. 3-66 Data Readout During Revolution 6

Table 3-13

COMMAND SYSTEM SUMMARY

Active Mission		
Real-Time Commands Transmitted and Executed (RTC)		848
Stored Program Commands Transmitted and Stored (SPC)		
Executed	409	
Erased (Because of Mission Changes)	255	
Erase Commands (All "O")	1151	
Total SPC	1815	1815
Spacecraft Commands Transmitted and Executed (SCC)		
L-Band	11	
Hardline	34	
Total SCC	45	45
Total Commands, Active Mission		2708
Commands Transmitted and Accepted after Mission		2731
Total Commands During Orbital Life of GATV 5003		5439

All of the 64 memory rows were properly loaded with desired commands. Of those stored commands that were executed, only 18 rows were not exercised for any command execution. (This was due to these rows being reloaded by all zeros in preparation for a new command load.) During the mission, 20 emergency reset timer (ERT) reset commands were executed, ranging from a minimum of 1 hr between reset commands to a maximum of 7 hr between reset commands. In the post-mission activities, the ERT was allowed to time out, and the time was 77 sec from expected time. (Specification limit is ±324 sec.)

Vehicle clock reset was performed successfully to coincide with GMT. Due to ground station problem with verifying the proper memory load, the initial reset was not performed because the memory was inhibited from executing the stored commands at the time reset would have been accomplished. Figure 3-67 shows the execution time for clock reset and the apparent drift of vehicle time in respect to GMT. The first reset was 1 sec in error due to the improper time label associated with the command as established by the ground station.

3.6.2.4 Instrumentation. The instrumentation system permitted monitoring of 185 analog and direct measurements, 47 bi-level status indicators, and memory readout of the 64-row memory for a total of 296 measurements. Operation of the instrumentation system was satisfactory and provided adequate data coverage for all portions of the flight. The following instrumentation anomalies were noted:

a. A14-A/A separation monitor did not provide the expected signal upon Agena/Atlas separation. Three steps of 1.25 volts each were expected, but the first step was 4.3 volts, the second step was 5.0 volts, and the third step was not seen. However, this measurement, in conjunction with activation of the Agena attitude control system, did provide enough data to determine the separation rate. Tests have shown this to be a problem of mechanical resonance in the switch actuation arm, and action has been taken to correct this problem.
b. A523-Accel Z No. 1 (TDA) measurement was inoperative during ascent from +140.9 to +201.8 sec. At all other times its operation was normal.
c. B184-Nozzle extension skin temperature No. 1 measurement was probably detached from the nozzle extension after orbit injection and is believed to have been suspended within the plume of the +Y 16-lb SPS engine, because its temperature indication increased each time this particular 16-lb engine was fired. It gave no indication of a PPS burn. All other propulsion system instrumentation was nominal throughout the mission.
d. Status Bit 50, Status display bright/dim, indicated that the display was on bright when it should have been on dim. The signal condition for this measurement would hold the status gate in a "1" condition if the dim bus were 14v dc or greater. The dim bus can vary from 12v dc to 18v dc, dependent upon main bus voltage and the display light loading.

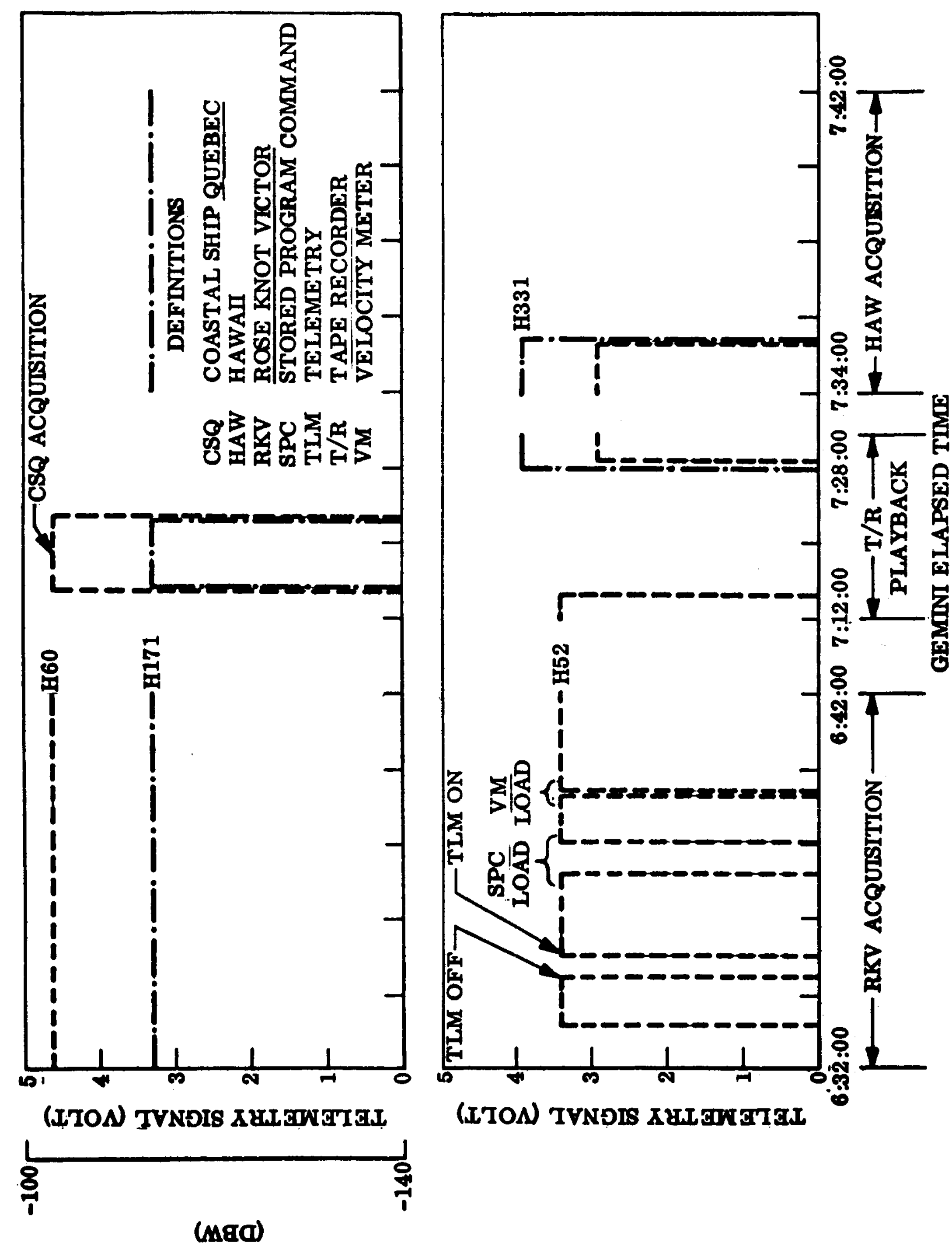

Fig. 3-67 Command Activity

As the main bus was 27.8v dc and the display current load was not at a maximum, the dim bus voltage was at least 14v dc. Tests are in process to determine the main bus voltage at which status bit 50 will function properly.

3.6.2.5 Tracking System. The performance of the tracking system conformed to the design requirements. The temperatures of C- and S-band transponders were higher than expected, but stayed well within the design limitations. The reason for higher than expected temperature is that the thermal analysis was based on a 27 percent duty cycle,. whereas the actual transponder duty cycle was much higher (90 percent on C-band and 73 percent on S-band).

3.6.2.6 UHF Receiver. The performance of the UHF receiver was in accordance with the design requirements throughout the flight. The data shows that phase lock occurred at an input signal level of about -131 dbw. The temperature of the UHF receiver varied between 78° F and 96.7° F and that of transmitter No. 2 varied between 42° F and 72° F The primary reason for this difference is that transmitter No. 1 was on 90 percent of the time, whereas transmitter No. 2 was on for 7 percent of the time.

3.7 RELIABILITY

Equipment performance during Gemini VIII was satisfactory. The most significant anomaly was the yaw c. g. offset, which did not interfere with the accomplishment of mission objectives.

3.7.1 Reliability Prediction

The estimated reliability for GATV 5003, as presented in the most recent GATV Reliability Estimate and Analysis Report (LMSC-A605200-10, Classified Appendix, 30 July 1965) and modified in the GATV Program Progress Report (LMSC-A605200-16) for December 1965 was 0. 676.

3.7.2 Product Assurance Review of Flight

During ascent and subsequent PPS engine firing, the vehicle experienced a yaw c. g. displacement. This was not the result of equipment malfunction. None of the other anomalies that were observed interfered with the accomplishment of mission objectives.

The primary propulsion system performed satisfactorily during the flight of 5003. A total of 9 PPS burns (including ascent) and 11 SPS burns (including propellant orientation firings) were achieved. The mission requirement was for a maximum of 5 PPS burns.

Aerospace ground equipment satisfactorily supported the checkout of launch of the vehicle. Pad damage was minimal.

The flight of Vehicle 5003 has been categorized as a three-sigma ascent and orbit success and will be recorded as such in the Agena Ascent Flight History Summary dated 1 April 1966.

Investigations have been conducted to fully determine the effects of all flight anomalies. All corrective action judged to be necessary has been, or is being, taken.

Section 4
CONCLUSIONS AND RECOMMENDATIONS

Section 4
CONCLUSIONS AND RECOMMENDATIONS

GATV 5003 was launched on schedule after an uninterrupted countdown. All subsystems of the GATV functioned within design parameters, and the telemeter and radar tracking data received by the Manned Space Flight Network stations indicated nominal performance from liftoff through 45 orbital revolutions, which constitute the scope of this report.

The outstanding success of the GATV 5003 during the programmed maneuvers shows the adequacy of the change programs recommended in GATV 5002 Systems Test Evaluation, LMSC-A774454, (C), dated 9 Dec 1965 and instituted after a thorough analysis and evaluation of the GATV 5002 flight results. The change programs consisted mainly of: "Project Sure-Fire", a modification and test program which installed an oxidizer manifold-pressure switch and an oxidizer discharge-pressure switch coupled so as to prohibit fuel lead into the combustion chamber; relocation of sensitive accelerometers and shock mounting aft rack equipments in the separation shock area; and revision of the electrical power to the PPS so as to bypass the turbine overspeed shutdown gate.

4.1 CONCLUSIONS

1. Tracking data indicated that the vehicle was injected into a nearly perfect circular orbit at 161 nm. An incremental velocity of 8246 ft/sec was imparted to the GATV by the Primary Propulsion System at velocity meter cutoff. The computer simulation of the ascent portion of the flight and examination of flight data indicated that the wind environment was not severe and did not create loading conditions beyond the predicted structural or control capability of the vehicle.

2. A temporary loss of TDA accelerometer A523 was experienced during the ascent portion of the flight; however, after recovery it remained nominal for the remainder of the mission. Some slosh motion was observed during the orbital burns, although the accelerations were not excessive as compared to other missions.

3. All Primary Propulsion System objectives were met. The PPS provided the required impulse to attain orbit as well as an orbit apogee/perigee adjust and plane changes. Due to precise orbit attainment, the PPS was not called upon for either plane or phase adjust to effect rendezvous and docking with Gemini VIII. The multiple-restart capability was demonstrated by eight successful PPS restarts on orbit with data indicating no anomalous performance during any restart. The tankage, feed and load, and engine vent systems performed as predicted with data indicating no leakage in either main propellant tank. Therefore, proper pressure bias was maintained throughout Vehicle 5003 useful life.

4. The Secondary Propulsion System was operated 11 times and performed satisfactorily during the entire Agena mission. Some slight variations in pressure were experienced during the ascent burn; however, the performance was within specification limits, and this variation did not occur during subsequent burns.

5. Vehicle Electrical Power performance was nominal through the 45 revolutions and satisfactory power levels for 8 1/2 days were substantiated by random data samples from Texas Tracking Station.

6. All Guidance and Control systems performed satisfactorily throughout the flight. The flight control electronics, hydraulic control system, and pneumatics properly compensated for the yaw c. g. offset. The velocity meter provided the programmed cutoff for each burn. Pneumatic operation was satisfactory with the exception of a short duration pressure drop of the attitude control gas regulator during the first yaw attitude change on Revolution 3.

7. The Communications and Control system performed satisfactorily during the Gemini VIII mission and subsequent Agena maneuvers. PCM telemetry performance, beacon tracking response, and command performance were very satisfactory. Instrumentation performance was nearly perfect.

8. Thermodynamic evaluation of the flight data received through the forty-fifth revolution indicates that the thermal design of the Gemini forward equipment racks, tanks, and aft rack is satisfactory.

4.2 RECOMMENDATIONS

The GATV systems have now been adequately tested in a space environment, and all systems performed as programmed and predicted.

There is only one significant recommendation resulting from the Gemini VIII flight: correction of the c. g. offset. To provide predictable attitude control capability, the c. g. of the vehicle will be placed on the longitudinal axis. This will be accomplished by removal of one Type XVII and one Type I-C battery and the addition of sufficient ballast to locate the c. g. on the longitudinal axis.

All other recommendations are in the nature of product improvements that will be submitted to the appropriate Customer agency for consideration.

Appendix A

COMMANDS EXECUTED BY GATV 5003

Table A-1

TOTAL COMMANDS EXECUTED BY GATV 5003

Command Source	RTC Commands	SPC Commands	Total Commands
Spacecraft*	45	–	45
Canary Islands (CYI)	154	195	349
Rose Knot Victor (RKV)	97	241	338
Carnarvon (CRO)	151	286	437
Coastal Ship Quebec (CSQ)	118	479	597
Eastern Test Range (ETR)	141	486	627
Hawaii (HAW)	87	128	215
TOTAL	893	1815	2708
Corpus Christi (TEX)	2731**		2731
TOTAL VEHICLE COMMANDS			5439

*Spacecraft Commands: 11 L-Band Link
34 Hardline

**Command Breakdown Not Available.

Table A-2

STORED COMMANDS UTILIZED FOR VEHICLE ACTIVITY

Activity	Executed	Cleared	Scrubbed	Cum. Total
Minus 90 Deg Yaw	27			27
		128		155
Docked Yaw			54	209
Memory and Guidance Test	19	62		290
Hohmann Transfer (Burn No. 2)	18	46		354
Circularization (Burn No. 3)	21			375
		64		439
Plane Change (Burn No. 4)	36	128	80	683
		64		747
MTI Adjust (Burn No. 5)	30			777
		64		841
INCL Adjust (Burn No. 6)	40			881
		64		945
Height Adjust (Burn No. 7)	30			975
		64		1039
Height Adjust (Burn No. 8)	32	64		1135
		64		1199
Height Adjust (Burn No. 9)	30			1229
		64		1293
SPS Translation (Burn No. 10)	37		37	1367
		64		1431
SPS Translation (Burn No. 11)	20	44		1495
		64		1559
SPS Translation (Burn No. 12)		44	20	1623
Vehicle Time-Word Special Test	28		100	1751
Mission Shutdown	5	59		1815
TOTAL	373	1151	291	1815

Table A-3

COMMANDS FOR MINUS 90 DEGREE YAW

Cmd	Event	Agena Time of Execution
9	Tape Recorder On – Record	0.016
78	ACS Gain High – Undocked	1:00.047
74	ACS Deadband Narrow	1:00.062
63	ACS Pressure High	1:00.078
50	Roll H/S to Yaw IRP On	1:02.031
47	Power Relay Reset	1:10.094
66	Pitch/Yaw Minus	1:10.109
68	Pitch/Yaw Low Rate	1:10.125
58	Geocentric Rate Off	1:11.141
73	Yaw Rate On (3:03.58)	1:12.156
51	Pitch H/S to Yaw IRP On	1:12.171
53	H/S to Yaw In Phase	1:12.188
60	Geocentric Rate Reverse	1:12.203
72	Yaw Rate Off	2:11.219
59	Geocentric Rate On	2:12.234
57	Gyrocompassing On	2:12.250
76	ACS Gain Low	2:17.265
75	ACS Deadband Wide	2:17.281
62	ACS Pressure Low	2:17.297
47	Power Relay Reset	2:27.313
6	TLM Off	2:29.328
5	TLM On	2:29.344

Table A-4

COMMANDS FOR HOHMANN TRANSFER (BURN NO. 2)

Cmd	Event	Agena Time of Execution
9	Tape Recorder On – Record	00.016
78	ACS Gain High – Undocked	02.047
74	ACS Deadband Narrow	02.062
63	ACS Pressure High	02.078
50	Roll H/S to Yaw IRP On	04.031
47	Power Relay Reset	12.094
81	PPS Start "C" (21:42:31)	6:12.109
94	Hydraulics Gain – Undocked	6:12.125
85	V/M Enable	6:27.141
80	PPS Cutoff (Backup)	7:39.156
84	V/M Disable	8:39.171
57	Gyrocompassing On	8:39.188
76	ACS Gain Low	8:44.203
75	ACS Deadband Wide	8:44.219
62	ACS Pressure Low	8:44.234
47	Power Relay Reset	8:54.250
6	TLM Off	8:56.265
5	TLM On	8:56.281

Table A-5

COMMANDS FOR CIRCULARIZATION (BURN NO. 3)

Cmd	Event	Agena Time of Execution
9	Tape Recorder On – Record	00.016
78	ACS Gain High – Undocked	2.047
74	ACS Deadband Narrow	2.062
63	ACS Pressure High	2.078
50	Roll H/S To Yaw IRP On	4.031
47	Power Relay Reset	12.094
81	PPS Start "C" (27:03:19)	6:12.109
94	Hydraulics Gain – Undocked	6:12.125
85	V/M Enable	6:27.141
80	PPS Cutoff (Backup)	7:39.156
84	V/M Disable	9:40.171
57	Gyrocompassing On	9:40.188
76	ACS Gain Low	9:45.203
75	ACS Deadband Wide	9:45.219
62	ACS Pressure Low	9:45.234
47	Power Relay Reset	9:55.250
6	TLM Off	9:57.265
5	TLM On	9:57.281

Table A-6

COMMANDS FOR PLANE CHANGE (BURN NO. 4)

Cmd	Event	Agena Time of Execution
9	Tape Recorder On – Record	0.016
22	Arm/Stop Disable	1.500
78	ACS Gain High – Undocked	2.047
74	ACS Deadband Narrow	2.062
63	ACS Pressure High	2.078
51	Pitch H/S to Yaw IRP On	4.031
47	Power Relay Reset	12.094
66	Pitch/Yaw Minus	6:12.109
68	Pitch/Yaw Low Rate	6:12.125
58	Geocentric Rate Off	6:13.141
73	Yaw Rate On	6:13.156
82	PPS Start "A" (39:16:10)	6:15.360
94	Hydraulics Gain – Undocked	6:15.375
72	Yaw Rate Off	6:16.656
85	V/M Enable	6:30.391
59	Geocentric Rate On	6:30.406
80	PPS Cutoff (Backup)	7:12.422
84	V/M Disable	8:13.438
67	Pitch/Yaw Plus	8:13.453
58	Geocentric Rate Off	8:14.469
73	Yaw Rate On	8:15.485
72	Yaw Rate Off	8:17.171
59	Geocentric Rate On	8:18.188
57	Gyrocompassing On	8:18.203
76	ACS Gain Low	8:23.219
75	ACS Deadband Wide	8:23.234
62	ACS Pressure Low	8:23.250
23	Arm/Stop Enable	8:32.516
47	Power Relay Reset	8:33.265
6	TLM Off	8:35.281
5	TLM On	8:35.297

Table A-7

COMMANDS FOR MTI ADJUST (BURN NO. 5)

Cmd	Event	Agena Time of Execution
9	Tape Recorder On – Record	0.016
22	Arm/Stop Disable	1.453
78	ACS Gain High – Undocked	2.047
74	ACS Deadband Narrow	2.062
63	ACS Pressure High	2.078
51	Pitch H/S To Yaw IRP On	4.031
47	Power Relay Reset	12.094
66	Pitch/Yaw Minus	12.109
68	Pitch/Yaw Low Rate	12.125
58	Geocentric Rate Off	13.141
73	Yaw Rate On	14.156
50	Roll H/S to Yaw IRP On	14.171
52	H/S to Yaw Out of Phase	14.188
60	Geocentric Rate Reverse	14.203
72	Yaw Rate Off	1:14.219
59	Geocentric Rate On	1:15.234
57	Gyrocompassing On	1:15.250
81	PPS Start "C" (44:01:06)	7:15.265
94	Hydraulics Gain Undocked	7:15.281
85	V/M Enable	7:30.297
80	PPS Cutoff (Backup)	8:41.313
84	V/M Disable	9:42.328
57	Gyrocompassing On	9:42.344
76	ACS Gain Low	9:47.360
75	ACS Deadband Wide	9:47.375
62	ACS Pressure Low	9:47.391
47	Power Relay Reset	9:57.406
23	Arm/Stop Enable	9:58.469
6	TLM Off	9:59.422
5	TLM On	9:59.438

Table A-8

COMMANDS FOR INCL ADJUST (BURN NO. 6)

Cmd	Event	Agena Time of Execution
9	Tape Recorder On – Record	0.016
22	Arm/Stop Disable	1.485
78	ACS Gain High – Undocked	2.047
74	ACS Deadband Narrow	2.062
63	ACS Pressure High	2.078
50	Roll H/S to Yaw IRP On	4.031
47	Power Relay Reset	12.094
67	Pitch/Yaw Plus	12.109
68	Pitch/Yaw Low Rate	12.125
58	Geocentric Rate Off	13.141
73	Yaw Rate On	14.156
51	Pitch H/S to Yaw IRP On	14.171
53	H/S to Yaw In Phase	14.188
60	Geocentric Rate Reverse	14.203
72	Yaw Rate Off	1:14.219
59	Geocentric Rate On	1:15.234
57	Gyrocompassing On	1:15.250
66	Pitch/Yaw Minus	7:15.265
58	Geocentric Rate Off	7:16.281
73	Yaw Rate On	7:17.297
82	PPS Start "A" (47:39:02)	7:17.906
94	Hydraulics Gain – Undocked	7:17.922
72	Yaw Rate Off	7:24.984
85	V/M Enable	7:32.938
59	Geocentric Rate On	7:32.953
80	PPS Cutoff (Backup)	8:04.969
84	V/M Disable	9:04.453
67	Pitch/Yaw Plus	9:06.000
58	Geocentric Rate Off	9:06.313
73	Yaw Rate On	9:07.328

Table A-8 (Cont.)

Cmd	Event	Agena Time Of Execution
72	Yaw Rate Off	9:14.344
59	Geocentric Rate On	9:15.360
57	Gyrocompassing On	9:15.375
76	ACS Gain Low	9:20.391
75	ACS Deadband Wide	9:20.406
62	ACS Pressure Low	9:20.422
47	Power Relay Reset	9:30.438
23	Arm/Stop Enable	9:31.500
6	TLM Off	9:32.469
5	TLM On	9:32.516

Table A-9

COMMANDS FOR HEIGHT ADJUST (BURN NO. 7)

Cmd	Event	Agena Time of Execution
9	Tape Recorder On – Record	00.016
22	Arm/Stop Disable	1.453
78	ACS Gain High – Undocked	2.047
74	ACS Deadband Narrow	2.062
63	ACS Pressure High	2.078
51	Pitch H/S to Yaw IRP On	4.031
47	Power Relay Reset	12.094
66	Pitch/Yaw Minus	12.109
68	Pitch/Yaw Low Rate	12.125
58	Geocentric Rate Off	13.141
73	Yaw Rate On	14.156
50	Roll H/S to Yaw IRP On	14.171
52	H/S to Yaw Out of Phase	14.188
60	Geocentric Rate Reverse	14.203
72	Yaw Rate Off	1:13.219
59	Geocentric Rate Off	1:15.234
57	Gyrocompassing On	1:15.250
82	PPS Start "A" (50:46:35)	7:15.265
95	Hydraulics Gain – Docked	7:15.281
85	V/M Enable	7:30.297
80	PPS Cutoff (Backup)	7:57.313
84	V/M Disable	8:56.328
57	Gyrocompassing On	8:56.344
76	ACS Gain Low	9:01.360
75	ACS Deadband Wide	9:01.375
62	ACS Pressure Low	9:01.391
47	Power Relay Reset	9:11.406
23	Arm/Stop Enable	9:12.469
6	TLM Off	9:13.422
5	TLM On	9:13.438

Table A-10

COMMANDS FOR HEIGHT ADJUST (BURN NO. 8)

Cmd	Event	Agena Time Of Execution
9	Tape Recorder On – Record	00.016
22	Arm/Stop Disable	1.453
78	ACS Gain High – Undocked	2.047
74	ACS Deadband Narrow	2.062
63	ACS Pressure High	2.078
50	Roll H/S to Yaw IRP On	4.031
47	Power Relay Reset	12.094
67	Pitch/Yaw Plus	12.109
68	Pitch/Yaw Low Rate	12.125
58	Geocentric Rate Off	13.141
73	Yaw Rate On	14.156
50	Roll H/S to Yaw IRP On	14.171
53	H/S to Yaw In Phase	14.188
61	Geocentric Rate Normal	14.203
72	Yaw Rate Off	2:14.219
59	Geocentric Rate On	2:15.234
57	Gyrocompassing On	2:15.250
82	PPS Start "A" (54:38:51)	8:15.265
95	Hydraulics Gain-Docked	8:15.281
85	V/M Enable	8:30.297
80	PPS Cutoff (Backup)	8:56.313
84	V/M Disable	9:56.328
57	Gyrocompassing On	9:56.344
76	ACS Gain Low	10:01.360
75	ACS Deadband Wide	10:01.375
62	ACS Pressure Low	10:01.391
47	Power Relay Reset	10:11.406
23	Arm/Stop Enable	10:12.469
6	TLM Off	10:13.422
5	TLM On	10:13.438

Table A-11

COMMANDS FOR HEIGHT ADJUST (BURN NO. 9)

Cmd	Event	Agena Time Of Execution
9	Tape Recorder On – Record	0.016
22	Arm/Stop Disable	1.453
78	ACS Gain High – Undocked	2.047
74	ACS Deadband Narrow	2.062
63	ACS Pressure High	2.078
50	Roll H/S to Yaw IRP On	4.031
47	Power Relay Reset	12.094
67	Pitch/Yaw Plus	12.109
68	Pitch/Yaw Low Rate	12.125
58	Geocentric Rate Off	13.141
73	Yaw Rate On	14.156
50	Roll H/S to Yaw IRP On	14.171
52	H/S to Yaw Out of Phase	14.188
60	Geocentric Rate Reverse	14.203
72	Yaw Rate Off	2:14.219
59	Geocentric Rate On	2:15.234
57	Gyrocompassing On	2:15.250
82	PPS Start "A" (59:27:43)	8:15.265
95	Hydraulics Gain Docked	8:15.281
85	V/M Enable	8:30.297
80	PPS Cutoff (Backup)	8:57.313
84	V/M Disable	9:57.328
57	Gyrocompassing On	9:57.344
76	ACS Gain Low	10:02.360
75	ACS Deadband Wide	10:02.375
62	ACS Pressure Low	10:02.391
47	Power Relay Reset	10:12.406
23	Arm/Stop Enable	10:13.469
6	TLM Off	10:14.422
5	TLM On	10:14.438

Table A-12

COMMANDS FOR SPS TRANSLATION (BURN NO. 10)

Cmd	Event	Agena Time of Execution
9	Tape Recording On – Record	0.016
22	Arm/Stop Disable	1.453
78	ACS Gain High – Undocked	2.047
74	ACS Deadband Narrow	2.062
63	ACS Pressure High	2.078
50	Roll H/S to Yaw IRP On	4.031
47	Power Relay Reset	12.094
66	Pitch/Yaw Minus	12.109
68	Pitch/Yaw Low Rate	12.125
58	Geocentric Rate Off	13.141
73	Yaw Rate On	14.156
51	Pitch H/S to Yaw IRP On	14.171
52	H/S to Yaw Out of Phase	14.188
61	Geocentric Rate Normal	14.203
72	Yaw Rate Off	1:14.219
59	Geocentric Rate On	1:15.234
57	Gyrocompassing On	1:15.250
62	ACS Pressure Low	1:16.485
47	Power Relay Reset	1:26.500
79	ACS Gain High – Docked	7:03.531
63	ACS Pressure High	7:04.547
74	ACS Deadband Narrow	7:12.562
51	Pitch H/S to Yaw IRP On	7:13.578
47	Power Relay Reset	7:14.594
93	SPS Ready (64:30:30)	7:15.265
85	V/M Enable	7:30.281
92	SPS 200-lb Thrust Initiate	7:31.297
90	SPS Cutoff (Prime)	7:52.313
84	V/M Disable	8:02.328
57	Gyrocompassing On	8:02.344

Table A-12 (Cont.)

Cmd	Event	Agena Time of Execution
76	ACS Gain Low	8:07.360
75	ACS Deadband Wide	8:07.375
62	ACS Pressure Low	8:07.391
47	Power Relay Reset	8:17.406
23	Arm/Stop Enable	8:18.469
6	TLM Off	8:19.422
5	TLM On	8:19.438

Table A-13

COMMANDS FOR SPS TRANSLATION (BURN NO. 11)

Cmd	Event	Agena Time of Execution
9	Tape Recorder On – Record	0.078
22	Arm/Stop Disable	1.360
79	ACS Gain High – Docked	2.109
51	Pitch H/S to Yaw IRP On	4.094
74	ACS Deadband Narrow	6:00.125
63	ACS Pressure High	6:01.141
47	Power Relay Reset	6:11.156
93	SPS Ready (67:38:32)	6:12.171
85	V/M Enable	6:27.188
92	SPS 200# Thrust Initiate	6:28.203
90	SPS Cutoff (Prime)	7:19.219
84	V/M Disable	7:29.234
57	Gyrocompassing On	7:29.250
76	ACS Gain Low	7:34.265
75	ACS Deadband Wide	7:34.281
62	ACS Pressure Low	7:34.297
47	Power Relay Reset	7:44.313
23	Arm/Stop Enable	7:45.375
6	TLM Off	7:46.328
5	TLM On	7:46.344

Table A-14

COMMANDS FOR VEHICLE TIME – WORD SPECIAL TEST

Cmd	Event	Gemini Elapsed Time
2	S-Band Beacon On	69:53:46
1	C-Band Beacon On	69:53:46
5	TLM On	69:56:16
6	TLM Off	70:07:33
10	C- & S-Band Beacons Off	70:12:13
2	S-Band Beacon On	70:21:01
1	C-Band Beacon On	70:21:01
5	TLM On	70:23:31
6	TLM Off	70:58:03
5	TLM On	71:34:26
6	TLM Off	71:45:44
10	C- & S-Band Beacons Off	71:48:03
1	C-Band Beacon On	71:55:34
2	S-Band Beacon On	71:58:07
5	TLM On	72:00:37
6	TLM Off	72:42:52
10	C- & S-Band Beacons Off	73:03:15
2	S-Band Beacon On	73:10:37
1	C-Band Beacon On	73:10:37
5	TLM On	73:13:07
10	C- & S-Band Beacons Off	73:22:42
6	TLM Off	73:22:42
1	C-Band Beacon On	73:32:49
2	S-Band Beacon On	73:36:31
5	TLM On	73:39:01
6	TLM Off	74:24:26
10	C- & S-Band Beacons Off	74:41:28

Table A-15

MISSION SHUTDOWN

Cmd	Event	Gemini Elapsed Time
5	TLM On	74:59:46
1	C-Band Beacon On	Not Executed
2	S-Band Beacon On	Memory Load
10	C- & S-Band Beacons Off	Changed for
6	TLM Off	Mission Shutdown
		Load.
13	Time Word Reset	79:18:55
12	Reset Timer Reset	80:18:55
12	Reset Timer Reset	86:18:55
12	Reset Timer Reset	92:18:55
12	Reset Timer Reset	98:18:55
0	Flush Load (All other rows)	98:18:55

Appendix B

STATION CONTACT SCHEDULE

Table B-1

STATION CONTACT SCHEDULE

MJD	U. T. (sec)	Rev	Station	Pass No.	Fit No.	Used	Comments
39200	54018	0	Patrick AFB 3	2		No	Before Injection
	54108	0	Merritt I. 4	3		No	Before Injection
	54222	0	Bermuda 5	4		No	Before Injection
	54252	0	Bermuda 2	9		No	Before Injection
	54282	0	G. Bahama 4	5		No	Before Injection
	54330	0	Grand Turk 4	6		No	Before Injection
	54462	0	Antigua 3	8		No	Before Injection
	54960	0	G. Canary 7	10	1		
	55086	0	G. Canary 2	11	1		
	57102	0	Carnarvon 3	15		No	Bad Header
	57048	0	Carnarvon 3	7	1		
	57066	0	Carnarvon 3	13		No	Short
	57438	0	Woomera 0	14		No	Questionable Data
	57564	0	Woomera 0	12		No	Questionable Data
	57696	0	Woomera 0	16		No	Questionable Data
	58650	1	Hawaii 2	18	1		
	58644	1	Hawaii 5	19	1		
	59274	1	Pt. Arguello 5	20		No	Bad Data
	59316	1	Gym 2	21	1		
	59796	1	Tex 2	22	1		
	62856	1	Carnarvon 2	24	1		
	64332	2	Hawaii 2	25	1		
	65332	2	Tex 2	26		No	Short Pass
	64994	2	Pt. Arguello 2	28		No	Bad Data
	65748	2	Bermuda 2	27	1		
	71286	3	Merritt I. 4	30	1		
	71370	3	Eglin AFB 0	31		No	
	71316	3	G. Bahama 4	32	1		
	76422	4	Pt. Arguello 2	34		No	Bad Data
	76704	4	Gym 2	33	1		
39201	15090	9	Ascension 4	35		No	Short
	26622	11	G. Canary 7	37	2		
	26634	11	G. Canary 2	38	2		
	31734	12	Antigua 3	39	2		
	32334	12	G. Canary 7	40	2		
	32310	12	G. Canary 2	41	2		
	34974	12	Woomera 0	42		No	Questionable Data
	37308	13	G. Turk 4	43	2		
	37398	13	Antigua 3	44	2		
	38076	13	G. Canary 7	45	2		
	38040	13	G. Canary 2	46	2		

Table B-1 (Cont.)

MJD	U.T. (Sec)	Rev	Station	Pass No.	Fit No.	Used	Comments
39201	40206	13	Carnarvon 2	53	2		
(cont.)	40374	13	Carnarvon 3	51	2		
	40578	13	Woomera 0	52	2		
	42780	14	Tex 2	47	2		
	42966	14	Eglin AFB 0	48		No	
	43026	14	G. Turk 4	49	2		
	43032	14	Patrick AFB 3	50	2		
	43230	14	Bermuda 5	54	2		
	48276	15	Gym 2	55	2		
	48414	15	Tex 2	56	2		
	48576	15	Eglin AFB 0	57	2		
	48630	15	Merritt I. 4	58	2		
	48696	15	G. Bahama 4	59	2		
	48762	15	G. Turk 4	60		No	
	48840	15	Bermuda 2	62	2		
	48846	15	Bermuda 5	63	2		
	49044	15	Antigua 3	61	2		
	49566	15	G. Canary 7	64	2		
	49530	15	G. Canary 2	65	2		
	51678	15	Carnarvon 3	73	2		
	52032	15	Woomera 0	74		No	
	53364	16	Hawaii 5	66	3		
	53910	16	Gym 2	67	3		
	53964	16	Pt. Arguello 0	68		No	Bad Data
	54174	16	Tex 2	69	3		
	54312	16	Eglin AFB 0	70	3		
	54420	16	G. Bahama 4	71	3		
	54552	16	Bermuda 5	72	3		
	54582	16	G. Bahama 4	75	3		
	54576	16	Tex 2	76	3		
	54504	16	G. Turk 4	78	3		
	54582	16	Eglin AFB 0	77	3		
	54558	16	Bermuda 2	79	3		
	54576	16	Bermuda 5	80	3		
	56412	16	Pretoria 0	81, 83	3		
	57582	16	Carnarvon 3	89	3		
	58992	17	Hawaii 5	82	3		
	59694	17	Pt. Arguello 0	84		No	Questionable Data
	60120	17	Eglin AFB 0	85	3		
	60330	17	G. Turk 4	86	3		
	60168	17	Patrick AFB 3	87	3		
	60504	17	Antigua 3	88	3		
	61386	17	Ascension 4	90	3		

Table B-1 (Cont.)

MJD	U. T. (Sec)	Rev	Station	Pass No.	Fit No.	Used	Comments
39201 (cont.)	62214	17	Pretoria 0	91→107		No	A set of short passes which should be one pass
	64776	18	Hawaii 5	108	3		
	65484	18	Pt. Arguello 0	109	3		
	65988	18	Eglin AFB 0	110	3		
	66006	18	Patrick AFB 3	111	3		
	66042	18	G. Bahama 4	112	3		
	66156	18	G. Turk 4	113	3		
	66324	18	Antigua 3	114	3		
	67188	18	Ascension 4	115	3		
	69210	18	Carnarvon 3	116	3		
	70614	19	Hawaii 5	117		No	
	70632	19	Hawaii 2	119		No	
	71226	19	Pt. Arguello 2	122		No	Bad Data
	71292	19	Pt. Arguello 0	118		No	Bad Data
	71442	19	Gym 2	120	4		
	71622	19	Tex 2	121	4		
	72204	19	G. Turk 4	123	4		
	73974	19	Pretoria 0	124	4		
	76512	20	Hawaii 5	125	4		
	79602	20	Pretoria 0	126	4		
	82898	20	Hawaii 5	127	4		
	85506	21	Pretoria 0	129	4		
39202	1902	22	Hawaii 5	128	4		
	8070	23	Hawaii 5	130	4		
	10572	24	Ascension 4	131	4		
	16284	25	Ascension 4	132	4		
	22464	26	G. Canary 7	133	4		
	22476	26	G. Canary 2	134	4		
	27678	27	Antigua 3	136	4		
	28266	27	G. Canary 7	137	4		
	28260	27	G. Canary 2	138	4		
	30810	27	Carnarvon 2	141	5		
	30912	27	Woomera 0	140		No	Questionable Data
	33546	28	G. Turk	143	5		
	33576	28	Antigua 3	144	5		
	34266	28	G. Canary 2	142	5		
	34290	28	G. Canary 7	145	5		
	36468	28	Carnarvon 3	146	5		
	36468	28	Carnarvon 2	148	5		
	36852	28	Woomera 0	147		No	Questionable Data
	39384	29	Tex 2	149	5		

Table B-1 (Cont.)

MJD	U.T. (Sec)	Rev	Station	Pass No.	Fit. No.	Used	Comments
39202	39444	29	Patrick AFB 3	154	5		
(cont.)	39480	29	G. Turk 4	156	5		
	39502	29	G. Bahama 4	150	5		
	29654	29	Bermuda 5	152	5		
	39612	29	Antigua 3	151		No	
	39660	29	Bermuda 2	155	5		
	40338	29	G. Canary 7	153	5		
	40296	29	G. Canary 2	157	5		
	42468	29	Carnarvon 3	158	5		
	46278	29	Carnarvon 2	160	5		
	43014	29	Woomera 0	159		No	Questionable Data
	45096	30	Gym 2	161	5		
	45096	30	Gym 2	162-176		No	Same as 161, Short
	45204	30	Tex 2	177		No	
	45366	30	Eglin AFB 0	178		No	
	45390	30	Patrick AFB 3	179		No	
	45432	30	G. Bahama 4	182		No	
	45630	30	Bermuda 5	183		No	
	45630	30	Bermuda 2	186		No	
	45726	30	Antigua 3	187		No	
	45528	30	G. Turk 4	185		No	
	46338	30	G. Canary 2	184	6		
	48534	30	Carnarvon 3	180	6		
	48996	30	Woomera 0	181		No	Questionable Data
	50982	31	Gym 2	189	6		
	51102	31	Tex 2	190	6		
	51342	31	Eglin AFB 0	191	6		
	51516	31	G. Bahama 4	192	6		
	51660	31	Bermuda 2	194	6		
	51570	31	Bermuda 5	195	6		
	51738	31	Antigua 3	193	6		
	53388	31	Pretoria 0	196	6		
	54510	31	Carnarvon 3	197	6		
	54510	31	Carnarvon 2	199	6		
	54900	31	Woomera 0	198		No	Questionable Data
	56250	32	Hawaii 2	200	6		
	56166	32	Hawaii 5	201	6		
	56868	32	Pt. Arguello 0	202		No	Bad Data
	56790	32	Pt. Arguello 2	203		No	Bad Data
	57066	32	Tex 2	204	6		
	57396	32	G. Bahama 4	205	6		
	57516	32	Bermuda 2	206	6		

Table B-1 (Cont.)

MJD	U. T. (Sec)	Rev	Station	Pass No.	Fit. No.	Used	Comments
39202	57564	32	Bermuda 5	207	6		
(cont.)	57672	32	Antigua 3	208	6		
	58542	32	Ascension 3	209		No	
	60444	32	Carnarvon 3	210	7		
	60462	32	Carnarvon 2	211	7		
	62004	33	Hawaii 5	212	7		
	62106	33	Hawaii 2	213	7		
	62940	33	Pt. Arguello 0	214		No	Bad Data
	62808	33	Pt. Arguello 2	217		No	Bad Data
	63162	33	Tex 2	215	7		
	63510	33	G. Bahama 4	216	7		
	63660	33	Bermuda 5	218	7		
	63642	33	Bermuda 2	219	7		
	63750	33	Antigua 3	220	7		
	64620	33	Ascension 4	221	7		
	65436	33	Pretoria 0	222	7		
	66624	33	Carnarvon 2	223	7		
	66576	33	Carnarvon 3	224	7		
	68286	34	Hawaii 5	225	7		
	68316	34	Hawaii 2	227	7		
	68934	34	Pt. Arguello 2	229		No	Bad Data
	69090	34	Pt. Arguello 0	226		No	Bad Data
	69246	34	Gym 2	228	7		
	69714	34	G. Bahama 4	230		No	
	69960	34	Antigua 3	231		No	
	70998	34	Ascension 4	232	8		
	71616	34	Pretoria 0	233	8		
	74328	35	Hawaii 5	235	8		
	74382	35	Hawaii 2	237	8		
	75066	35	Pt. Arguello 0	236		No	Bad Data
	74946	35	Pt. Arguello 2	239		No	Bad Data
	75132	35	Gym 2	238	8		
	75456	35	Tex 2	234	8		
	77466	35	Pretoria 0	240	8		
	80292	36	Hawaii 5	241	8		
	80294	36	Hawaii 2	242	8		
	83406	36	Pretoria 0	244	8		
	86207	37	Hawaii 5	243	9		
	86208	37	Hawaii 2	245	9		
39203	5958	38	Hawaii 5	246	9		
	8748	38	Ascension 4	247	9		
	14868	39	Ascension 4	248		No	

Table B-1 (Cont.)

MJD	U.T. (Sec)	Rev	Station	Pass No.	Fit No.	Used	Comments
39203 (cont.)	21126	41	G. Canary 7	246	10		
	26358	42	Antigua 3	250	10		
	26868	42	G. Canary 7	252	10		
	29676	42	Woomera 0	253		No	Questionable Data
	32076	43	Antigua 3	254	10		
	32760	43	G. Canary 7	255	10		
	34998	43	Carnarvon 3	256	11		
	35418	43	Woomera 0	257		No	Questionable Data
	37800	44	Patrick AFB 3	258	11		
	37962	44	Antigua 3	259	11		
	38016	44	Bermuda 5	260	11		
	38664	44	G. Canary 7	261	11		
	40860	44	Carnarvon 3	264	11		
	41280	44	Woomera 0	265		No	Questionable Data
	43410	45	Tex 2	262	11		
	43632	45	Patrick AFB 3	263	11		
	43854	45	Bermuda 5	266	11		
	43908	45	Antigua 3	267	11		
	45562	45	G. Canary 7	268	12*		

*Could not obtain a good fit with just one pass of data.

Appendix C

ON-ORBIT TEMPERATURE MEASUREMENTS

Table C-1

ON-ORBIT TEMPERATURE MEASUREMENTS

Measurements	GTM 3	HAW 4	RKV 6	ANT 6	HAW 8	RKV 10	CRO 14	CRO 15	HAW 18	CYI 26	TEX 28	ASC 31	ANT 33	TAN 36	RKV 38	BDA 43	TEX 44	TEX 45
								TRACKING STATIONS										
A150 Shear Panel -1	87/80*	77/71	89 /83	84	76/70	71/67		86/83	66/60	73/69	74/69	71/66	83/79	60/59	76/70	54/ 51	53/51	76/71
A151 Shear Panel -2	76/74	73/70	82 /77	66/61	63	64/62		70/69	57	71/60	76/70	63/58	73/71	54/53	63/60	51/49	60/54	37/ 35
A152 Shear Panel -3	63/62	69/66	76	64/62	62	56/53		59	45	69/62	71/70	66/66	69/67	63/62	53/51	57/54	55/52	40/39
A153 Shear Panel -4	69/62	67/63	87 /85	69	77/73	57/54		67/63	44	60/57	70/68	82/76	78/73	76/69	60/58	63/55	62/56	84/79
A154 +Z Aft. Blkd	57	76/72	75/76	54	58	54/46		84/73	46	106 /62	84/57	94/61	62/58	42	46	50/38	46/34	16/ 8
A155 -Z Aft. Blkd	91/73	84/73	106/87	58/50	84/73	65/53		110/87	57/46	88/61	84/57	113 /91	102/98	65/64	76/65	61/ 38	66/33	98/87
A156 +Y SPS Mod. Blkd	79/75	88	93 /88	75	75	74/70		97/84	57	96 /82	88/84	79/66	82/79	43	66/61	38/ 29	46/43	43
A157 -Y SPS Mod. Blkd	66/61	84/70	93/84	84/70	75/70	57/52		61/57	48	75/70	93/79	97 /84	85/81	66	57	61/32	70/66	61
A158 +Y Mod. Rad. Shd.	134	141 /134	88/30	73/58	96/73	88/77		141 /114	106/92	112/69	73/62	26	118/112	26/22	96/77	54/46	50/42	30/ 26
A159 -Y Mod. Rad. Shd.	30/22	46	161 /124	81/69	84/80	22/18		30/126	15/10	58/50	84/65	136/127	73/69	91/77	18	124/81	120/113	91/88
B031 Fuel Pump Inlet	96/80	118/117	102	96/95	95/93	71		62/ 56	71/50	64/59	129 /118	91/62	90/70	105/64	90/61	74	67	64
B032 Oxidizer Pump Inlet	90	115	100	94/93	92	71		63/ 55	70/57	64/56	115	88/60	95/62	102/64	88/61	74/72	68	67
B083 Thrust Chamb. Skin	81	85/81	89	89/81	85/81	77/74		85/65	81/ 41	73/69	112/81	132 /53	100/65	80/57	97/57	53/49	49	57/53
B096 Fuel Tank -1	58/55	52	54/52	52	52	55		57/55	57	54	57	52	60	55/52	60/57	57/55	58	57
B097 Fuel Tank -2	48/47	51	52/51	52	52	48/47		50/45	45	55	60	64/58	59	67/58	52/47	58/57	61	66
B136 Ox. Tank +Z	53	54	54	55/54	55	54		52	54	55	58	58	60	60/57	54	57	60	58
B137 Ox. Tank -Z	51	52	55	54	57/54	54		52	52	54	57	60/57	62/55	61/57	56/52	57/54	58/55	75/70
B141 Ox. Start Tank	75	72	69	65	65	55		50	45	48	62	59	62/60	59	62	48	48	41
B142 Fuel Start Tank	63	63	63	63	63	56		50	46	46	56	56	60/56	58	53/50	49	50	46/43
B164 Nozzle Ext. Skin -1								LOST MEASUREMENT										
B165 Nozzle Ext. Skin -2	-32/14	-41/-4	83/14	23/-42	83/74	-60/-80		32/14	-113/-71	-32	82/66	700/106	332/78	180/-81	227/-80	601/-32	91/23	167/123
B216 +Y N_2 Sphere	92	86	89/86	86	86/82	76		76	73/66	79/75	92/63	69	76	60	66	50/36	50	46
B233 1, +Y Biprop Valve	80/76	76	84	80/76	76	67/63		63	58	75/72	89/67	58	76/73	50/45	54	24	24	37
B234 1, -Y Biprop Valve	58	63	76/71	71	71	50		54/45	54/45	73/67	54/76	76	80/75	71/67	54	50	45	50/45
B235 2, +Y Biprop Valve	84	76	84/80	80/76	76/71	71/67		71/67	63	72	84	54	72/66	45	50	58/41	50	33
B236 2, -Y Biprop Valve	63	63	76	71	71	54		50	45	72/66	90	71/67	75	67	54	58/54	58/44	58
B240 1, +Y Mod. Injector	54/20	85/58	111/77	50/27	66/46	31/27		305/85	320/35		340/20	336/77	295/78	335/0	332/20	-23	24/-23	77/60
B241 1, -Y Mod. Injector	34/22	48	92/70	55/34	48	26/18		345/41	345/3		345/41	345/70	345/60	335/22	345/34	26/7	37/14	37/26
B246 Skin Unit I, +Y	31	31	31	31	31	31		2042/31	2007/31		1953/31	1790/31	1750/30	1757/31	1757/31	31	31	31
B247 Skin Unit I, -Y	32	32	32	32	32	32		2178/186	2060/32		2179/32	1940/32	1920/30	1902/32	1961/32	87/32	32	32
B248 Skin Unit II, +Y	32	32	51/32	32	32	32		32	32		32	32	30	32	32	1239	32	32
B249 Skin Unit II, -Y	32	32	10/57	32	32	32		32	32		32	32	30	32	32	1400	32	57
B253 -Y N_2 Sphere	72	73	79	79	79	63		60	56		86	79	81	76	66/63	66/50	63	63
B260 Ox. Line I, +Y	93	96/93	100	93/90	89	90/86		90/76	76	80/76	96/76	73	90/76	73/39	80/76	45	45	49

*High/Low

Table C-1 (Cont)

Measurements	GTM	HAW	RKV	ANT	HAW	RKV	CRO	CRO	HAW	CYI	TEX	ASC	ANT	TAN	RKV		BDA	TEX	TEX
	3	4	5	6	6	10	14	15	18	26	28	31	33	35	36	41	43	44	46
B262 Ox. Line 1, -Y	63	69/66	86	93/90	76/73	59		62/56	50/48	66/63	63/56	56/66	63/66	73/66	63		56	52	50
B267 Fuel Line 2, +Y	93	96	96	90/86	86/83	83		63	73	83/79	96	66	79	86	73/69		69/62	56	46
B269 Fuel Line 2, -Y	73	76/73	86	83	83	66		63	56	83/90	89	83	90/86	80	69/66		69/66	66	69
B270 +Y Ox. Tank	73	73	73	69	69	73/69		73/69	69	71/69	76	73	73	69	69		66	66	66
B271 +Y Fuel Tank	80	80	80	73	76	76		76	76	76/73	83	76	80/76	76/73	73		69/66	66	63
B272 -Y Ox. Tank	66	66	66	66	66	66		63	59	63/59	66	66	66/63	66	63		66	66/63	66/63
B273 -Y Fuel Tank	69	69	73	73/69	69	69		66/62	63	69/63	73	69	69	69	66		66	66	66
C010 Battery Case -1	58	58	58	58	58	65/62		69	69	69/65	65	62	65	62	65		62	62	62
C013 Battery Case -2	62	62	62	62	62	65		69	69	62	73	69	73	69	73		69	73/69	69
C014 Battery Case -4	58	58	58	58	58	58		58	54	59	58	58	58	58	58		58	58	58
C015 Battery Case -5	54	54	54	54	54	54		54	50	50	50	50	50	54	54		54	54	58/54
C016 Battery Case -6	54	50	54	54	54	50		50	46	45	50	50	50	50	50		50	50	54
C021 400 cps 3-Phase Inv.	105/104	102	102	101/99	99	105/104		102	97	91	93	86	94	88/84	96/94		94/92	94	86/84
C022 Battery Case -3	58	58	58	58	58	62/58		58	58	60	62	62	58	61/58	62		61	62	58
C185 Reg. D.C. Conv. -2	77	77	77	73	73	73		70	65	62/60	62	58	58/56	62.	69/65		60	69	58
C186 Reg. D.C. Conv. -1	96	99	103	- 103	102/99	92		88	84	91	92	92	91	92	88/84		92	92	88
D005 Hyd BTL Return Line	144/124	88/68	72/64	102/47	148/124	51/47	83/75	80	90/28	33/28	38/33	88/76	91/83	56/51	60/56	33/28	47/38	38	154/158
D046 -1 Valve Cluster	109/78	80/78	90/84	16/12	5/0	64	81	82/76	66/60	78	80	73	78	68/64	64	66/62	68/66	61	37
D047 -2 Valve Cluster	109/105	104/96	114/51	-40/-25	0/-25	90/85	114/111	111/100	90/85	88	90	111/106	103/101	102/92	97/94	92	92	100/94	123/117
D054 Horiz. Sens. Hd. (RH)	89	87	86/84	82	82	87/86	90/89	89	84	85/82	79	73	85	73/72	83/82	70	82/80	83	68
D055 Horiz. Sens. Hd. (LH)	69	73	83	79	79	86	68	66	62	75/74	77	79	72	77/76	63	80/78	84/78	82/79	88
D070 Control Gas Supply	89	92	102/99	18/-4	35/31	76	110/106	115/111	111/96	120/109	115	118	115/102	121/106	111/106	111/102	115/88	118/105	148/137
D085 V/M Elec. Oven	168	168	168	168	168	168	168	172/168	173	172/168	168	168	171/167	168	168	168	168	168	168
D087 V/M Accel. Oven	172	172	172	172	172	172	176/172	172	172	178/172	172	172	178/172	176/172	176/172	168/164	176/182	172	180/162
D129 IRP Int. Case	144	144	144	147/144	144	144	142	144	158/143	148/141	144	144	148/142	144	144	142	144	147	144
H006 Clock	182	177	177	177	177	177/173		178/172	173	178/172	173	173	178/172	177	177/173		177/188	173	177
H007 Memory	64	64	64	64	64	59		50	51	55	55	59	63/59	64	59/55		64	64	64
H033 Programmer Pwr. Sup.	77	77	77	77	81/76	68		64	50	60	60	72	72	72	68		72	72	77
H040 S-Band Transponder	N.G.	104/97	136/133	140	140	157/153		152	102/96	134/132	148	148	152	144	148		160/136	136/129	136
H060 UHF Receiver	83	83/79	79	79	79	83		79	79	86	71	67	71/69	71	79		77	75	76
H062 VHF Xmtr. -1 Case	97	100/89	97	89	93/89	97		93	81	80/78	77	73	80	77	80/86		87	86	80/73
H063 VHF Xmtr. -2 Case	50	64/55	55	51	55/51	64/50		60	51	42/40	42	38	50/45	42	55		56	51	51
H172 C-Band Xpndr. Case	131	121/117	106	117	121	138		138	114	130	131/127	127	131	127	131/127		121/120	117	121
H180 PCM Tray	77	77	80	80	80	80		77	60	70	80	84	82/80	84	80/77		80	80/77	84
H234 L-Band Face Plate	47	62	50	47/44	53/50	47/44		41	50	46	38	41	50	47	65/62		62/50	62	47